Title
Saturation Mutagenesis and Structure-Activity Relationship of a Natural Product Antibiotic

Author
Tran, Hai Long

Publication Date
2017

Peer reviewed|Thesis/dissertation

Saturation Mutagenesis and Structure-Activity Relationship of a Natural Product Antibiotic

by

Hai Long Tran

DISSERTATION

Submitted in partial satisfaction of the requirements for the degree of

DOCTOR OF PHILOSOPHY

in

Chemistry and Chemical Biology

in the

GRADUATE DIVISION

of the

UNIVERSITY OF CALIFORNIA, SAN FRANCISCO

Acknowledgments

First and foremost, I want to thank my research advisor Jim Wells for his unending support, enthusiasm, and creative thinking that has shaped the scientist that I am today. The wonderful laboratory environment has fostered great scientific conversations and lasting friendships that has made my time as a graduate student incredibly enjoyable. I thank my thesis committee, Michael Fischbach and Susan Miller, for their guidance and support throughout my PhD. I would also like to thank my collaborators, Matthew Jacobson, Katrina Lexa, Susan Miller, Adam Renslo, Christopher Walsh, and Travis Young for sharing a common interest and willingness to work together.

I would like to thank all members of the Wells lab, SMDC, and the Antibiome group for providing support in various ways. In particular, I want to thank all of the graduate students and postdocs of the Wells lab whom I have had the great pleasure of interacting with: Nicholas Agard, Wentao Chen, Emily Crawford, Daniel Gray, Juan Diaz, Zachary Hill, Sean Hudson, Olivier Julien, Emily Kang, JT Koerber, Peter Lee, Kevin Leung, Paul Marinec, Alex Martinko, Christopher McClendon, Charles Morgan, Kurt Mou, Duy Nguyen, Sam Pollock, Jason Porter, Justin Rettenmaier, Nicholas Rettko, Jack Sadowsky, Julia Seaman, Kazutaka Shimbo, Ashley Smart, Benjamin Spangler, Amy Weeks, Arun Wiita, Min Zhuang, Xin Zhou, and Julie Zorn. A special thanks to Marja Tarr who truly cares about each and every one of us. In addition, the lab wouldn’t be able to run without these individuals: Mary Betlach, Maria-Elena Diaz, Allison Doak, Ninwe Maraha, Rong Mao, Kazuko Olsen, and Ula Soegianto.

I want to thank Charles Craik, Christine Olson, Julia Molla, and Nicole Flowers for running a top-notch graduate program in chemical biology. What made my graduate experience great was being able to do it together with my wonderful classmates: Yi-Chang Liu, Brittany Gulledge, Christopher Novotny, Florentine Rutaganira, and Christopher Williams.

Finally, I would like to give a big thanks to my parents, Minh and Minh-Hieu Tran, for supporting me in my decision to get a PhD. My siblings, ViLinh, Dung, Viet, MyLan, and Phong Tran, have been my biggest support group through this journey and I can always count on them for anything.

Statement concerning previously published materials

The material in Chapter 1 was originally published as communications in the *Journal of the American Chemical Society* (2017) 139: 2541-2544. Hai Tran performed most of the work described in this chapter. Katrina Lexa provided the BRIKARD computational modelling of mutants. Olivier Julien provided support with NMR acquisition and analysis. All authors contributed to the writing and/or editing of the manuscript. James Wells supervised the research.

The material in Chapter 2 has not been submitted for publication. Hai Tran performed all of the work described in this chapter. James Wells supervised the research.

Abstract

Antibiotics are some of the most important drugs ever developed to save human lives. These drugs are essentially cures for microbial infections. Despite how important these drugs are, the current antibiotic drug discovery and development pipeline has been met with many challenges. With the constant and rapid rise of resistance to our current antibiotics, new antibiotics are needed more than ever. This problem is exacerbated by the lack of new antibiotics approved for use in the past few decades. In the search for new antibiotics, natural products are a great place to look since most FDA approved antibiotics are natural products or derivatives thereof. This thesis project studies a particular antibiotic called thiocillin, produced by the soil bacterium *Bacillus cereus*. Thiocillin is a ribosomally synthesized and post-translationally modified peptide (RiPPs) natural product. Thiocillin exhibits potent antimicrobial activity against a broad spectrum of gram-positive bacteria including dangerous pathogens such as methicillin-resistant *Staphylococcus aureus* (MRSA) and vancomycin-resistant *Enterococci* (VRE). This thesis project seeks to identify new and more potent analogs of thiocillin as well as to gain a better understanding of its properties which will enable better drug development in the future.

Chapter 1 describes the genetic exploitation of *B. cereus* biosynthetic machinery to generate a saturation mutagenesis library of thiocillin's macrocycle in order to study the structure-activity relationship of this potent antimicrobial natural product. Since thiocillin is built from a ribosomally translated peptide scaffold, this enables the use of site-directed mutagenesis as a powerful tool to rapidly generate thiocillin analogs. This work discovered many new potent thiocillin analogs, the best showing an 8-fold

increase in potency over wild-type. Combining our experimental work with BRIKARD computational modelling, we gain a deep appreciation for the role of thiazoles and dehydro post-translational modifications in further restricting entropy beyond simple macrocyclization. Our results exemplify nature's chemical logic of using rigidifying elements in macrocycle design and we hope that this work may impact future macrocycle drug design.

Chapter 2 explores the use of a redox-reactive oxaziridine reagent to site-specifically label thiocillin analogs engineered with a methionine residue. Probes such as biotin, an alkyne, or an azide are installed onto the engineered methionine. These probes can be used to further study the biology of thiocillins or as a starting point for semi-synthetic medicinal chemistry. Here, we attempt to increase compound solubility by generating thiocillin prodrugs via click chemistry. We demonstrate the ease of site-specific labelling with the oxaziridine reagent, but at the expense of a loss of activity. This exemplifies some of the semi-synthetic challenges in the drug development of thiocillins.

Table of Contents

List of Figures

Page

List of Tables

Page

Chapter 1

Structure–Activity Relationship and Molecular Mechanics Reveal the Importance of Ring Entropy in the Biosynthesis and Activity of a Natural Product

Hai L. Tran, Katrina W. Lexa, Olivier Julien, Travis S. Young, Christopher T. Walsh, Matthew P. Jacobson, and James A. Wells

This work was published in the *Journal of the American Chemical Society* (2017) 139: 2541-2544

Abstract

Macrocycles are appealing drug candidates due to their high-affinity, specificity, and favorable pharmacological properties. In this study, we explored the effects of chemical modifications to a natural product macrocycle upon its activity, 3D geometry, and conformational entropy. We chose thiocillin as a model system, a thiopeptide in the ribosomally-encoded family of natural products that exhibits potent antimicrobial effects against gram-positive bacteria. Since thiocillin is derived from a genetically-encoded peptide scaffold, site-directed mutagenesis allows for rapid generation of analogs. To understand thiocillin's structure-activity relationship, we generated a site-saturation mutagenesis library covering each position along thiocillin's macrocyclic ring. We report the identification of eight unique compounds more potent than WT thiocillin, the best having an 8-fold improvement in potency. Computational modeling of thiocillin's macrocyclic structure revealed a striking requirement for a low entropy macrocycle for activity. The populated ensembles of the active mutants showed a rigid structure with few adoptable conformations while inactive mutants showed a more flexible macrocycle which is unfavorable for binding. This finding highlights the importance of macrocyclization in combination with rigidifying post-translational modifications to achieve high potency binding.

Introduction

Natural products are critical modulators of microbial and multicellular biology. Roughly one-third of the pharmacopeia are derived from small molecule natural products. Many of these exceed Lipinski's rules with sizes in the range of 500-1500 Da but retain favorable pharmacokinetic properties, enabling oral dosing in many cases. Macrocycles are conformationally constrained by cyclization, which has been suggested to reduce their apparent size and pre-organize the compound into a low entropy state, facilitating permeation and target binding. However, macrocyclic rings of the same size can vary dramatically in their conformational flexibility, due to the presence or absence of rigidifying elements such as double bonds or backbone rings. Here we assess the effect of ring entropy on binding and activity in a model natural product system, by combining systematic mutational analysis with computational modeling of ring entropy.

We chose to study the natural product thiocillin, a thiopeptide in a class called RiPPs, ribosomally synthesized and post-translationally modified peptides. Thiocillin undergoes a cascade of post-translational modifications (PTMs) to form a mature macrocyclic natural product.[1] Thiopeptide antibiotics inhibit the growth of gram-positive bacteria including MRSA and VRE at nanomolar concentrations.[2] Like many other thiopeptides, thiocillin targets the interface between ribosomal protein L11 and the 23S rRNA.[3] Thiocillin's prepeptide contains a C-terminal core peptide and an N-terminal leader sequence, which is removed once modifications are completed.[4] Common thiopeptide PTMs include thiazole (from Cys), oxazole (from Ser), methyloxazole (from Thr), dehydroalanine (Dha) (from Ser), and dehydrobutyrine (Dhb) (from Thr); all of these modifications rigidify the peptide.[5] The modified core peptide undergoes an

enzyme-catalyzed [4+2] cycloaddition reaction to close the macrocycle and forms a pyridine core.[6,7] One of our goals was to understand the importance of rigidifying modifications in the peptide to macrocyclization and potency.

We present a systematic SAR analysis of thiocillin by saturation mutagenesis and computational modeling. Thiocillin has previously been subjected to alanine scanning, cysteine-to-serine scanning, ring-size variants, incorporation of noncanonical amino acids, and various point mutants.[8-11] In this work, we conducted saturation mutagenesis on macrocycle residues 2-9, the 8 residues not involved in macrocycle linkage, thus producing a total of 152 single point mutants. This provided a comprehensive understanding of tolerated amino acid replacements, including variants with enhanced antibacterial activity. Importantly, we noted sharp SAR that separated active and inactive analogs. Molecular mechanics modeling combined with NMR studies showed the steep loss of activity seen with certain mutants was the result of dramatic increases in ring entropy. Thus, conformational constraints beyond macrocyclization are critical for the activity of this natural product.

Results and Discussion

To rapidly generate mutants of thiocillin, we used a plasmid complementation strategy (**Figure 1-1B**). By expressing the prepeptide gene, tclE, in *Bacillus cereus* ΔtclE-H, a strain lacking the endogenous prepeptide gene, we demonstrate the rescue of thiocillin production (**Figure 1-S1**).

The mature form of thiocillin contains a large macrocycle closed via a pyridine ring which absorbs light at 350 nm. To screen for macrocycle formation, methanolic extracts from small-scale 1.5 mL cultures were analyzed by LC/MS. Presence of a 350 nm peak and a mass consistent with the mutation indicated the successful macrocyclization of 25 mutants (**Figure 1-2)**. Our results suggest mutations to non-thiazole forming residues 3, 4, 6, and 8 are tolerant to mutations, with 6 and 8 being the most tolerant without loss of activity. Only residue 8 was able to accept large aromatic side chains such as phenylalanine and tyrosine. Mutating thiazole-forming Cys residues was poorly tolerated, consistent with a previous publication.[8] These mutants were not detectable in our small scale high-throughput assay, which deliberately focused on identifying highly-expressing and well-tolerated mutants.

To screen for active mutants, an overlay assay was used against *Bacillus subtilis* 168, a representative gram-positive bacterium. Engineered *B. cereus* strains producing an active thiopeptide create a zone of inhibition when overlaid with *B. subtilis* (**Figure 1-S3**). This screen identified 18 thiocillin mutants with antibiotic activity (**Figure 1-2**). Production of these 18 active mutants and an inactive negative control mutant were scaled up and purified for quantitative minimal inhibitory concentration (MIC) determination. Since each mutant produces multiple unique compounds due to auxiliary

PTMs on residues 6 and 8, we isolated and screened all unique compounds with yields greater than 0.1 mg/L. In total, 33 unique analogs were purified from the active mutants and 2 from the negative control. The MIC assay resulted in 7 compounds more active than WT (**Table 1-1**). The most potent compound was V6A2 with an MIC of 0.06 μg/mL, an 8-fold increase in potency. This particular mutant was previously discovered to have a 4-fold increase in potency when assayed as a mixture of compounds.[8] Interestingly, we identified mutants such as T8F, which showed activity on solid media, but not in liquid culture. This may be due to the hydrophobic Phe side-chain limiting its solubility.

To examine the influence of each single point mutation on conformational entropy, we sampled the potential energy landscape for every analog using BRIKARD.[12] BRIKARD applies inverse kinematics to enable efficient generation of low-energy conformations of macrocycles. We initially validated our computational approach by reproducing near-native states extracted from crystallography data for similar thiopeptides, including one bound to ribosomal protein L11.[3] Detailed methods are available in the SI. The conformations generated for each thiopeptide by BRIKARD were then clustered using a stringent Cartesian RMSD metric (0.25 Å) to eliminate redundant (nearly identical) conformations. While this collection of low-energy states cannot be interpreted as a true thermodynamic ensemble, the number of such states varied dramatically among the thiocillin variants (**Table 1-2**), reflecting the rigidity of the macrocycle and hence its entropy.

Our results showed a strong correlation to the experimental activity data, with a clear division between the highly rigidified active analogs having a maximum of 4-7 conformational states compared to the >250 conformational states accessible to the

inactive mutants (**Table 1-2**). This finding suggests that, within the thiocillin family, mutations that dramatically increase the flexibility of the macrocycle ablate binding, due at least in part to the increased entropic loss required for binding. We cannot, of course, rule out other effects of the mutations also impacting binding affinity and activity. Conversely, conformational rigidity does not guarantee activity, i.e., the data suggests that rigidity is necessary but not sufficient for activity.

One dramatic example with mutant T4A shows that breaking the planar character of the Dhb residue at position 4, which resulted in a mature macrocycle with no detectable activity. In this case, simply changing a planar sp^2 alpha carbon to a tetrahedral sp^3 geometry leads to a dramatic increase in backbone entropy (**Figure 1-3**). These striking changes in macrocycle entropy exemplify the need for computational sampling of ring entropy.

Following our computational study of the potential energy landscape of thiocillin and our mutant analogs, NMR was used to determine the structure of WT thiocillin in DMSO. The 3D HNHA NMR experiment was used for structural determination because it is an accurate method for measuring homonuclear three-bond $^3J_{HNH\alpha}$ coupling constants and was used to help elucidate the structure of lassomycin.[13] The $^3J_{HNH\alpha}$ values obtained from ^{15}N-labelled thiocillin were used to estimate dihedral phi angles for Thr-3, Val-6, and Thr-8 according to the Karplus equation (**Table 1-S5**).[14] These values were used as restraints in BRIKARD to generate an ensemble of conformations consistent with the NMR data (**Figure 1-S4A**). Five similar conformations were obtained with and without experimental restraints, further supporting the use of BRIKARD for conformational sampling. Our predominant NMR structure (**Figure 1-S4B**) (31%

occupancy) showed a similar folded conformation to a previous NMR structure obtained using ROESY data.[8]

Based on our experimental and computational SAR, we developed a second generation combinatorial thiocillin library randomizing residues 6 and 8, the most tolerated sites. 1200 colonies were screened by overlay assay, observing many previously known single mutants as well as 16 new double mutants. Six double mutants that were combinations of potent single mutants were purified to produce 8 unique compounds and subjected to MIC testing. Only the V6A-T8V double mutant showed a 2-fold increase in potency over WT (**Table 1-S2**). These double mutants did not show the expected synergy, suggesting that other global molecular properties such as solubility or permeability may be limiting their activity.

The three PTMs characteristic of thiopeptides are formation of (1) five-membered heterocyclic thiazoles and oxazoles, (2) sp^2 side chains of Dha/Dhb, and (3) a macrocycle enclosing pyridine/dehydropiperidine ring. All are rigidifying modifications. The conformational analyses in this study suggest the entropy restricting property of these planar Dha/Dhb side chains may be as important as their previously appreciated chemical reactivity, as electrophiles in lanthionine residue formation and as dual electrophiles and nucleophiles in pyridine/dehydropiperidine ring formation. If generalizable, the Dha/Dhb-forming PTM may reveal yet another layer of chemical logic used in nature to create high affinity molecular scaffolds.

Our studies suggest that a rigid macrocycle is a requirement for binding in this system and that very small chemical changes can lead to substantial increases in entropy as measured by computational modelling. The formation of a macrocycle

greatly reduces backbone entropy, however, macrocyclization alone appears insufficient for preorganization of the compound. Particularly in thiopeptides, the presence of rigidifying PTMs such as heterocyclization and dehydrations appears to lower the entropic barrier for binding. In other macrocycle systems that are not heavily modified, entropy reduction can be achieved by intramolecular hydrogen bonding. Entropy is an often overlooked parameter in macrocycle design and the principles learned here can be applied to other natural and synthetic macrocycle systems.

Acknowledgments

We thank Professors Michael Fischbach and Susan Miller for useful discussion, Dr. Evangelos Coutsias for advice on BRIKARD, Dr. Hector Huang for help with HRMS, and Drs. Mark Kelly and Greg Lee for help with NMR. Molecular graphics and analyses were performed with the UCSF Chimera package. This research was supported by the NIH (AI111662 and GM100619).

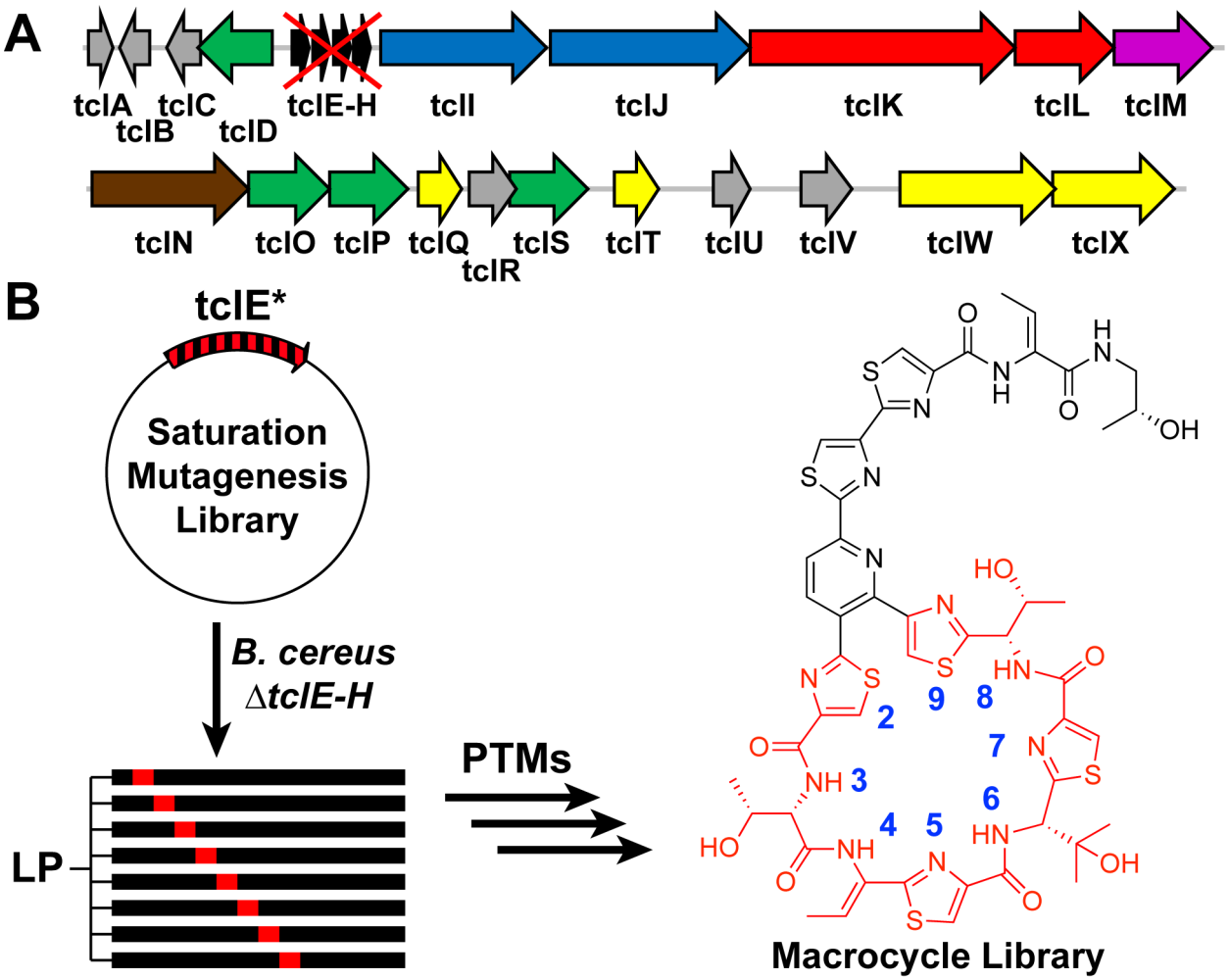

Figure 1-1: **Saturation mutagenesis of thiocillin. A)** Thiocillin gene cluster with genomic deletion of endogenous prepeptide genes tclE-H, *B. cereus* ATCC 14579 ΔtclE-H. **B)** A plasmid complementation method to generate site-saturation mutagenesis libraries at residues 2-9 of the macrocycle. LP = leader peptide.

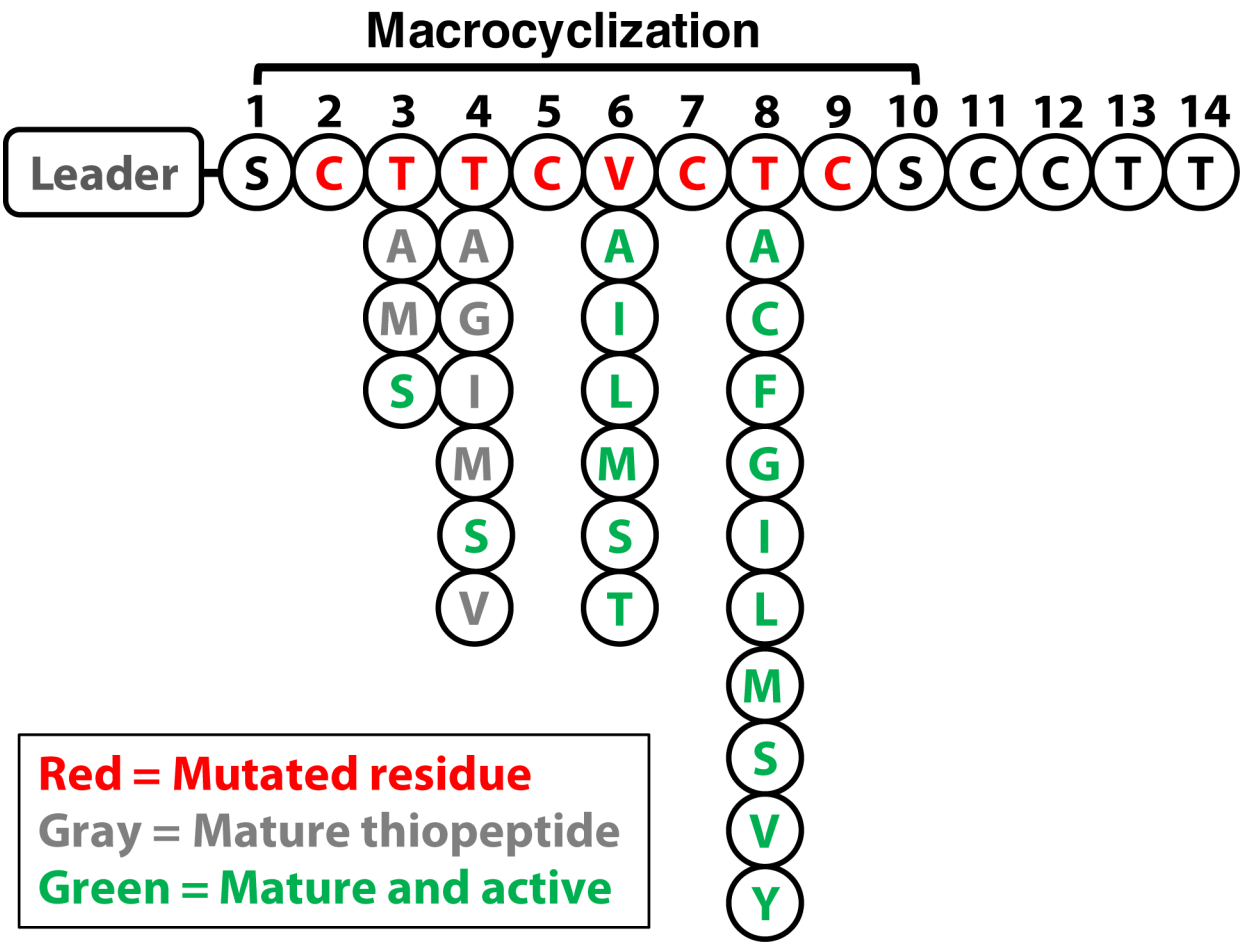

Figure 1-2: Mutations leading to macrocyclization and activity. Thiocillin prepeptide shown as a drop-down diagram designating tolerated mutations leading to macrocyclization (gray and green) and activity (green).

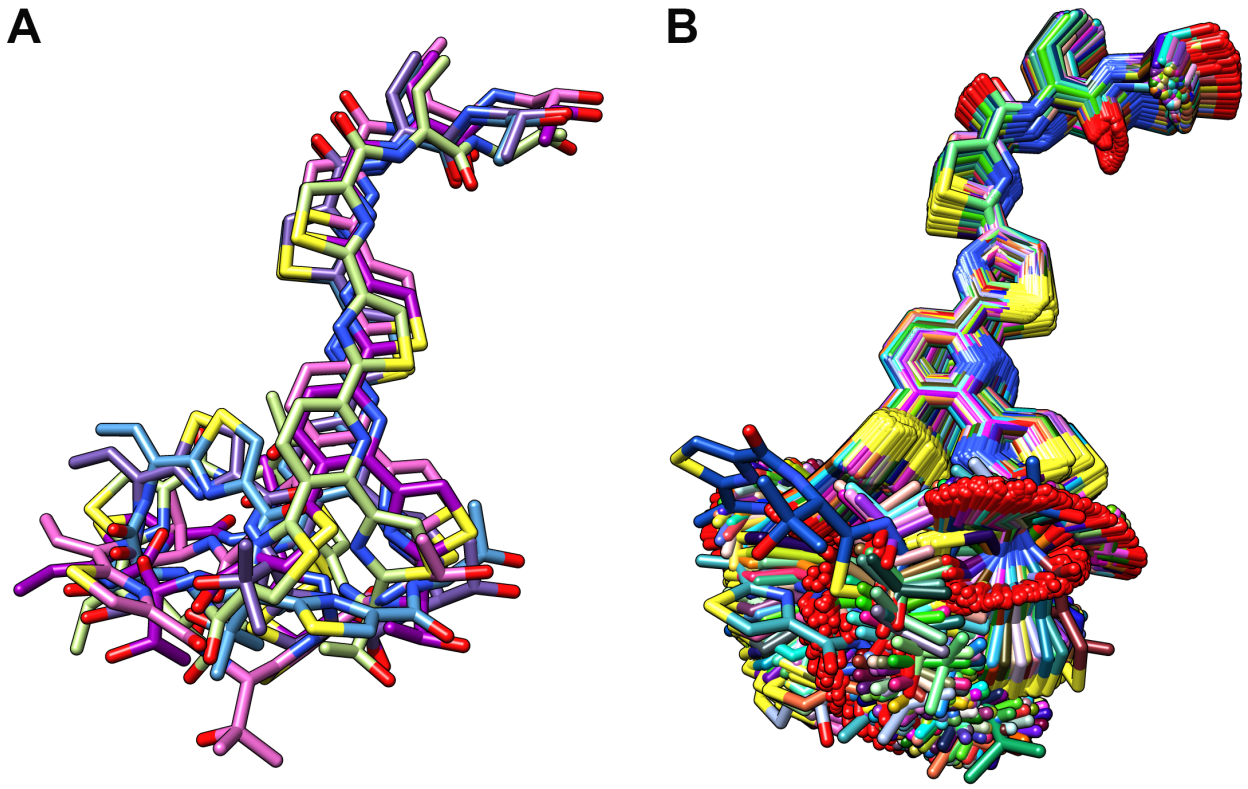

Figure 1-3: BRIKARD modelling of an active and inactive analog. BRIKARD simulations identified the populated ensembles of low energy conformations for **A)** WT thiocillin (low entropy) and **B)** T4A mutant (high entropy).

Mutant[a]	Yield[b]	MIC[c]	Modifications[d]
WT	3.9	0.5	All variants
T3S1	1.3	>8	V6-OH
T3S2	1.9	>8	
T3S3	0.3	>8	T8-CH_3
T3S4	0.3	>8	T3-Dha
T4A1 (-)	0.7	>8	V6-OH
T4A2 (-)	1.1	>8	
T4S1	0.6	2	T4-Dha; V6-OH
T4S2	0.3	1	T4-Dha; V6-OH; T8-CH_3
T4S3	0.1	>8	T4-Dha
V6A1	0.5	1	
V6A2	1.9	0.06	T8-CH_3
V6I1	2.1	0.5	I6-OH
V6I2	0.3	0.5	
V6L1	0.3	0.5	L6-OH; T8-CH_3
V6L2	0.5	2	T8-CH_3
V6M1	1.1	0.25	M6-OH; T8-CH_3
V6M2	2.4	0.13	T8-CH_3
V6S1	0.6	0.5	T8-CH_3
V6T1	1.6	0.13	T8-CH_3
T8A1	1.2	0.5	V6-OH
T8C1	0.4	8	V6-OH; C8-CH_3
T8F1	1.0	>8	
T8G1	0.9	2	V6-OH
T8G2	0.4	0.5	
T8I1	0.7	0.13	V6-OH
T8L1	1.3	1	V6-OH
T8L2	0.7	>8	
T8M1	1.4	1	V6-OH
T8M2	1.3	2	
T8S1	0.9	>8	V6-OH
T8S2	0.1	1	V6-OH; S8-Dha
T8V1	2.0	0.13	V6-OH
T8V2	0.3	1	
T8Y1	1.6	0.25	V6-OH
T8Y2	2.1	1	

Table 1-1: MIC table of thiocillin analogs. [a]Compound numbering is in order of chromatographic retention time. (-) indicates an inactive negative control. [b]mg/L. [c]μg/mL. [d]Modifications are predicted based on high-resolution MS, retention time, and NMR (structural characterizations are included in the SI).

Mutant	Conformations	Mutant	Conformations
WT[a]	5	V6I[a]	5
C2A	600	V6L[a]	4
C2S	591	V6S[a]	5
T3A	5	C7A	253
T3M	5	C7S	264
T3S[a]	5	T8A[a]	5
T4A	355	T8G[a]	7
T4L	380	T8I[a]	5
T4M	442	T8L[a]	4
T4S	384	T8M[a]	4
T4Dha[a]	7	T8S[a]	5
C5A	290	T8V[a]	5
C5S	340	C9A	501
V6A[a]	5	C9S	486

Table 1-2: Populated ensembles of conformations resulting from clustering the BRIKARD sampling results. [a]Active mutant.

Supplemental Information

Methods

I. Plasmid complementation

A plasmid complementation system was used to produce WT thiocillin and thiocillin mutants. The thiocillin prepeptide gene, tclE, was PCR amplified from WT *Bacillus cereus* ATCC 14579 and ligated into the BamHI and AatII sites of pHT01 (MoBiTec GmbH, Goettingen, Germany), an IPTG-inducible Bacillus expression plasmid, to create pHT01-tclE. Use of this plasmid for expressing thiocillin mutants have previously been shown.[10] Cloning and plasmid preparation was performed in *E. coli* XL10-Gold cells. *B. cereus* ΔtclE-H (KO cells), a strain lacking the endogenous thiocillin prepeptide gene, was generously provided by the Walsh lab (Harvard Medical School, Boston, MA). The plasmid was then electroporated into KO cells and selected on LB agarose plates containing 5 μg/mL chloramphenicol. Electroporation protocol for *B. cereus* ATCC 14579 has previously been reported.[15] 3 mL cultures were grown in LB with 10 μg/mL chloramphenicol +/- 1 mM IPTG for 72 hours at 30°C. WT and KO cells were grown in LB. Methanolic extracts of the pellet were dried and resuspended in 100 μL of 1:2 B:A (Solvent A = water/0.1% TFA; Solvent B = acetonitrile/0.1% TFA). 10 μL was loaded onto a Waters XBridge C18 3.5 μm 1x150 mm column with a flow rate of 50 μL/min and a linear gradient of 30-65% B over 24 min (Waters, Milford, MA).

II. Library construction

The thiocillin saturation mutagenesis library was constructed by individually mutating each of the macrocycle residues 2-9 to the remaining 19 amino acids. pHT01-tclE was restriction digested with AfeI and SmaI (New England Biolabs, Ipswich, MA) to create a linear vector. An oligo template for each mutant tclE construct was ordered from Integrated DNA Technologies (IDT, Coralville, IA) containing the full 14AA core sequence (**Table 1-S1**). Primers tclE-ins-F and tclE-ins-R was used to amplify the oligo templates to create DNA inserts. Gibson cloning was used to assemble the insert and vector into a plasmid. Plasmids were cloned in *E. coli* XL10-Gold and sequenced.

Combinatorial double mutant library was developed using Künkel mutagenesis. To develop the Künkel plasmid, an F1 origin sequence was inserted into the XhoI site of pHT01-tclE to create pHT08. Site-directed mutagenesis was used to replace residues 6-8 with a stop codon and SpeI cleavage site 'taaactagt' to prevent WT background in our screen. Primer 68NNK (**Table 1-S1)** was used as a Kunkel template to randomize residues 6 and 8 with NNK codons. The library was purified and electroporated directly into *B. cereus* ΔtclE-H.

III. Expression and extraction of thiocillin analogues

Plasmids containing thiocillin mutants were electroporated into *B. cereus* ΔtclE-H cells and selected on chloramphenicol selective plates. For small-scale expression, colonies were grown in 1.5 mL LB Lennox + 10 μg/mL chloramphenicol + 1 mM IPTG in 2.2 mL deep well blocks with shaking at 30°C for 72 hours. Cells were pelleted and

decanted. Compounds were extracted twice with 800 μL methanol. Methanol extracts were dried by Genevac and resuspended in 50 μL DMSO for downstream analysis.

For large-scale preparations of thiocillin analogues, fresh colonies were grown overnight in 30 mL LB Lennox + 10 μg/mL chloramphenicol at 30°C and 200 rpm. 7.5 mL overnight culture was innoculated into 1.5 L LB Lennox in 2.8 L baffled flask and were grown at 30°C and 200 rpm. 5 μg/mL chloramphenicol was added at 0, 24, and 48 hrs. 1 mM IPTG was added at 3 hr and 0.5 mM IPTG was added at 24 and 48 hrs. Cells were pelleted and decanted. 50 mL of methanol and 20 g of anhydrous sodium sulfate were added to the pellet and vortexed vigorously. The methanol was filtered with a Whatman no. 1 filter. A second methanol extraction was performed on the pellet and filtered. The methanol was removed by vacuum to leave a dark yellow residue. Ethyl acetate extractions was used to further purify the compounds. The residue was redisolved in 40 mL of 1:1 EtOAc:saturated NaCl solution and shaken in a separatory funnel. The EtOAc layer was collected. The aqueous layer was washed twice with 20 mL EtOAc. EtOAc layers were combined, dried with anhydrous Na_2SO_4 and filtered. EtOAc was removed by rotovap. Residue was dissolved in 1 mL DMSO, filtered, and purified by preparative HPLC. 500 μL was injected onto a Waters XBridge Prep C18 5 μm OBD 19x50 mm column with a flow rate of 20 mL/min. Solvent A = water/0.05% formic acid. Solvent B = methanol/0.05% formic acid. The method started at 50% B for 2 min, followed by a linear gradient from 50-75% B over 12 min, then a linear gradient to 100% B for 1 min, static at 100% B for 2 min, and then static at 50% B for 1 min. Major peaks with 350 nm absorption were collected and vacuumed to dryness. Mass of dried

residue was used to determine the yield. Compounds with yields greater than 0.1 mg were kept for further analysis.

[^{15}N]-labelled thiocillin was prepared for NMR analysis. Large-scale preparation protocol was followed exchanging the media with M9 minimal media containing [^{15}N]-ammonium chloride (Cambridge Isotope Laboratories, Tewksbury, MA) as the nitrogen source and supplemented with ATCC trace mineral supplement (ATCC) and BME vitamins (Sigma-Aldrich). WT *B. cereus* was grown without antibiotics or IPTG. The protocol described above was used to isolate [^{15}N]-thiocillin. The compound was dissolved in d_6-DMSO (Cambridge Isotope Laboratories) for NMR analysis.

IV. LC/MS macrocyclization assay

To assay for macrocyclization of thiocillin mutants, an LC/MS assay was used to detect the pyridine ring formed during macrocyclization (350 nm absorption) and the mass of the product. Samples were analyzed on a Waters 2795 HPLC with a Waters 2996 UV detector and a Waters ZQ-4000 quadrapole ESI mass spectrometer. 20 μL of the DMSO stocks from the small scale expression, described in Section III, were injected onto a Waters XBridge C18 3.5 μm 4.6x50 mm column with a flow rate of 1 mL/min and a linear gradient of 5-95% B:A over 8 min (Solvent A = water/0.1% TFA; Solvent B = methanol/0.1% TFA).

V. Overlay activity assay

To screen for active antibiotics, an overlay assay was used. Cultures of engineered *B. cereus* containing each tclE mutant from our saturation mutagenesis library were grown overnight in 96-well plates in LB media with 10 μg/mL chloramphenicol. A strain producing WT tclE via plasmid and a strain with an empty vector were used as positive and negative controls, respectively. After overnight growth, cultures were diluted 100-fold into LB media and spotted on LB agarose plates containing 10 μg/mL chloramphenicol and 1 mM IPTG. Colonies were allowed to grow for 30 hours at 30°C. Our "victim" strain for the overlay assay is *B. subtilis* BG2864 ATCC 47096 (a kanamycin resistant strain) which we transformed with pHT01 expressing LacZ (a β-galactosidase) to distinguish cell types in our assay when LacZ degrades X-gal to form a blue pigment. The overlay was prepared by cooling 25 mL of molten Top Agar (LB + 0.7% agarose) to 42°C and adding 10 μL of 50 mg/mL kanamycin (to prevent further growth of *B. cereus* colonies), 20 μL of 5 μg/mL chloramphenicol, 25 μL of 100 mM IPTG, 300 μL of 20 mg/mL X-gal dissolved in DMSO, and 25 μL of dense "victim" strain. The Top Agar solution was poured over the colonies and allowed to solidify. Plates were placed in a 37°C incubator overnight. Kill zones indicate a colony producing an active antibiotic.

VI. Minimal inhibitory concentration assay

A dense culture of *B. subtilis* 168 was diluted to an OD_{600} of 0.001 in LB media. 96-well plates were filled to 147 μL per well. A 2-fold serial dilution series was made in

DMSO (400 μg/mL - 0.39 μg/mL) for each purified compound. 3 μL of the serial dilution DMSO stock was added to the wells. The plates were sealed with foil and incubated for 16 hrs at 37°C with shaking at 280 rpm. OD_{600} of cultures were measured by plate reader. MIC is designated as the lowest concentration required to inhibit growth. Inhibited growth is defined as cultures showing less than 10% increases in OD_{600} over kanamycin (25 μg/mL) treated control.

A mixture of all WT thiocillin variants was used as a positive control. This was necessary to obtain the literature reported MIC value of 0.5 μg/mL.[16] T4A mutant was included as an inactive negative control mutant. The results for the single point mutant library are shown in **Table 1-1** and double mutants in **Table 1-S2**.

VII. LC/MS and HRMS structural characterization

LC/MS analysis was performed on all purified compounds as described in Section IV. High resolution mass spectrometry (HRMS) data was collected on a Q Exactive Plus (ThermoFisher Scientific) with resolution set to 140,000 at *m/z* 200. Purified compounds were diluted to 500 nM in 30% acetonitrile in water with 0.1% formic acid. 1.5 μL of the samples were direct injected into the mass spectrometer at a rate of 500 nL/min for analysis. HRMS and retention time data helped provide insight on PTMs. LC/MS and HRMS data is shown in **Figure 1-S3**. Summary of HRMS data is shown in **Table 1-S3**.

VIII. NMR structural characterizaion

All NMR experiments were performed on a Bruker Avance 800 MHz equipped with a cryoprobe at the UCSF NMR Facility. All data was collected at 298K. WT thiocillin YM-266183 variant, T4S1(Dha), and T8Y1 were dissolved to approximately 2-10 mg/mL in DMSO-d_6 (Cambridge Isotope Laboratories) and placed in 5 mm DMSO-matched SHIGEMI NMR tubes (Catalog #: DMS-005TB, SHIGEMI Co., Tokyo, Japan) or 5 mm Wilmad Thin Wall Precision NMR sample tubes (Catalog #: 535-PP-8, Wilmad LabGlass, Vineland, NJ). 1D ^{1}H NMR, 2D ^{1}H-^{13}C HSQC, 2D ^{1}H-^{13}C HMBC, and 2D ^{1}H-^{1}H ROESY spectra were taken for these samples. Chemical shift assignments are shown below (**Table 1-S4, Figure 1-S16,** and **Figure 1-S21**). {^{1}H-^{15}N} HSQC was taken on an [^{15}N]-labelled WT sample for ^{1}H and ^{15}N assignments. For 9 additional analogues, 1D ^{1}H NMR and 2D TOCSY spectra were taken including an additional COSY spectra for V6A2 (**Figures 1-S22 to 1-S40**).

Further 3D structural characterization was performed on WT thiocillin. 3D HNHA experiment was used to determine the homonuclear three-bond $^{3}J_{HNH\alpha}$ coupling constants (**Figure 1-S12**). The coupling constants for Thr-3, Val-6, and Thr-8 were used as phi angle restraints in BRIKARD modeling. **Table 1-S5** shows the phi angles and the percent occupancy from the top 5 NMR models. **Figure 1-S4a** shows the ensemble of the top 5 NMR models and **Figure 1-S4b** shows the most predominant conformation, WT_1.

IX. Computational details

A single input structure is required to run BRIKARD. We tested our approach to using BRIKARD to thoroughly sample experimentally relevant conformations using thiostrepton and nosiheptide; two thio-containing macrocycles with literature data.[3] These two molecules were used to benchmark the number of iterations required to generate sufficient conformational diversity for our purposes and the best clustering cut-off. Since our questions in this study focused solely on conformational diversity and the underlying conformational entropy of each mutant, we used a shortened version of the published BRIKARD protocol, in which 1000 iterations were performed for each compound of interest.[12]

An extended, linear pre-cursor peptide was built for the wild-type structure, the cycle was formed, and the resultant structure was minimized in Maestro. An opls2005-derived force field file describing the non-bonded and bonded terms for the compound was generated with the hetgrp_ffgen utility in the Schrodinger package. This was used as the input into BRIKARD to generate an initial conformational ensemble of 1000 PLOP-minimized structures. Energy-based clustering was performed with the tools available in BRIKARD. Further details into specific methods underlying BRIKARD and BRIKARD with PLOP are available in the citation Coutsias *et al* 2016. We identified an RMSD threshold of 0.25 Å to be optimum for clustering conformations into population families. These conformations were compared with the experimental data to ensure that a near-native state was contained within our final structural ensembles.

A similar build procedure was followed for thiocillin. All mutants of interest were built by making the corresponding backbone and/or side chain change to the initial wild

type input structure. The conformation of the long, rigid tail on thiocillin (residues 11-14) was based on our observations of the similar extended tail seen in nosiheptide (elongated, rigid but slightly bent). These input structures each had a force field file generated for the compound of interest and were subjected to 1000 iterations of BRIKARD with PLOP minimization. The output was clustered to identify the extent of conformational rigidity.

To explore the NMR ensemble of wild type thiocillin conformations, BRIKARD was run with restraints placed on the phi angles sampled on residues 3, 6, and 8. These restraints were derived from the ^{3}J couplings and enforced as follows: ±142°±5, ±165°±5, ±157°±5. We found no conformations satisfied all of these restraints absolutely and simultaneously. Instead, our best approximation of the NMR ensemble came from loosening the RMSD threshold to 0.75 Å and shifting the restraints slightly to ±142±5 & 22°±5 for phi3, ±160°±5 for phi6, and ±153°±5 for phi8 to enable successful sampling. No structures exactly matched all three constraints at once, but we were able to identify low-energy structures that approximately matched one or two of the ^{3}J coupling-derived restraint. This may be because the NMR results represent the average of a rapidly interconverting conformational ensemble rather than one single structure.

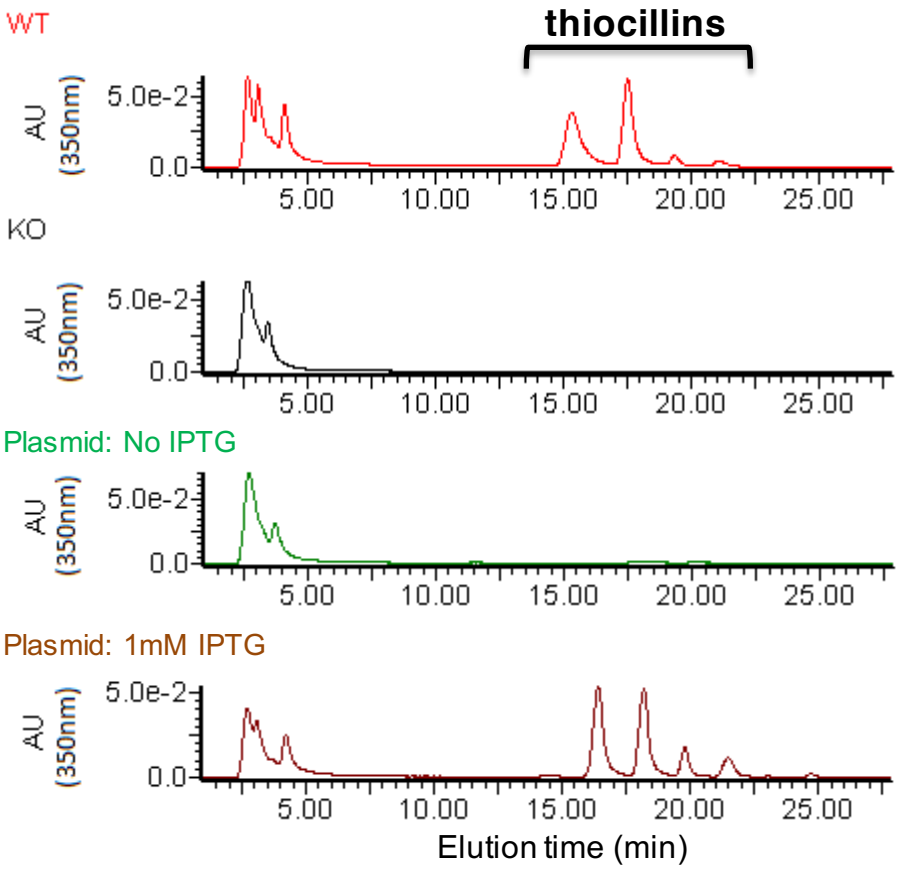

Figure 1-S1: Plasmid complementation shows rescue of thiocillin production under IPTG control.

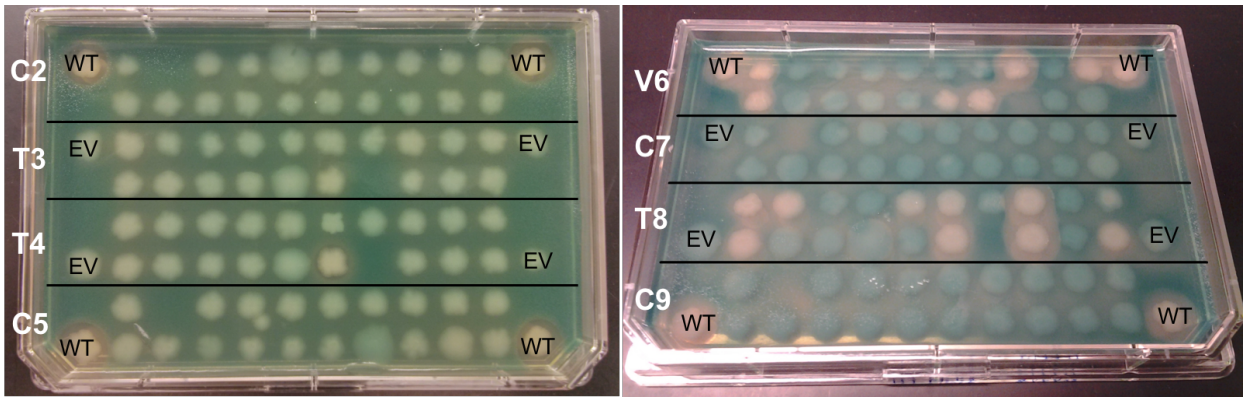

Figure 1-S2: Overlay assay for active antibiotics. Kill zones show colonies producing an active antibiotic. WT = *B. cereus* ΔtclE-H + pHT01-tclE. EV = *B. cereus* ΔtclE-H + pHT01-Empty Vector.

A) WT Thiocillin Mixture

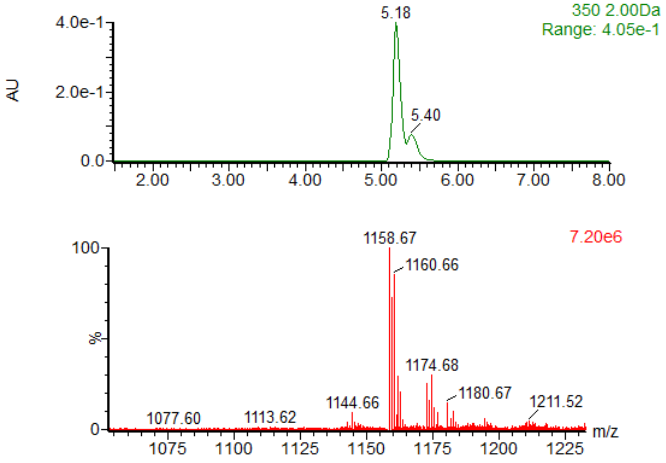

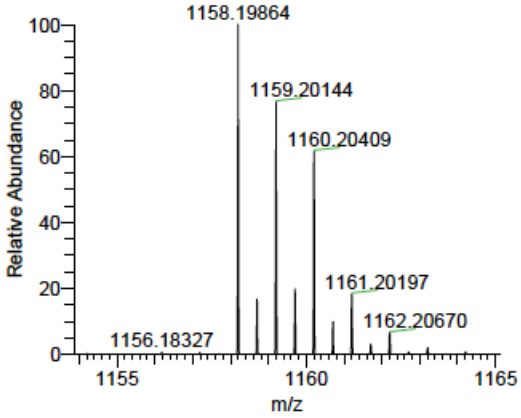

Q Exactive Plus: High Resolution MS1
Theoretical [M+H] = 1158.19659

B) T3S1

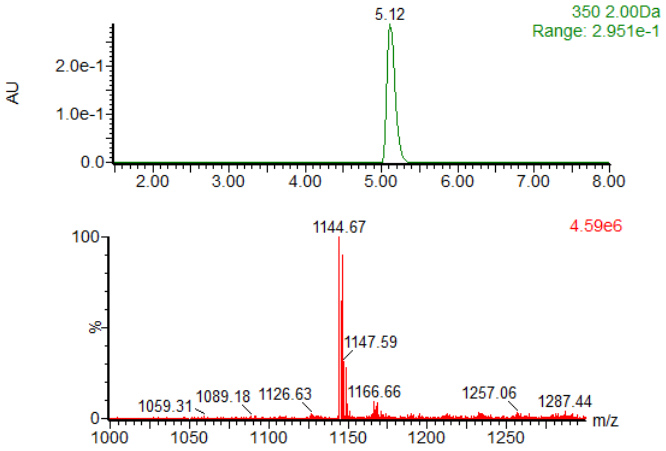

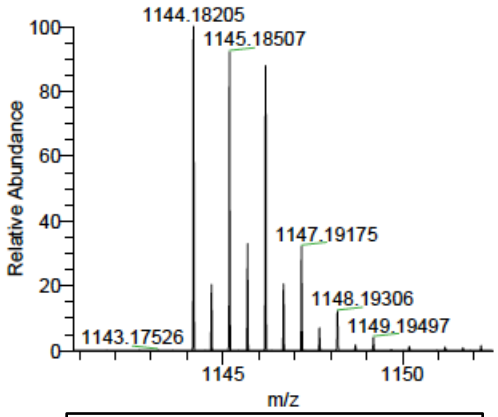

Q Exactive Plus: High Resolution MS1
Theoretical [M+H] = 1144.18094

C) T3S2

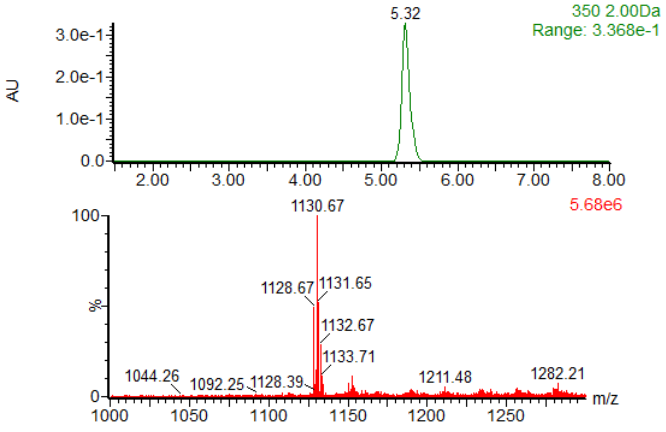

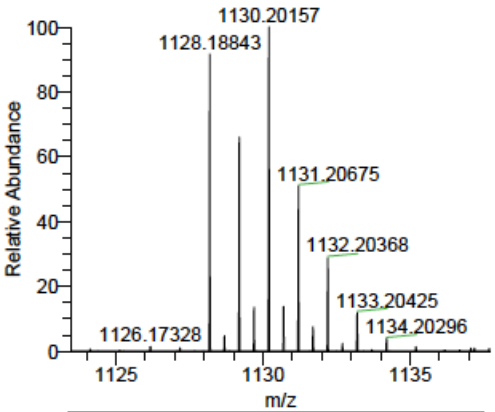

Q Exactive Plus: High Resolution MS1
Theoretical [M+H] = 1128.18602

D) T3S3

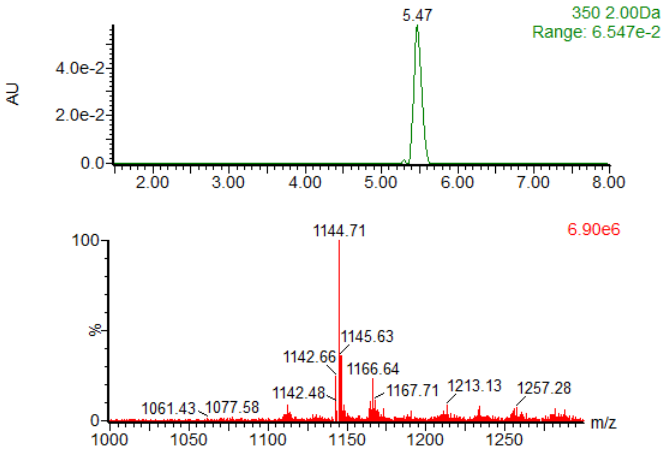

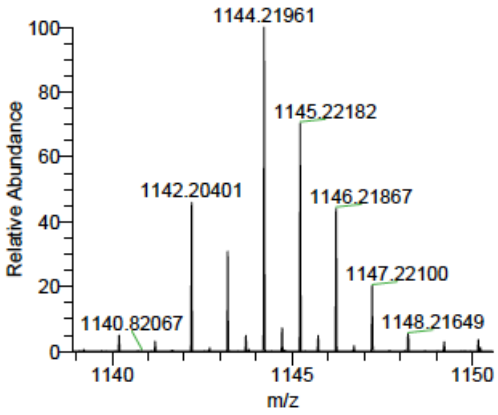

Q Exactive Plus: High Resolution MS1
Theoretical [M+H] = 1142.20167

E) T3S4

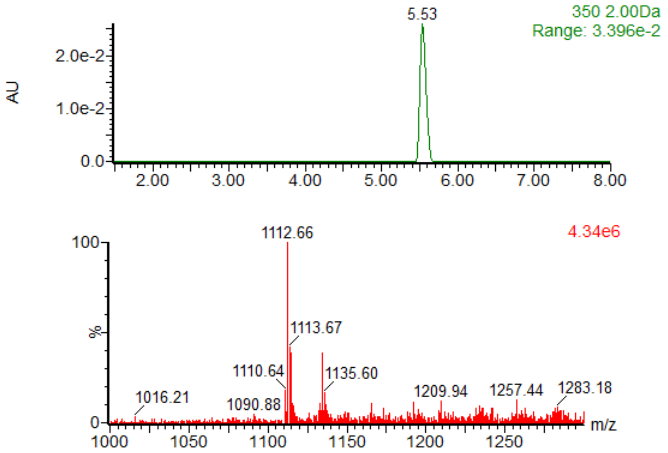

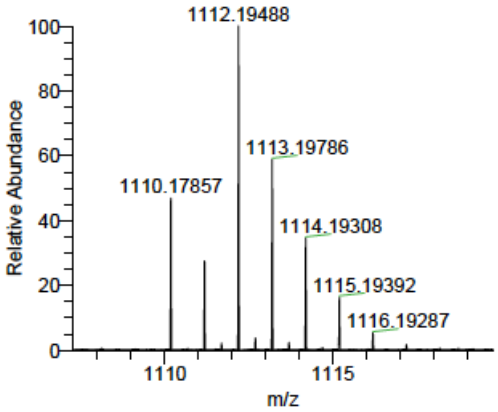

Q Exactive Plus: High Resolution MS1
Theoretical [M+H] = 1110.17546

F) T4A1

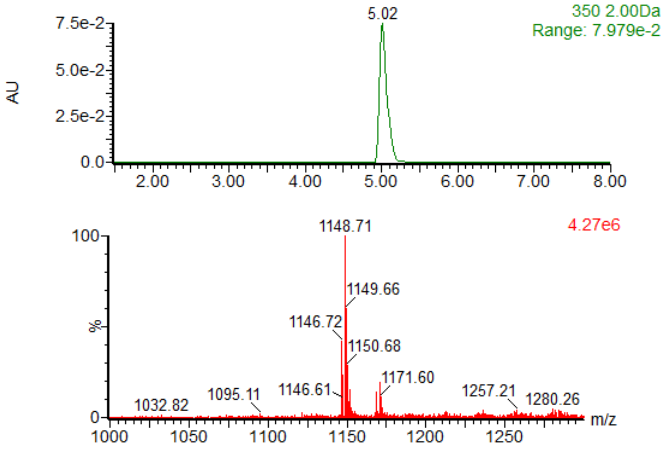

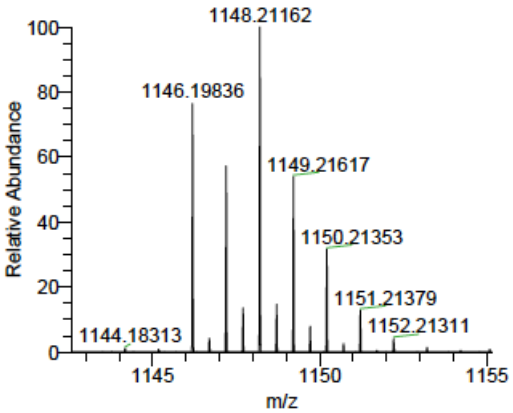

Q Exactive Plus: High Resolution MS1
Theoretical [M+H] = 1146.19659

G) T4A2

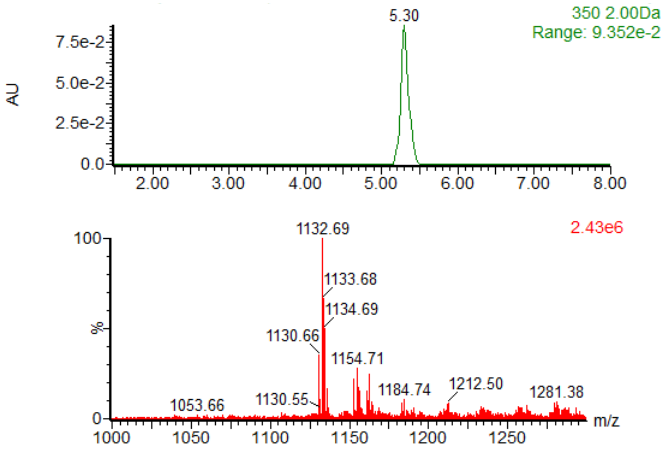

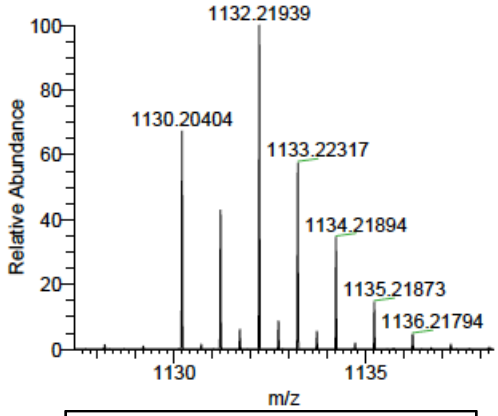

Q Exactive Plus: High Resolution MS1
Theoretical [M+H] = 1130.20167

H) T4S1

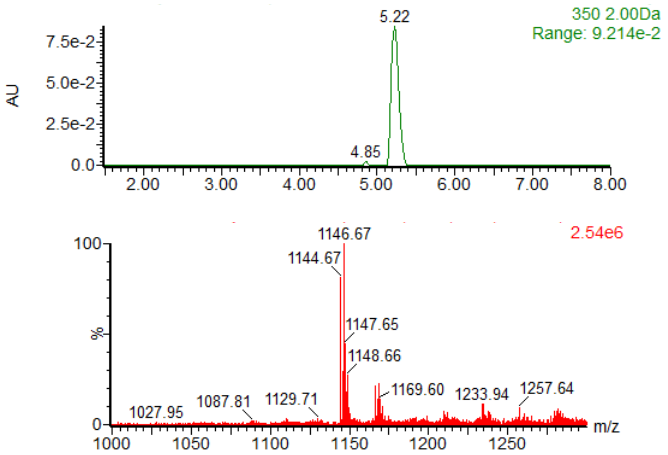

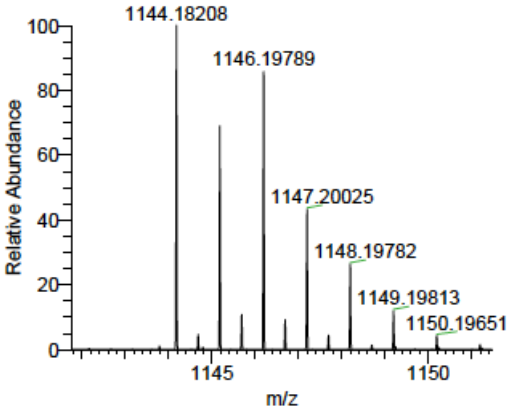

Q Exactive Plus: High Resolution MS1
Theoretical [M+H] = 1144.18094

I) T4S2

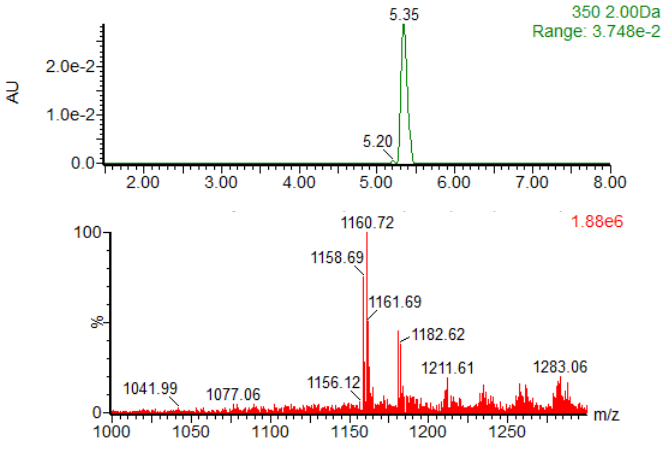

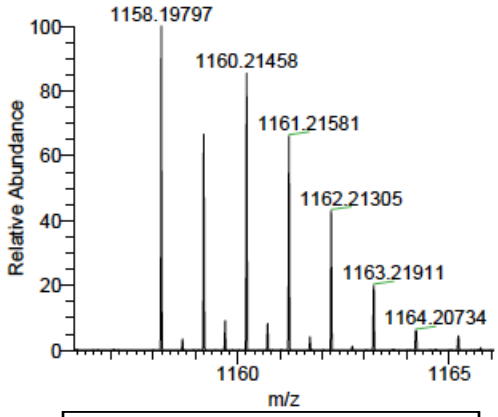

Q Exactive Plus: High Resolution MS1
Theoretical [M+H] = 1158.19659

J) T4S3

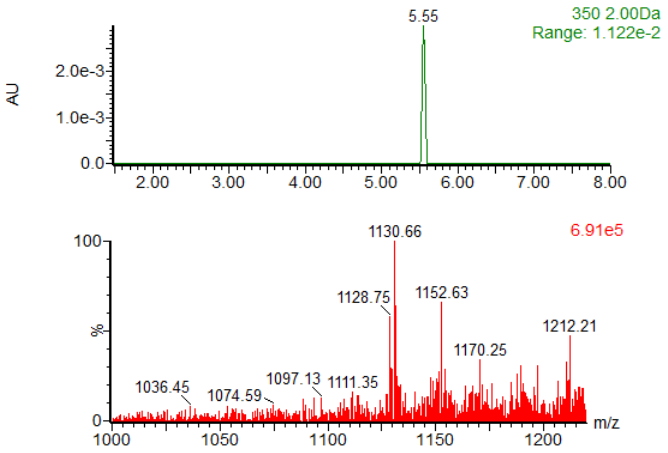

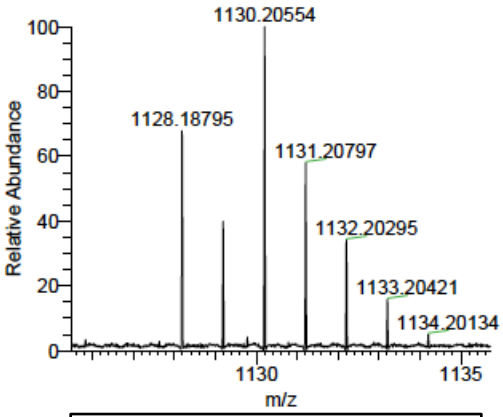

Q Exactive Plus: High Resolution MS1
Theoretical [M+H] = 1128.18602

K) V6A1

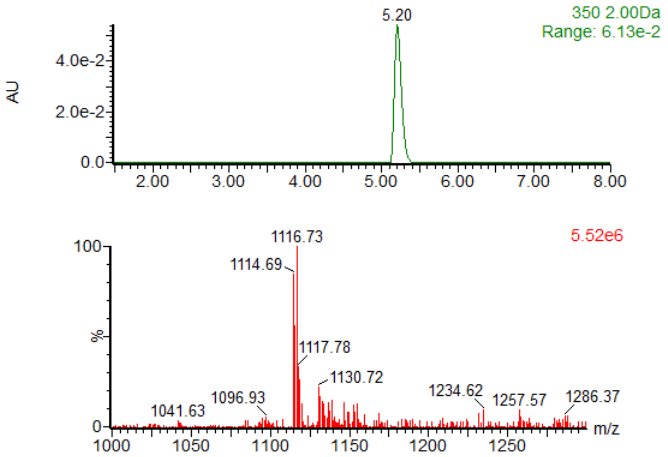

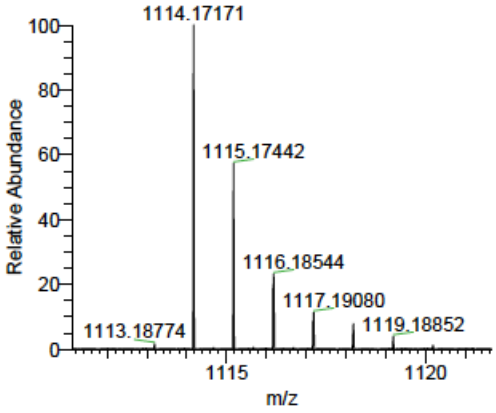

Q Exactive Plus: High Resolution MS1
Theoretical [M+H] = 1114.17037

L) V6A2

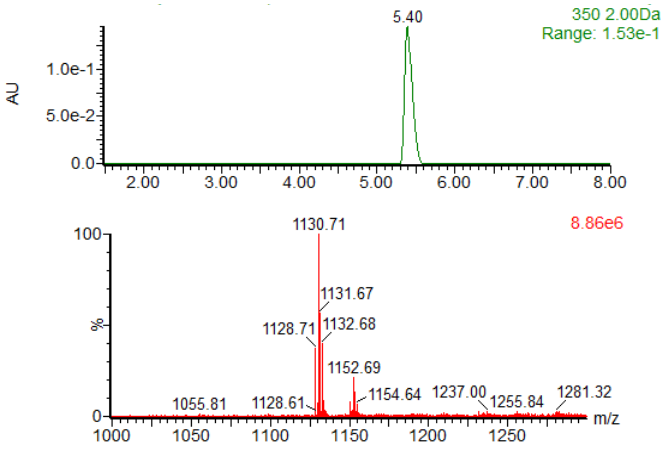

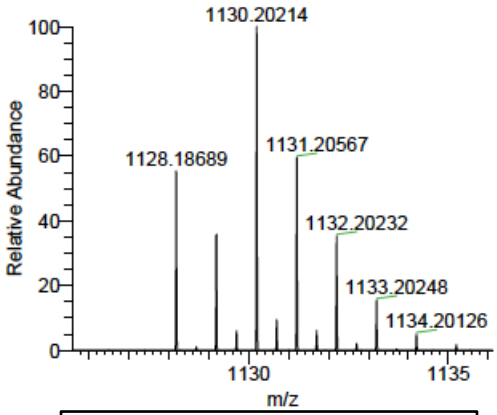

Q Exactive Plus: High Resolution MS1
Theoretical [M+H] = 1128.18602

M) V6I1

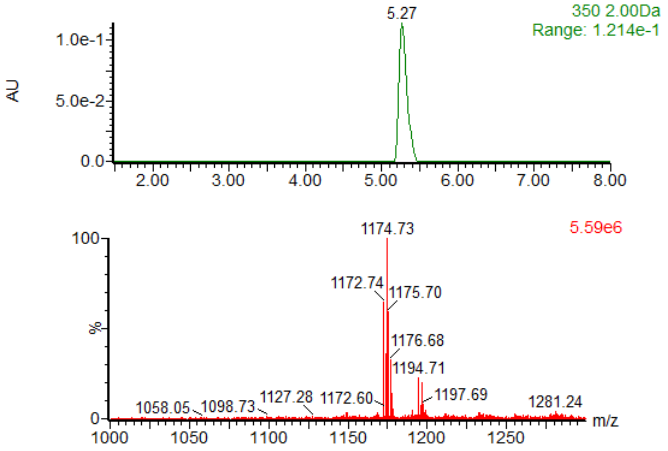

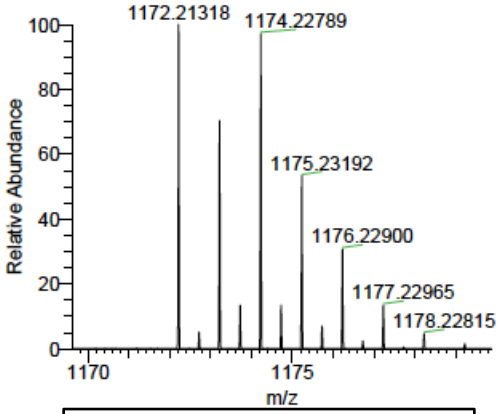

Q Exactive Plus: High Resolution MS1
Theoretical [M+H] = 1172.21224

N) V6I2

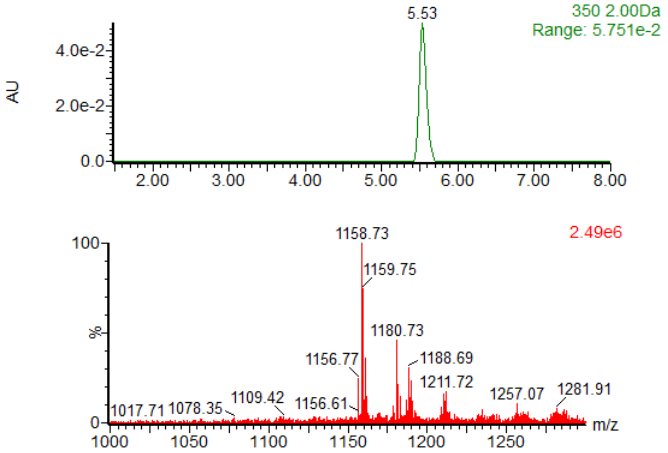

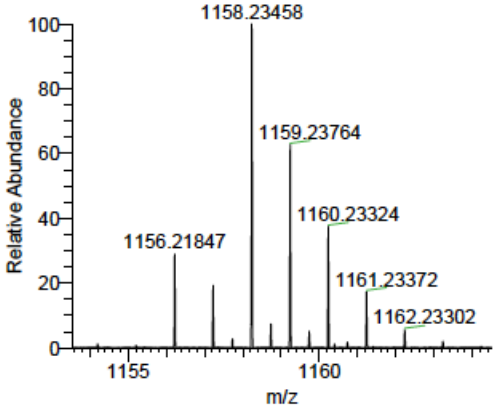

Q Exactive Plus: High Resolution MS1
Theoretical [M+H] = 1156.21732

O) V6L1

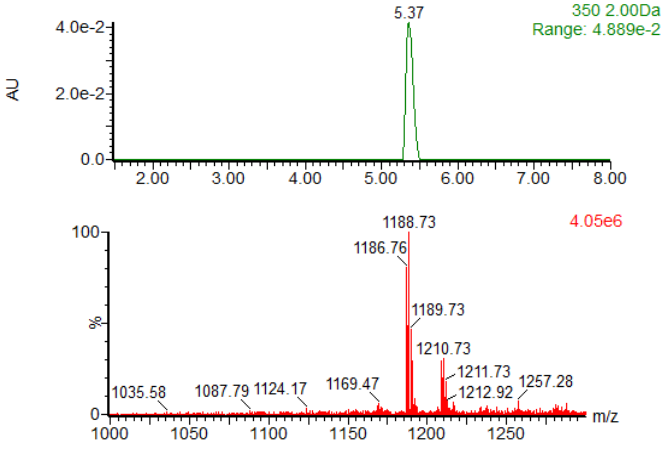

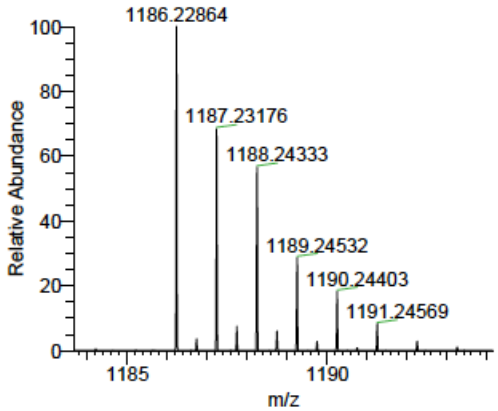

Q Exactive Plus: High Resolution MS1
Theoretical [M+H] = 1186.22789

P) V6L2

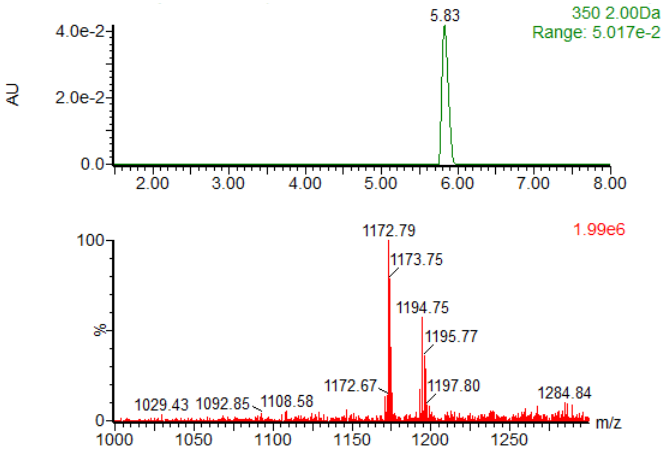

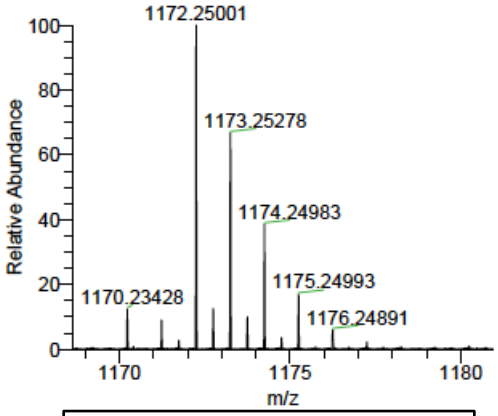

Q Exactive Plus: High Resolution MS1
Theoretical [M+H] = 1172.24862

Q) V6M1

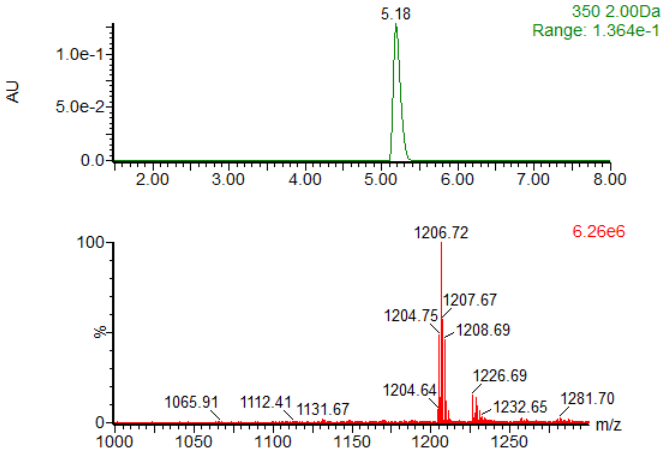

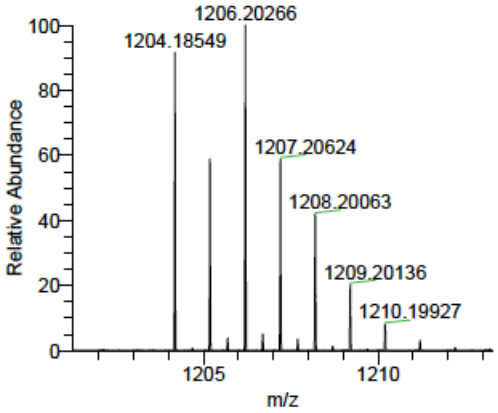

Q Exactive Plus: High Resolution MS1
Theoretical [M+H] = 1204.18431

R) V6M2

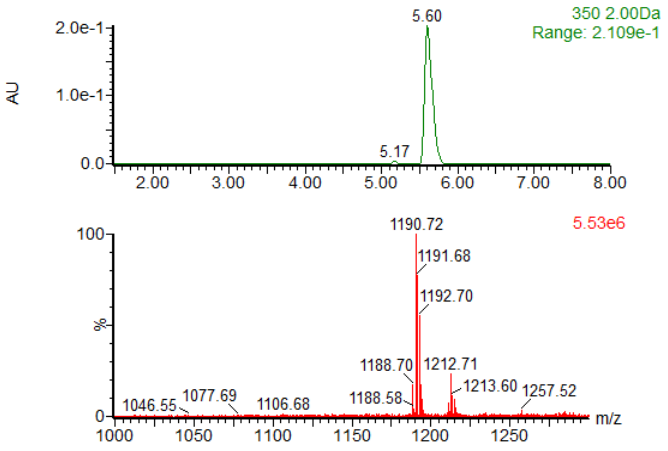

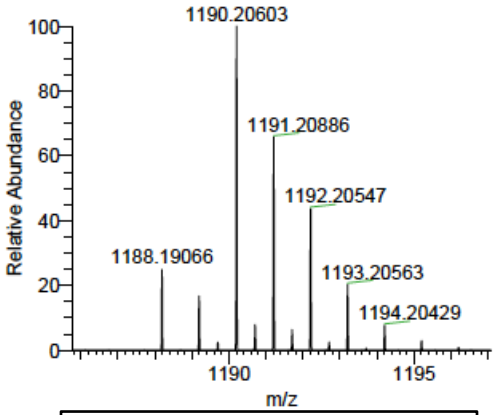

Q Exactive Plus: High Resolution MS1
Theoretical [M+H] = 1188.18939

S) V6S1

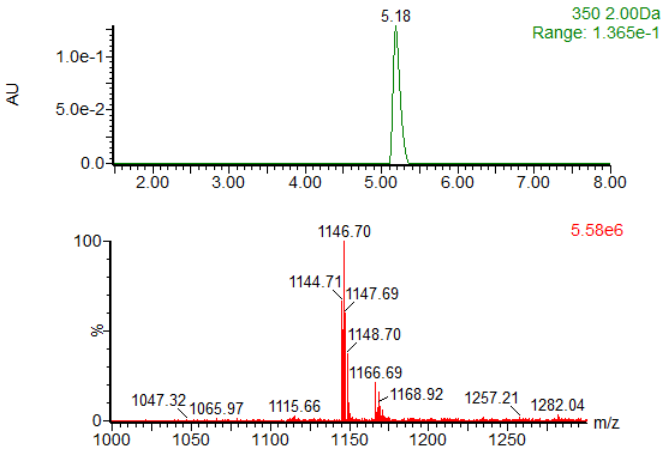

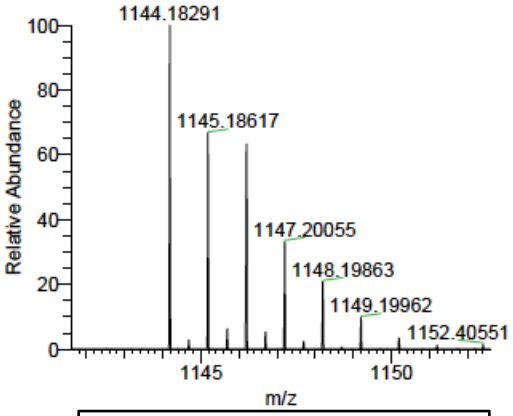

Q Exactive Plus: High Resolution MS1
Theoretical [M+H] = 1144.18094

T) V6T1

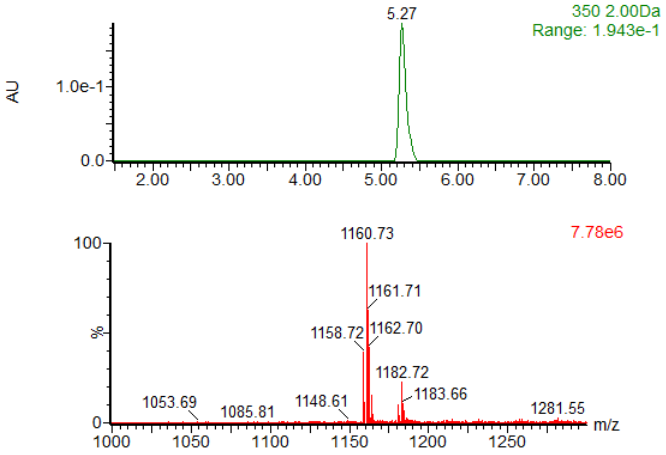

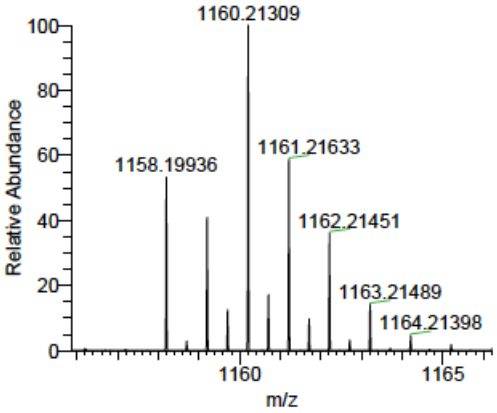

Q Exactive Plus: High Resolution MS1
Theoretical [M+H] = 1158.19659

U) T8A1

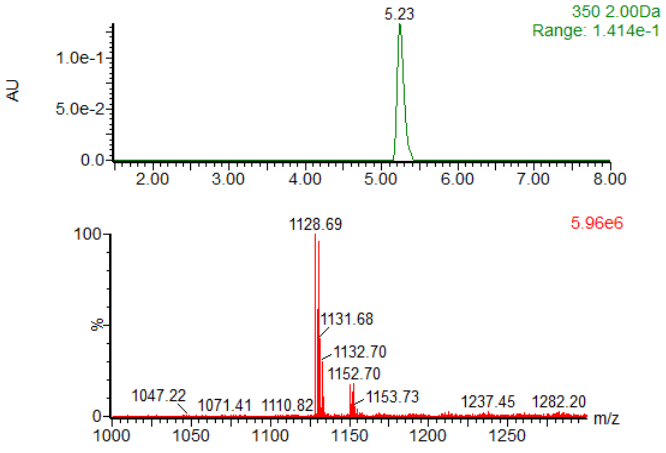

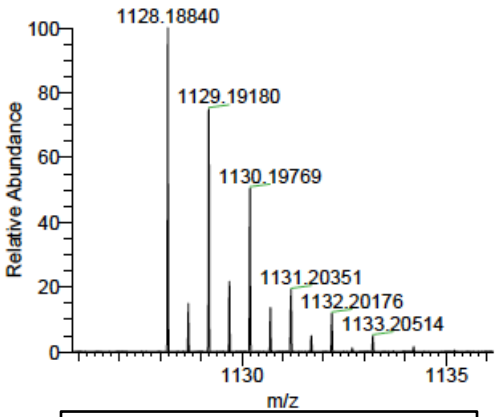

Q Exactive Plus: High Resolution MS1
Theoretical [M+H] = 1128.18602

V) T8C1

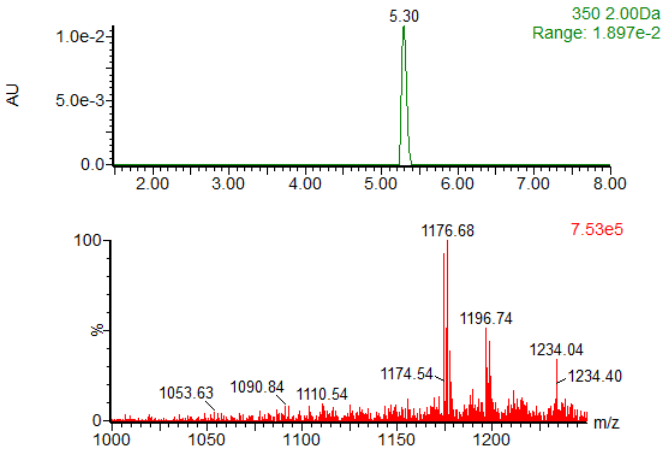

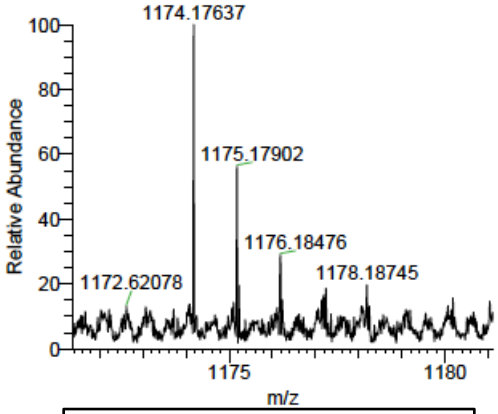

Q Exactive Plus: High Resolution MS1
Theoretical [M+H] = 1174.17374

W) T8F1

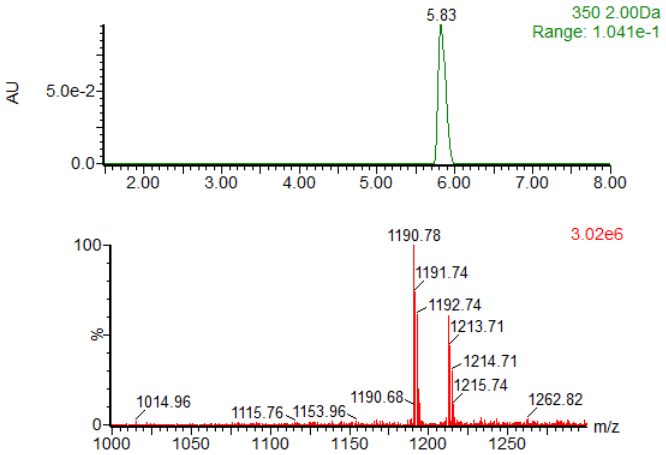

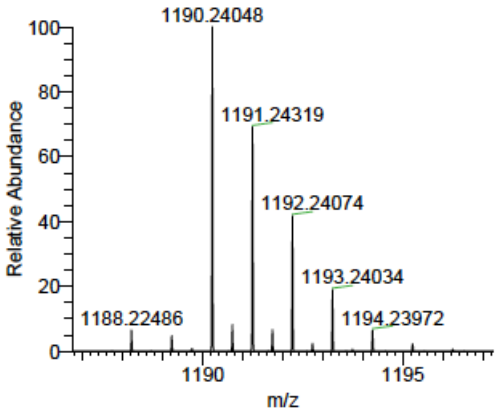

Q Exactive Plus: High Resolution MS1
Theoretical [M+H] = 1190.23806

X) T8G1

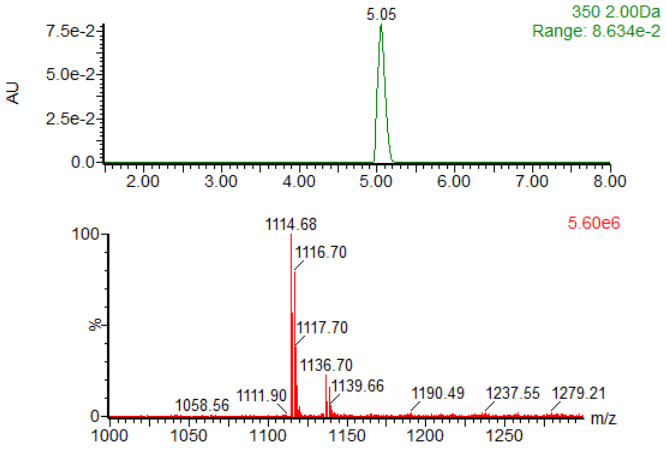

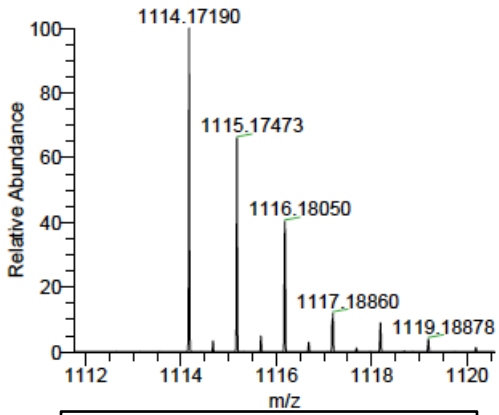

Q Exactive Plus: High Resolution MS1
Theoretical [M+H] = 1114.17037

Y) T8G2

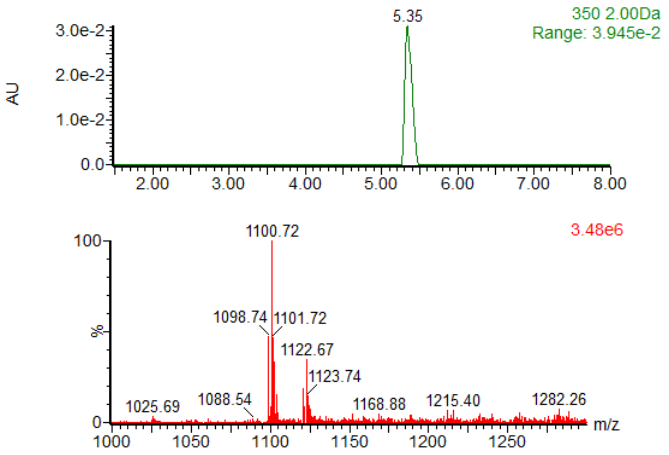

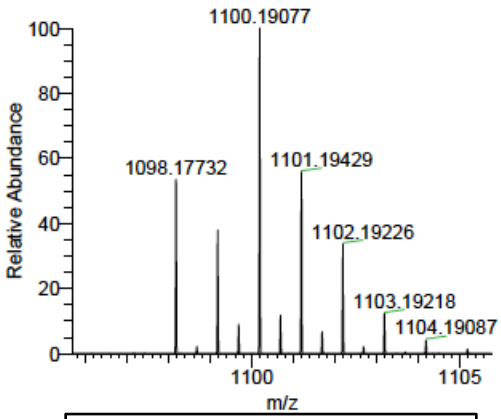

Q Exactive Plus: High Resolution MS1
Theoretical [M+H] = 1098.17546

Z) T8I1

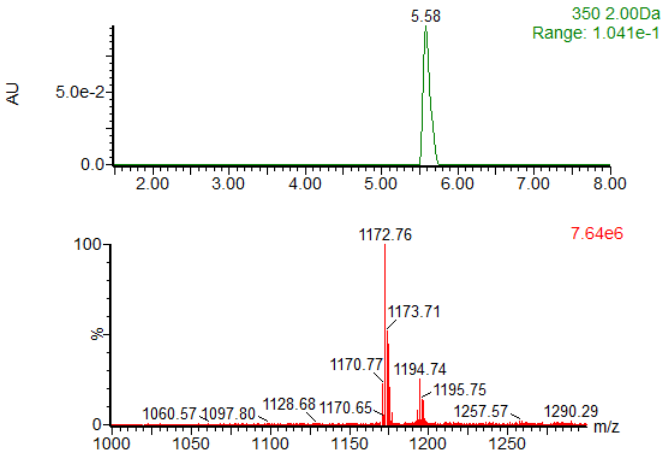

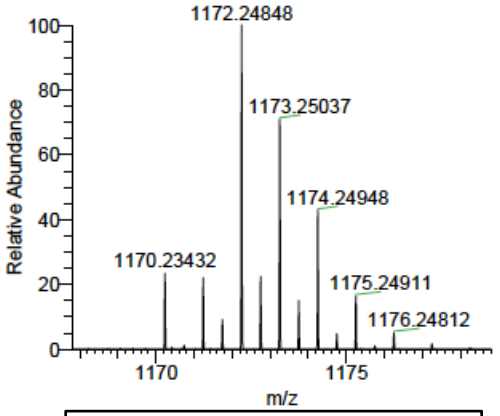

Q Exactive Plus: High Resolution MS1
Theoretical [M+H] = 1170.23297

AA) T8L1

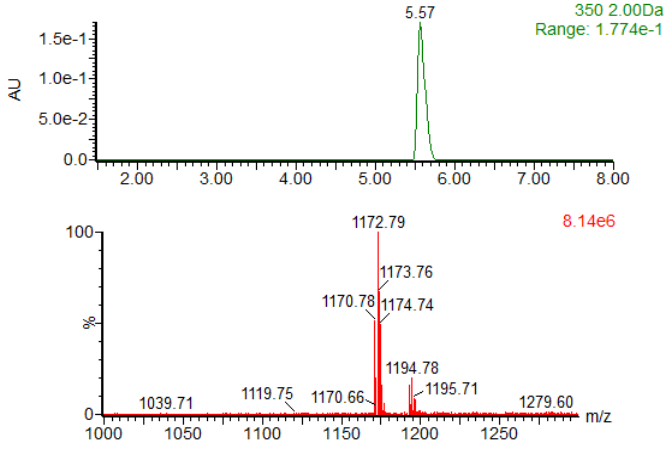

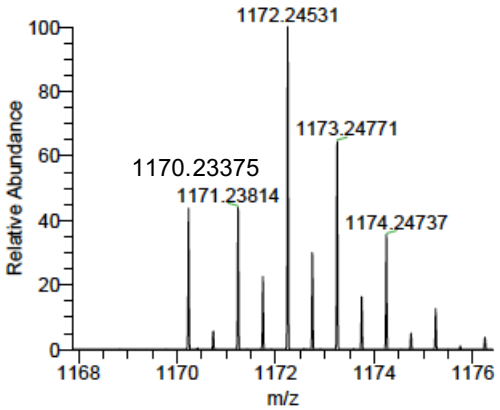

Q Exactive Plus: High Resolution MS1
Theoretical [M+H] = 1170.23297

BB) T8L2

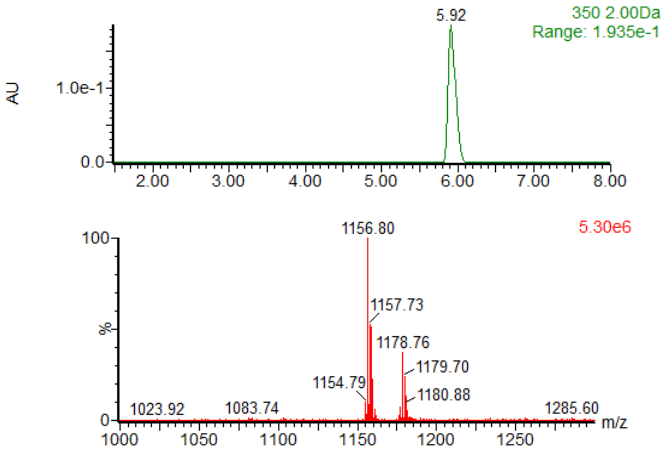

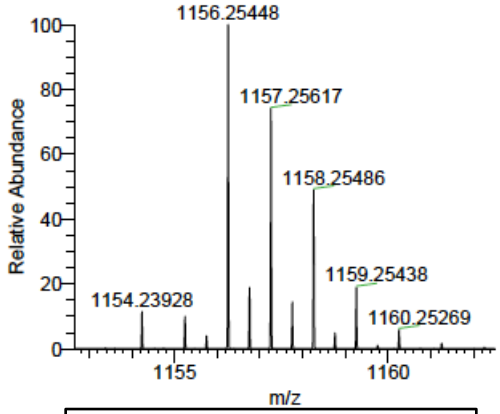

Q Exactive Plus: High Resolution MS1
Theoretical [M+H] = 1156.25371

CC) T8M1

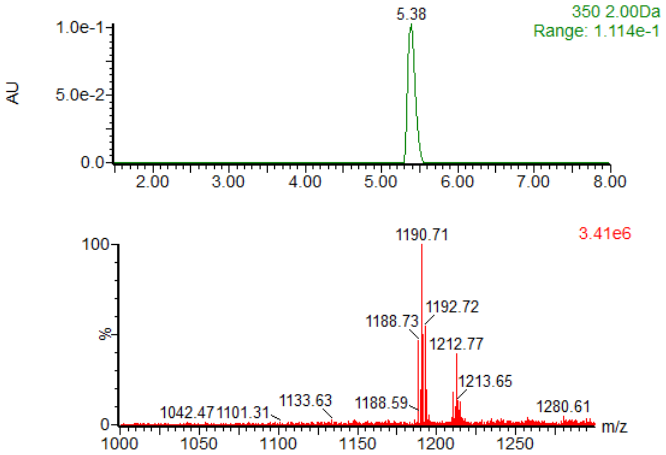

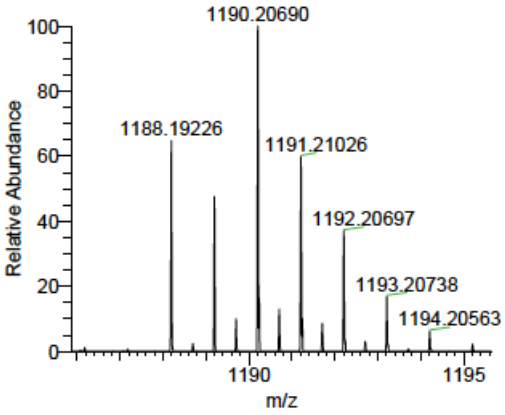

Q Exactive Plus: High Resolution MS1
Theoretical [M+H] = 1188.18939

DD) T8M2

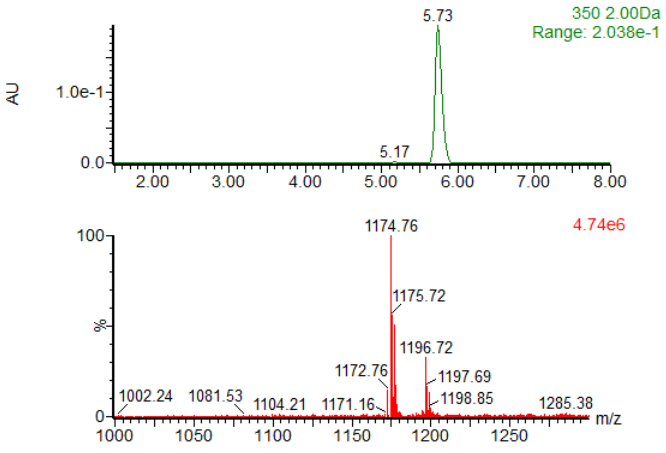

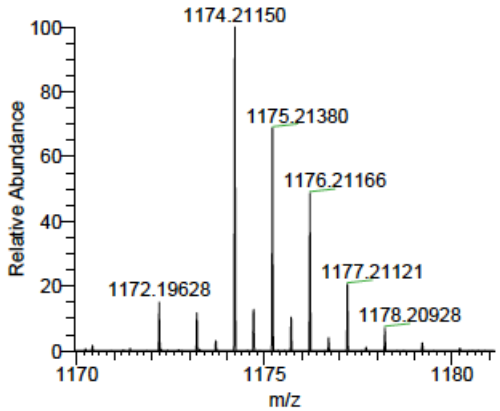

Q Exactive Plus: High Resolution MS1
Theoretical [M+H] = 1174.21013

EE) T8S1

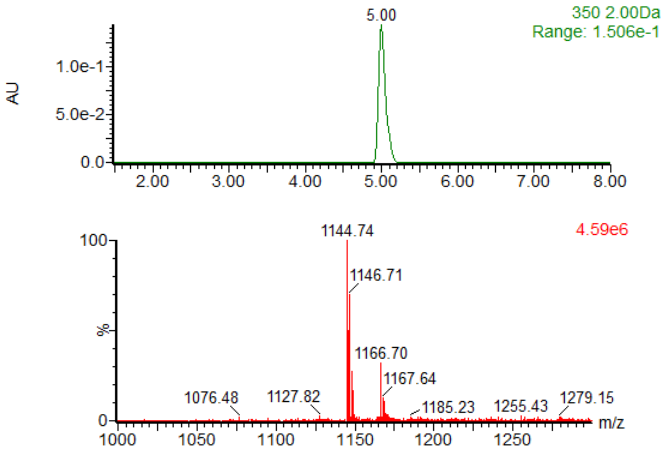

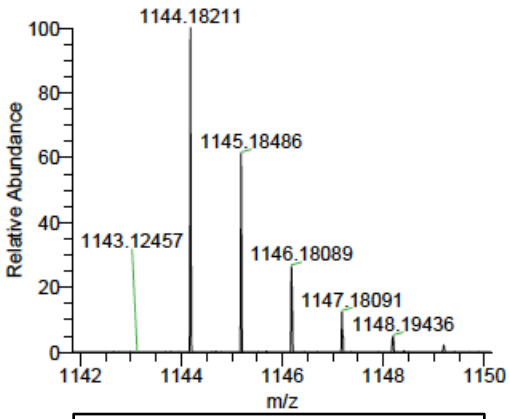

Q Exactive Plus: High Resolution MS1
Theoretical [M+H] = 1144.18094

FF) T8S2

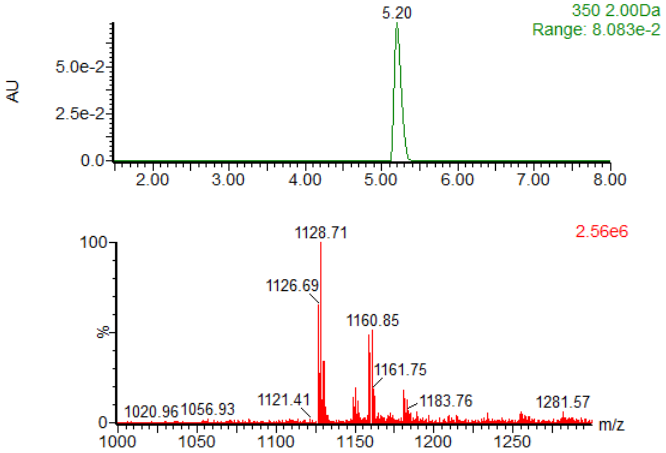

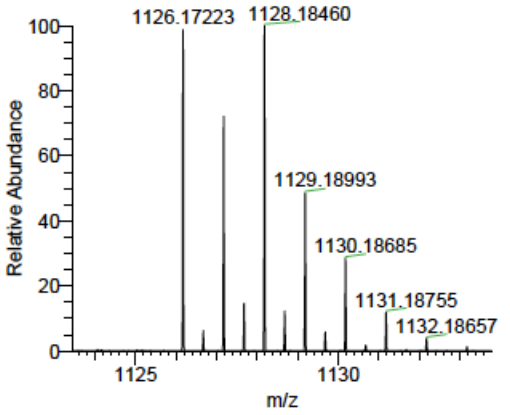

Q Exactive Plus: High Resolution MS1
Theoretical [M+H] = 1126.17037

GG) T8V1

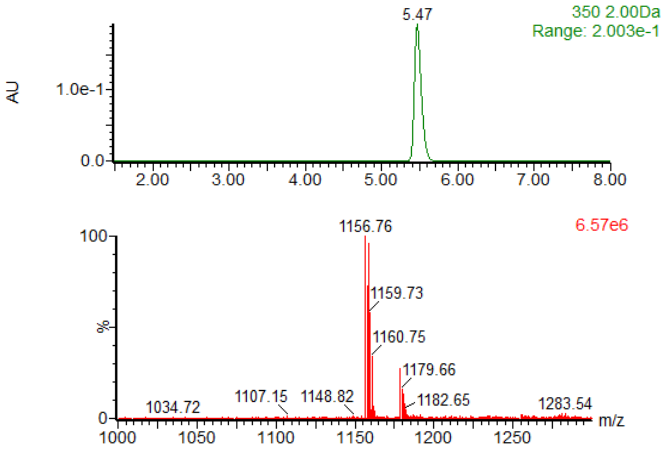

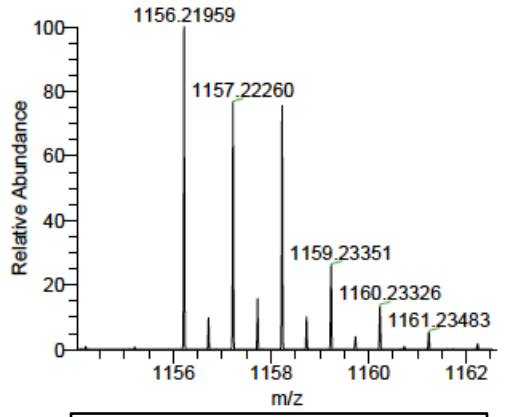

Q Exactive Plus: High Resolution MS1
Theoretical [M+H] = 1156.21732

HH) T8V2

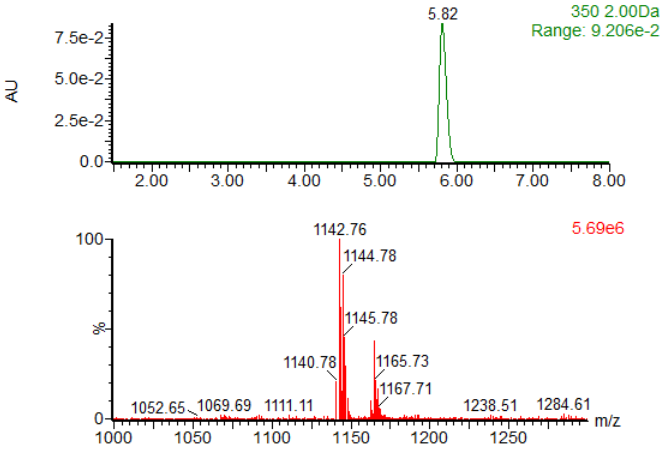

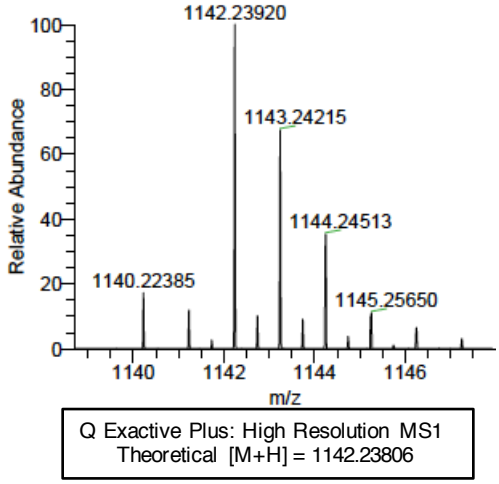

Q Exactive Plus: High Resolution MS1
Theoretical [M+H] = 1142.23806

II) T8Y1

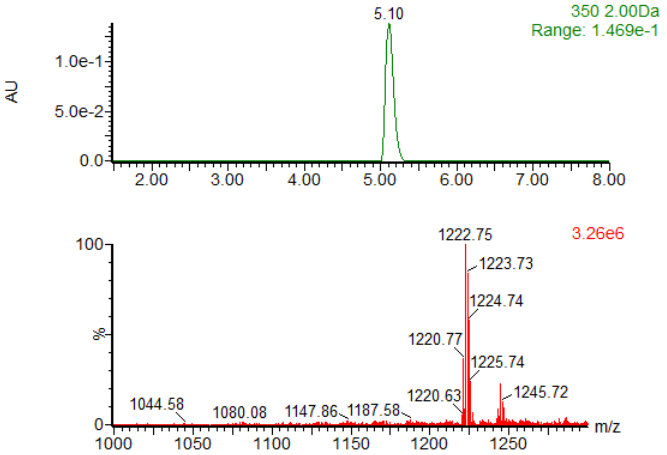

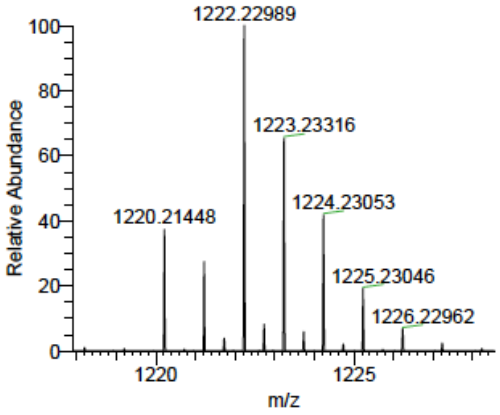

Q Exactive Plus: High Resolution MS1
Theoretical [M+H] = 1220.21224

JJ) T8Y2

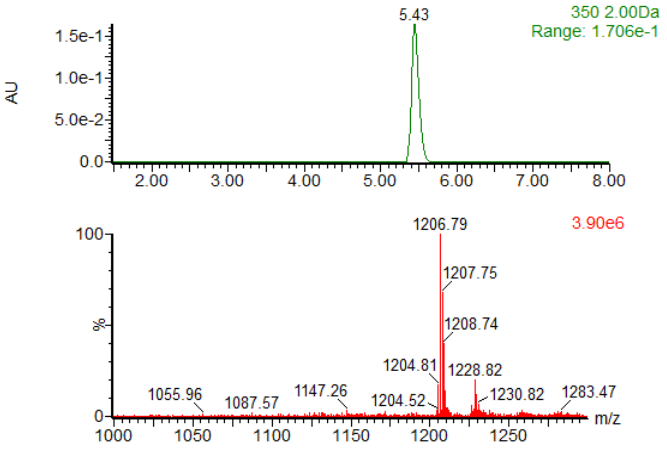

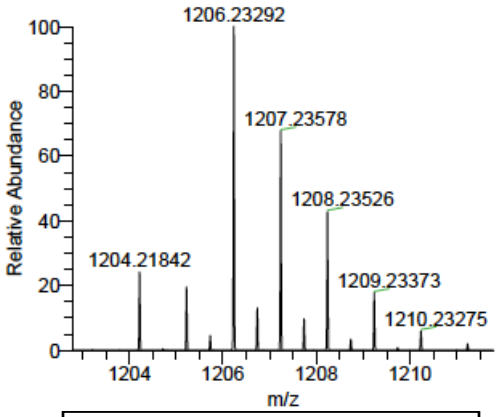

Q Exactive Plus: High Resolution MS1
Theoretical [M+H] = 1206.23297

KK) V6A-T8I1

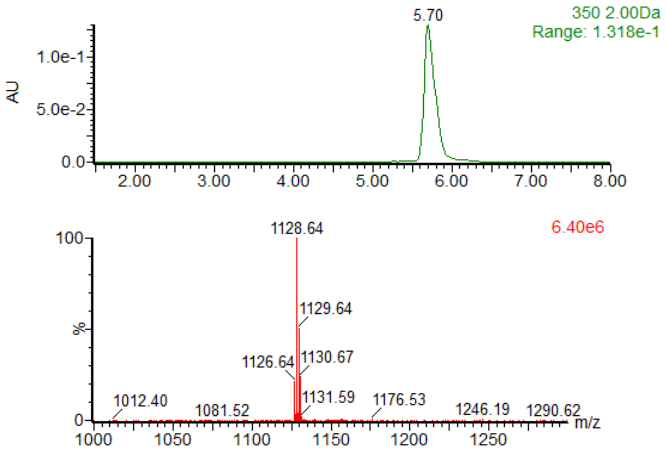

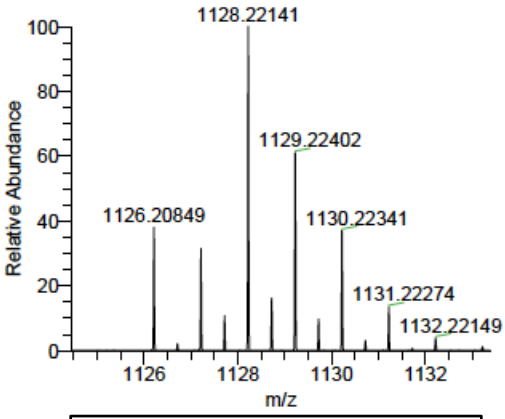

Q Exactive Plus: High Resolution MS1
Theoretical [M+H] = 1126.20676

LL) V6A-T8V1

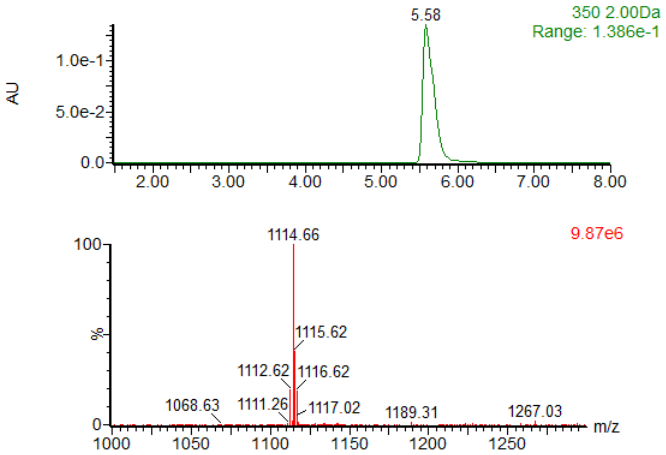

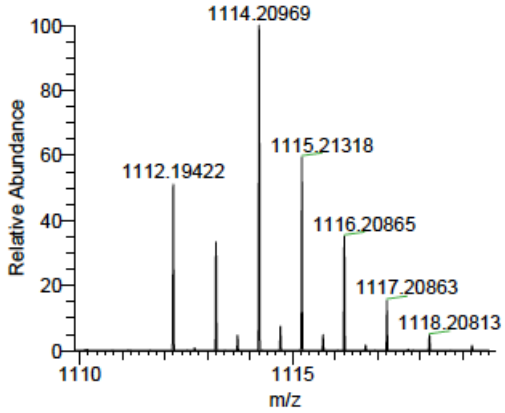

Q Exactive Plus: High Resolution MS1
Theoretical [M+H] = 1112.19111

MM) V6A-T8Y1

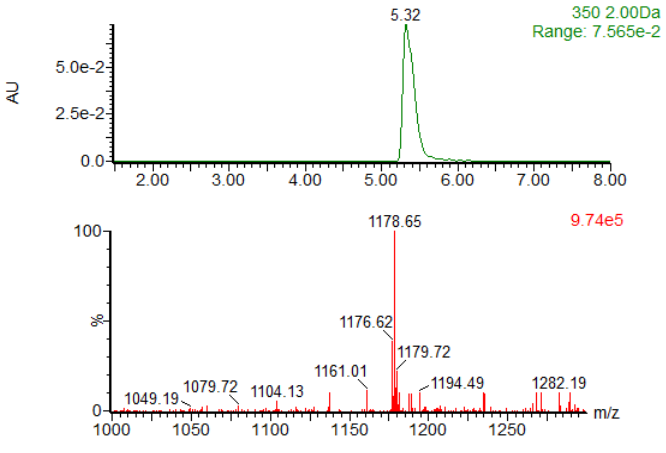

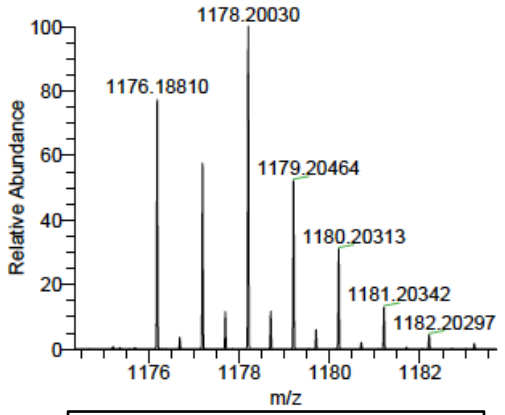

Q Exactive Plus: High Resolution MS1
Theoretical [M+H] = 1176.18602

NN) V6M-T8I1

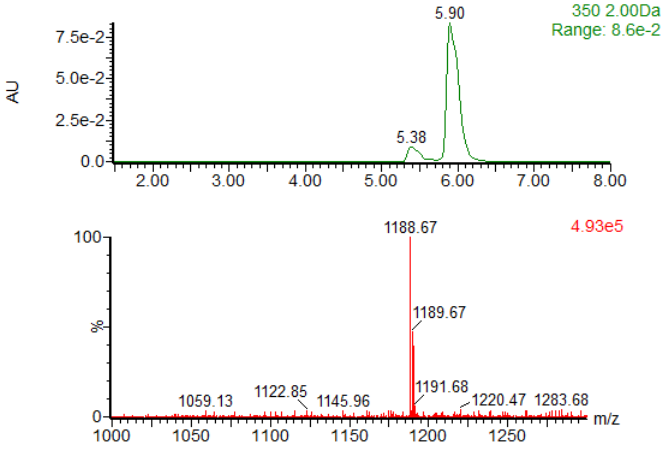

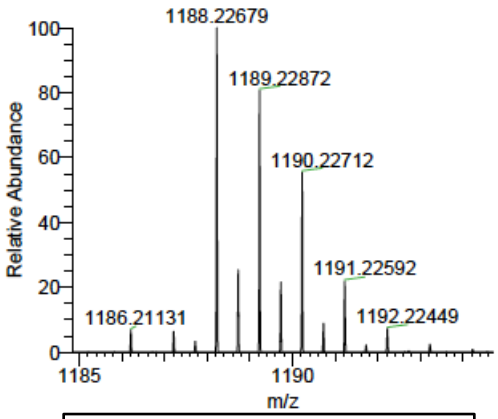

Q Exactive Plus: High Resolution MS1
Theoretical [M+H] = 1188.22578

OO) V6M-T8V1

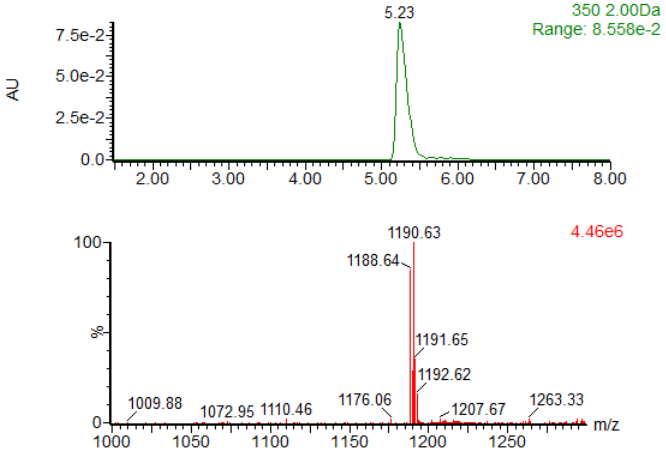

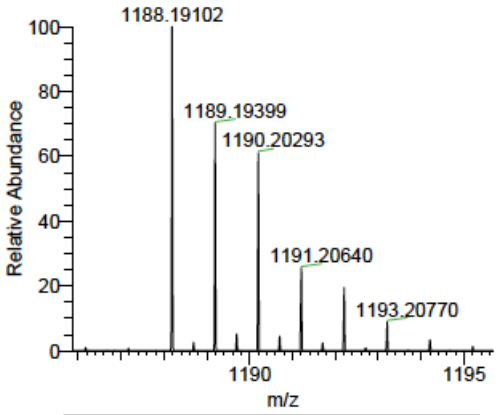

Q Exactive Plus: High Resolution MS1
Theoretical [M+H] = 1188.18939

PP) V6M-T8V2

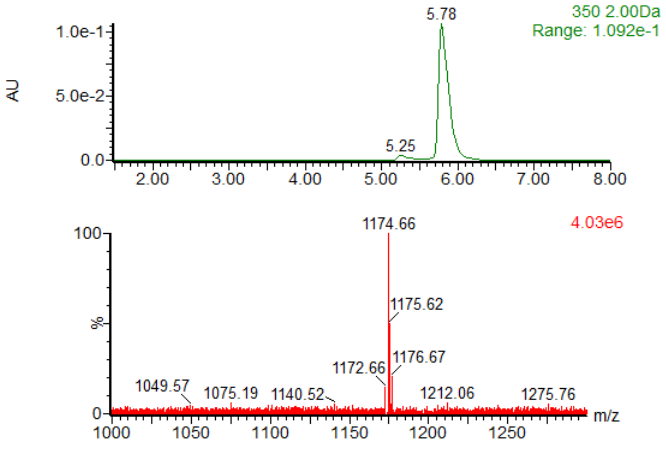

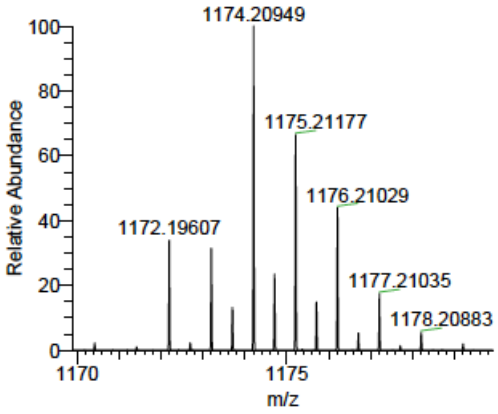

Q Exactive Plus: High Resolution MS1
Theoretical [M+H] = 1172.19448

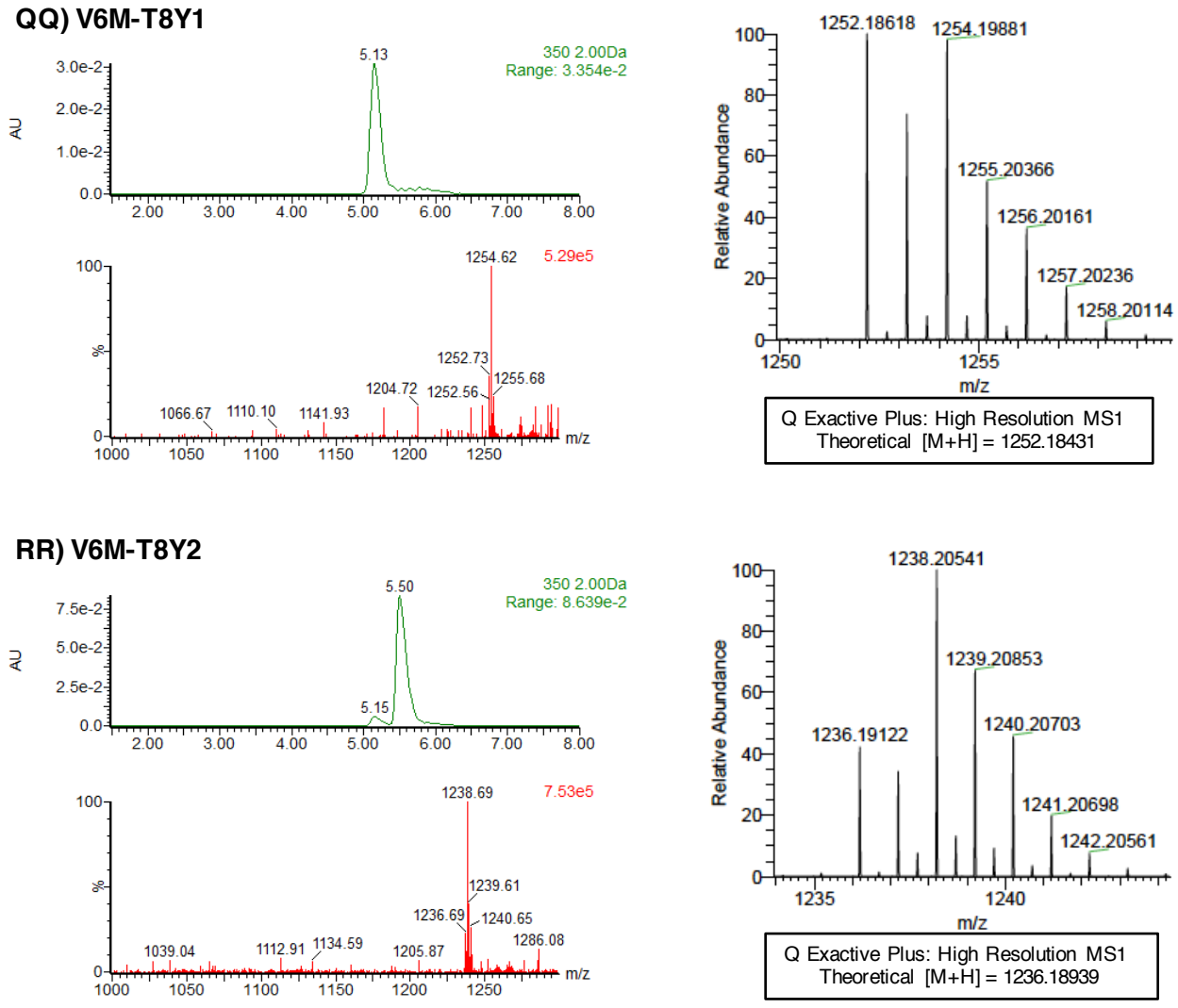

Figure 1-S3: **LC/MS and HRMS of all analogs in this study. A-RR)** Left panel: LC (green) and MS (red) data for each analogue in this study. Right panel: High Resolution MS1 data and theoretical [M+H].

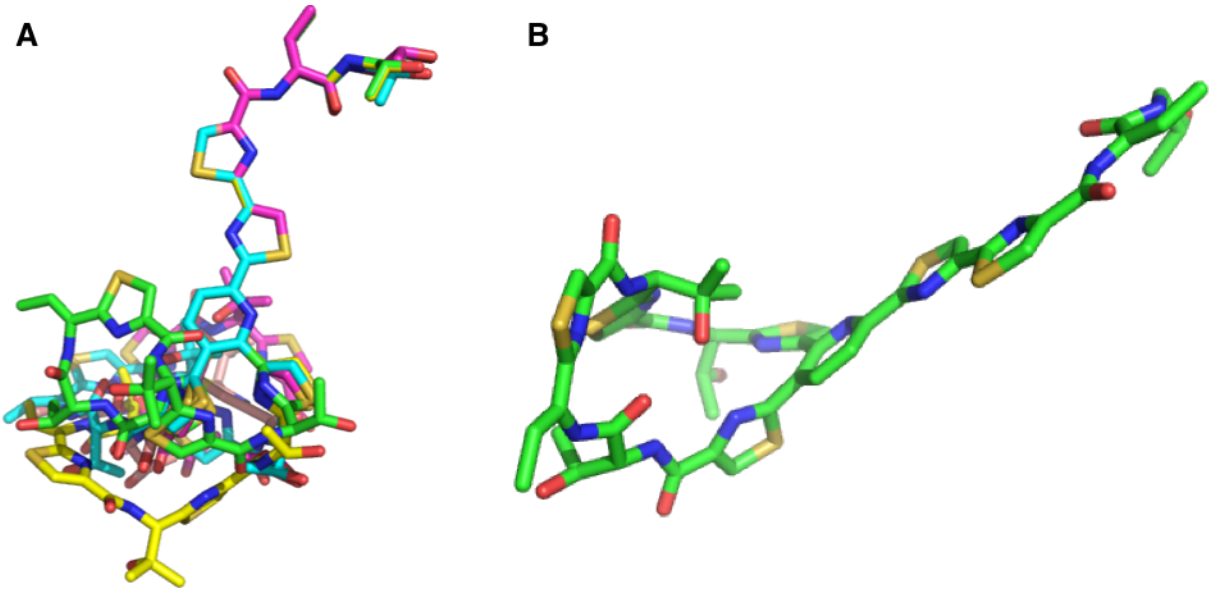

Figure 1-S4: 3D NMR structure of WT thiocillin. A) Ensemble of conformations as modeled by BRIKARD with NMR restraints. **B)** Structure of WT_1, the predominant 3D NMR solution structure (37% occupancy).

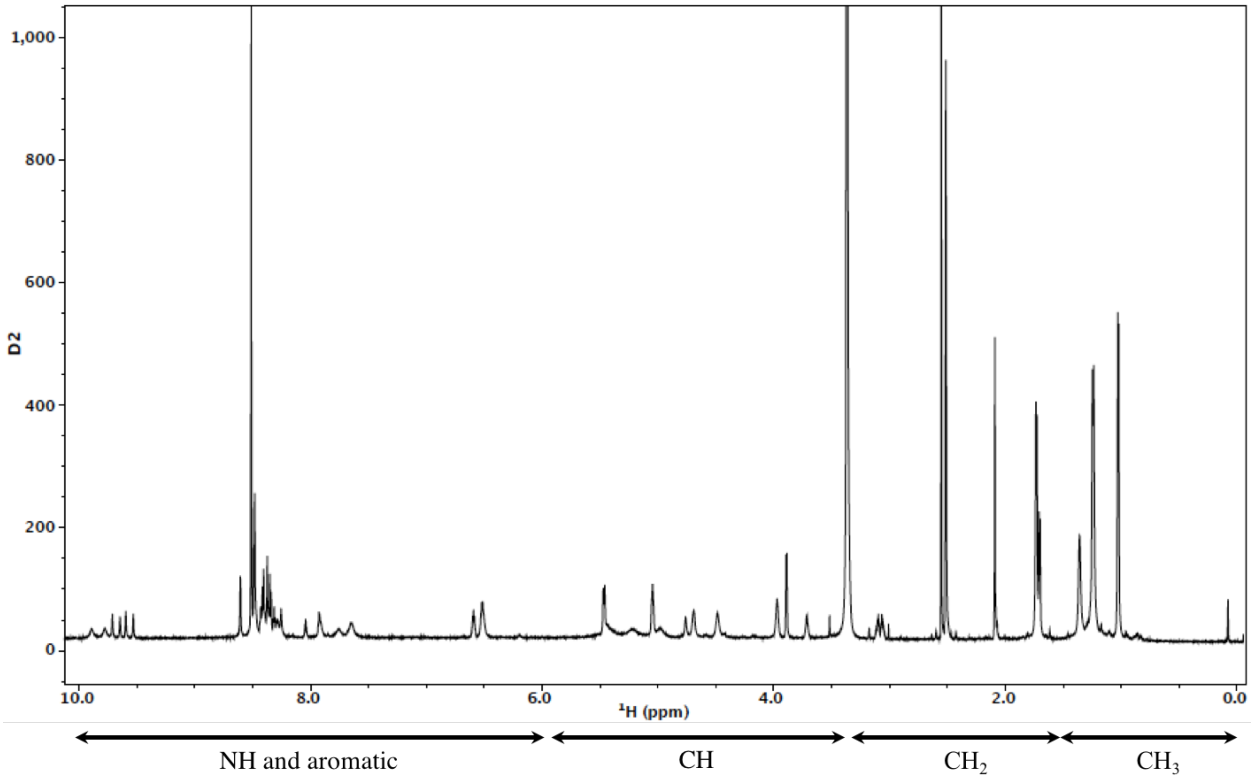

Figure 1-S5: **1D ^{1}H NMR spectrum of [^{15}N] WT Thiocillin YM-266183.**

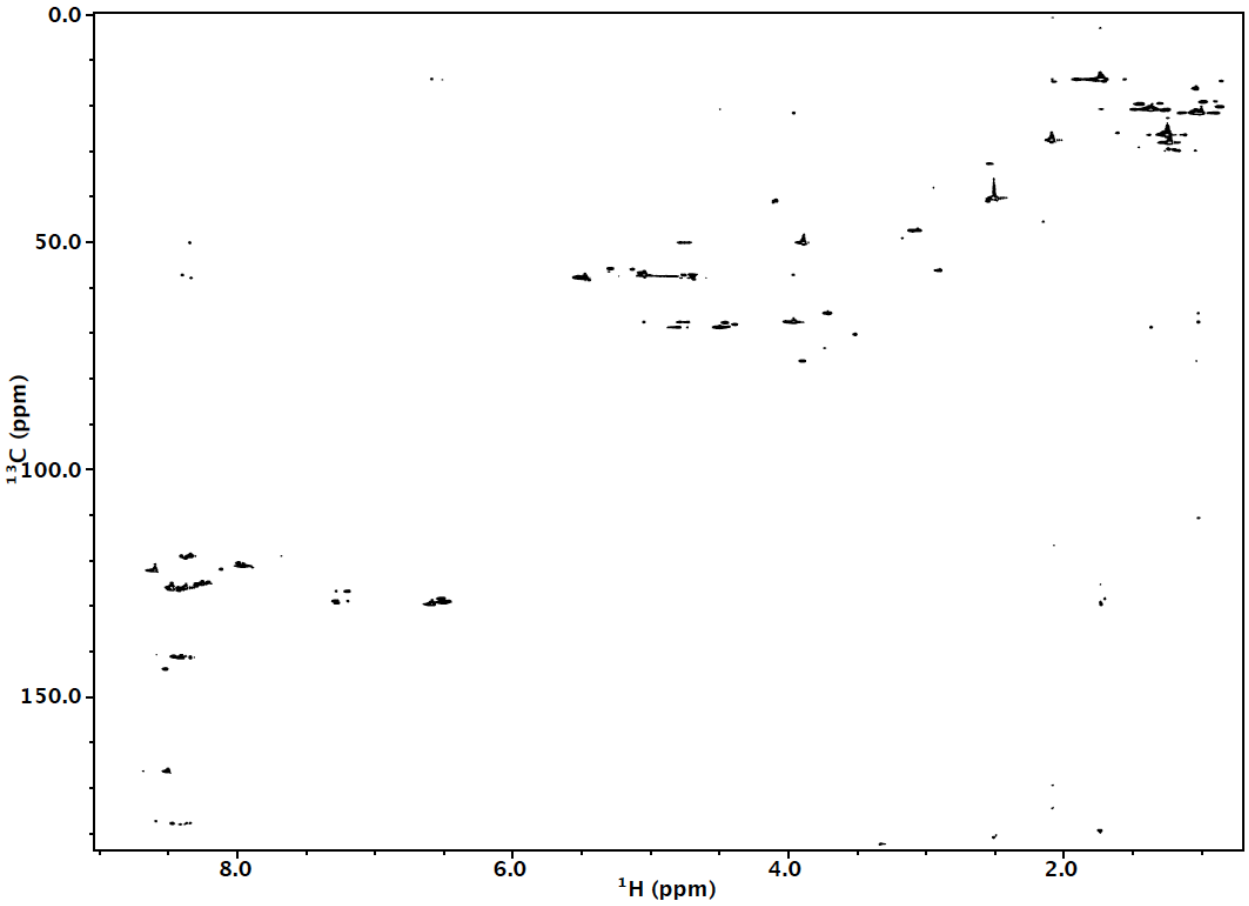

Figure 1-S6: **2D ^{1}H-^{13}C HSQC of WT Thiocillin YM-266183.**

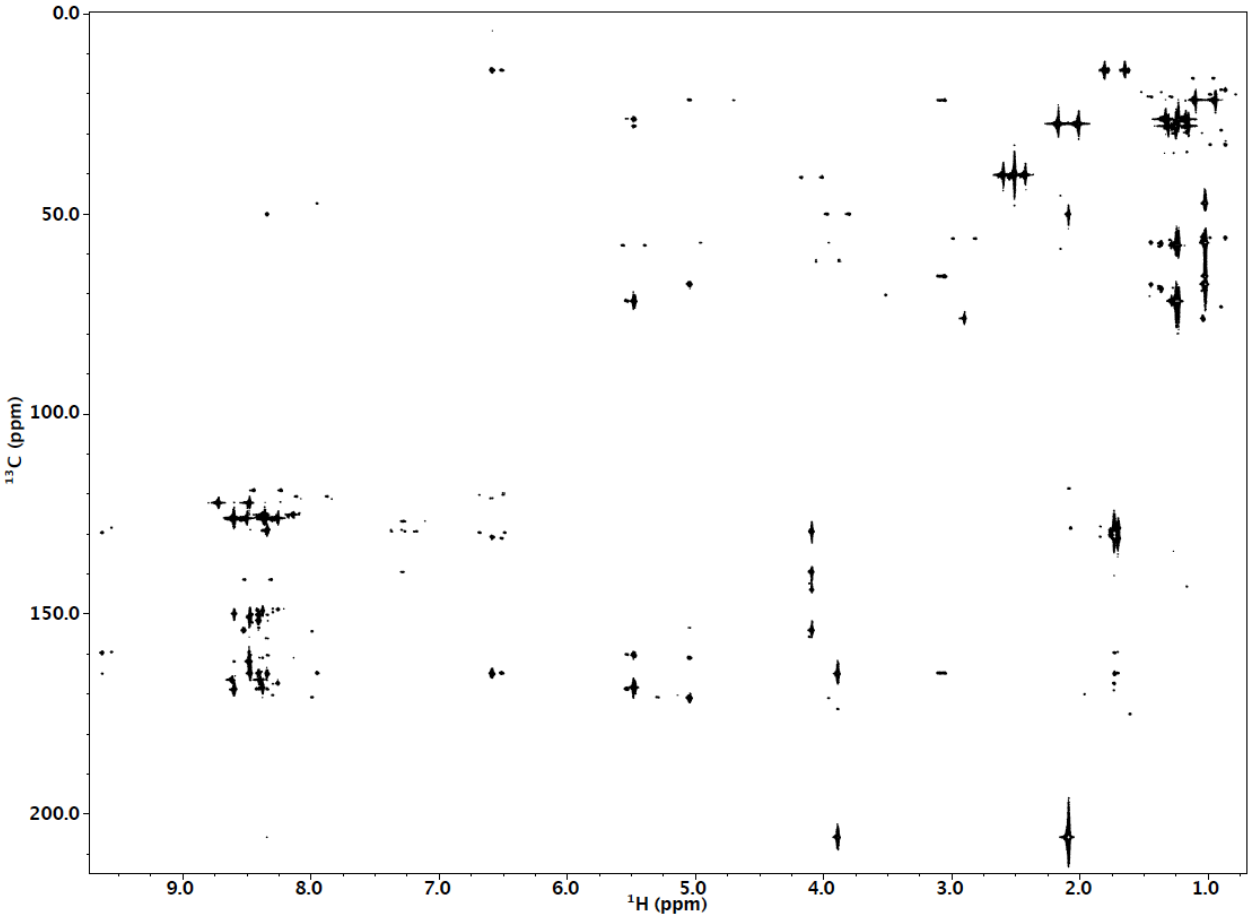

Figure 1-S7: **2D ^{1}H-^{13}C HMBC of WT Thiocillin YM-266183**.

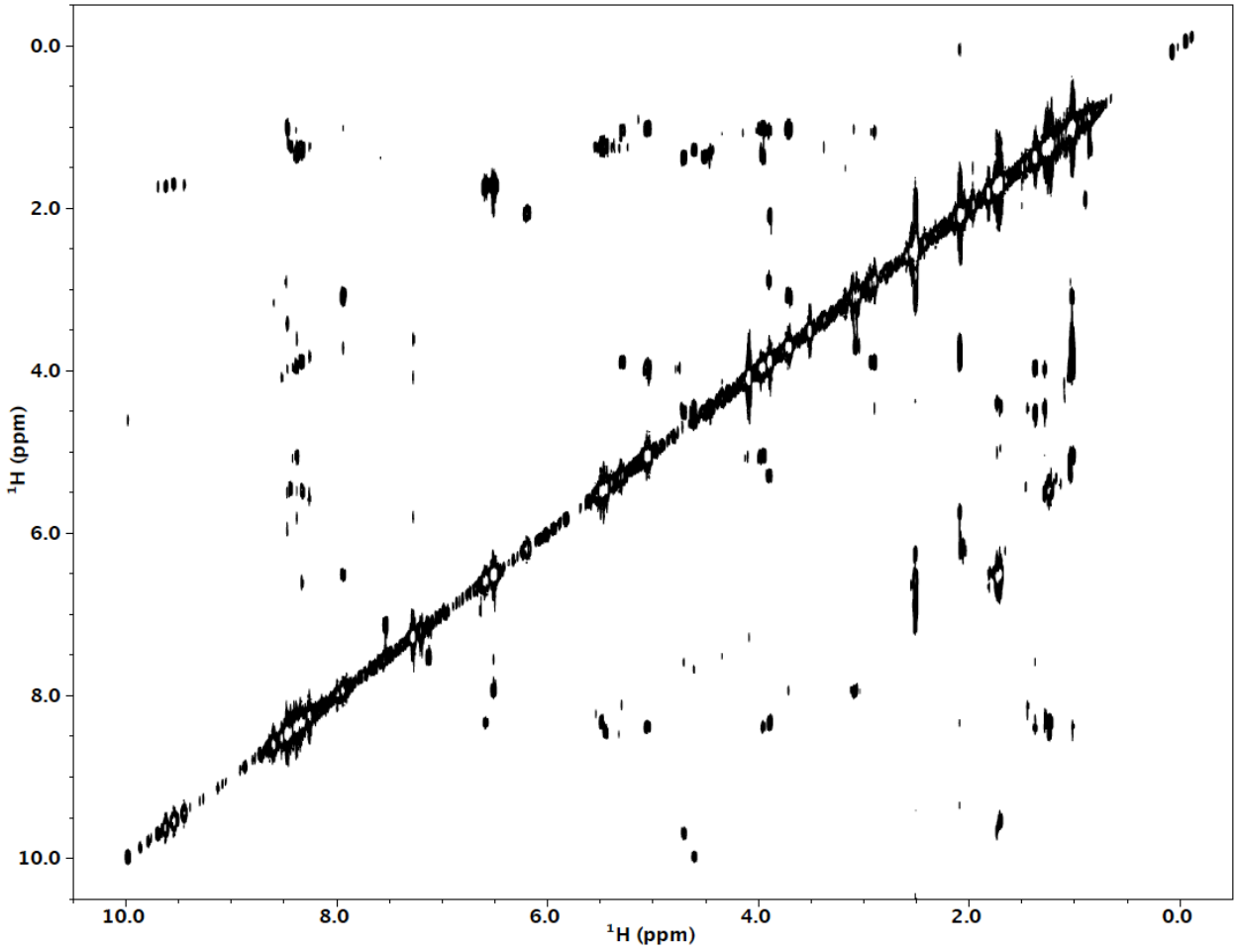

Figure 1-S8: **2D ^{1}H-^{1}H ROESY spectra of WT Thiocillin YM-266183 with a 300ms mixing time.**

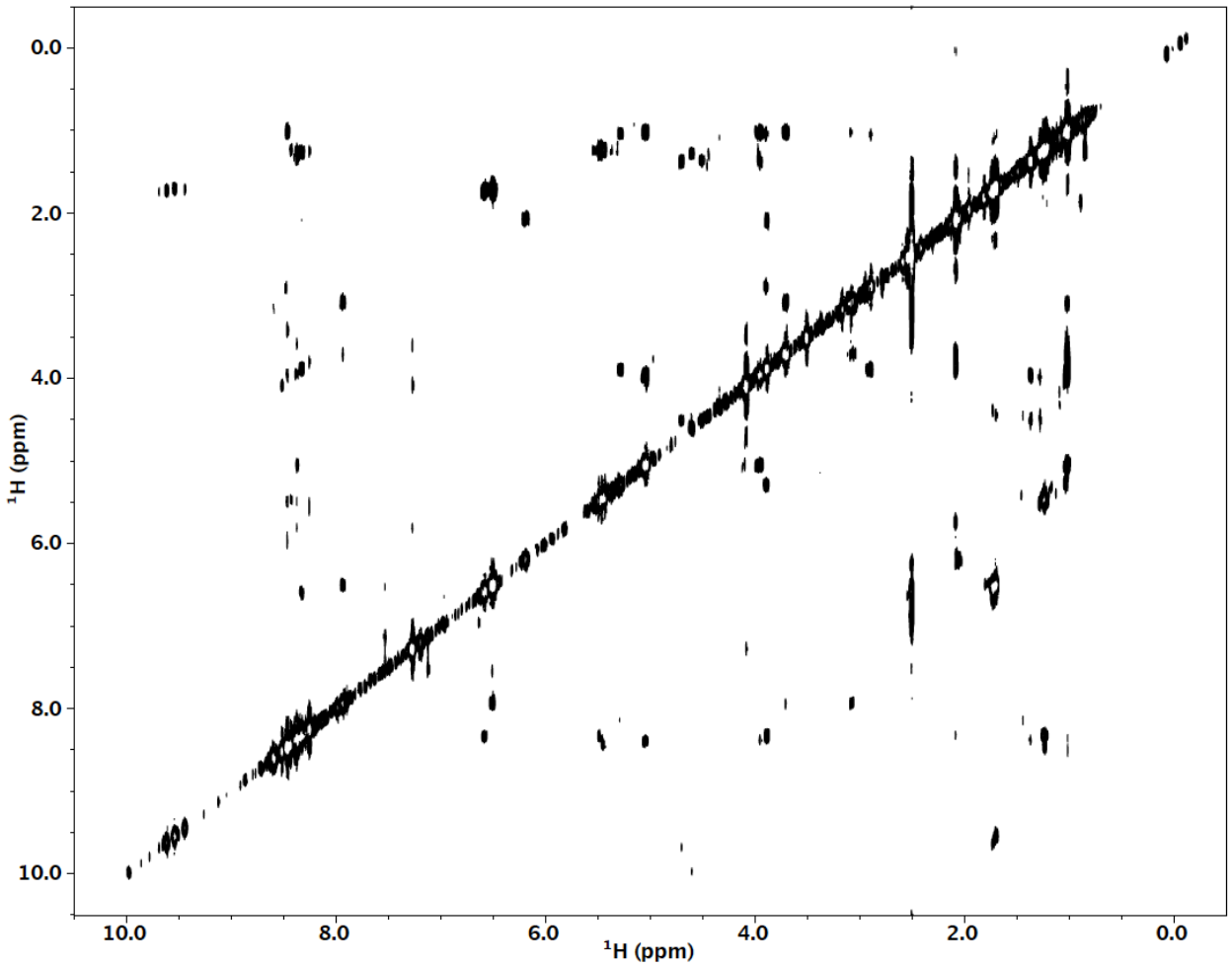

Figure 1-S9: **2D ^{1}H-^{1}H ROESY spectra of WT Thiocillin YM-266183 with a 500ms mixing time.**

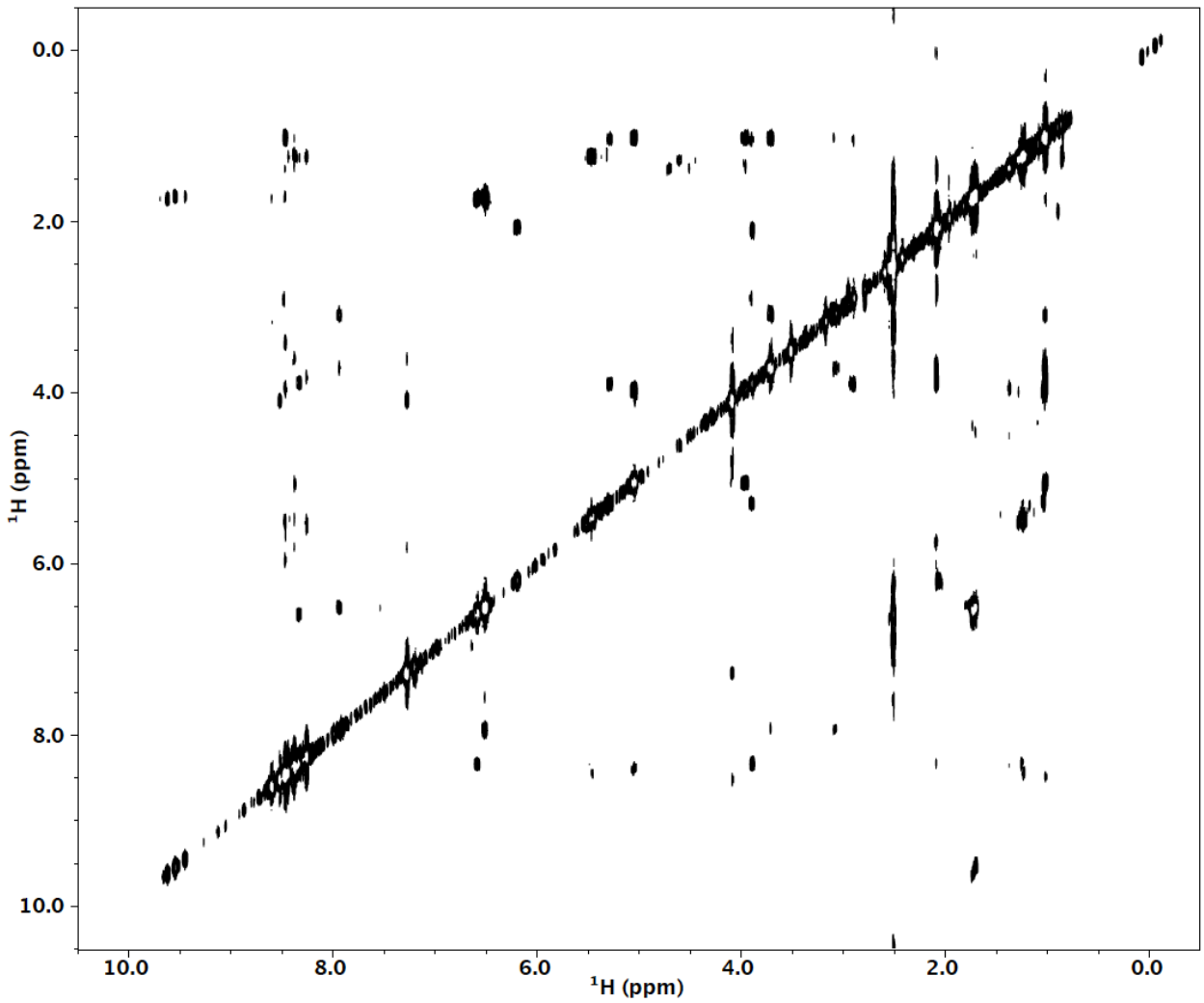

Figure 1-S10: **2D ^{1}H-^{1}H ROESY spectra of WT Thiocillin YM-266183 with an 800ms mixing time**.

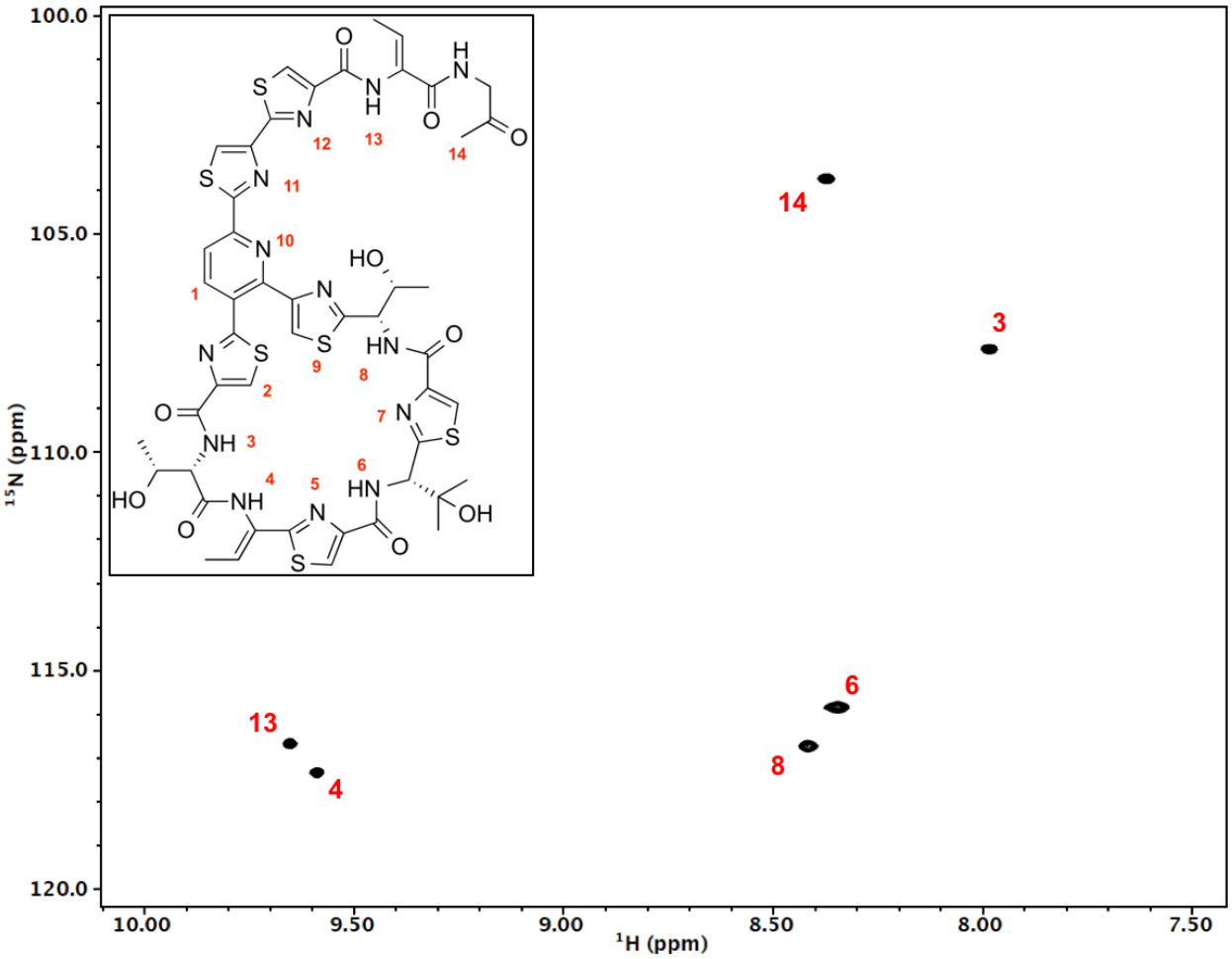

Figure 1-S11: 2D ^{1}H-^{15}N HSQC of ^{15}N WT Thiocillin YM-266183.

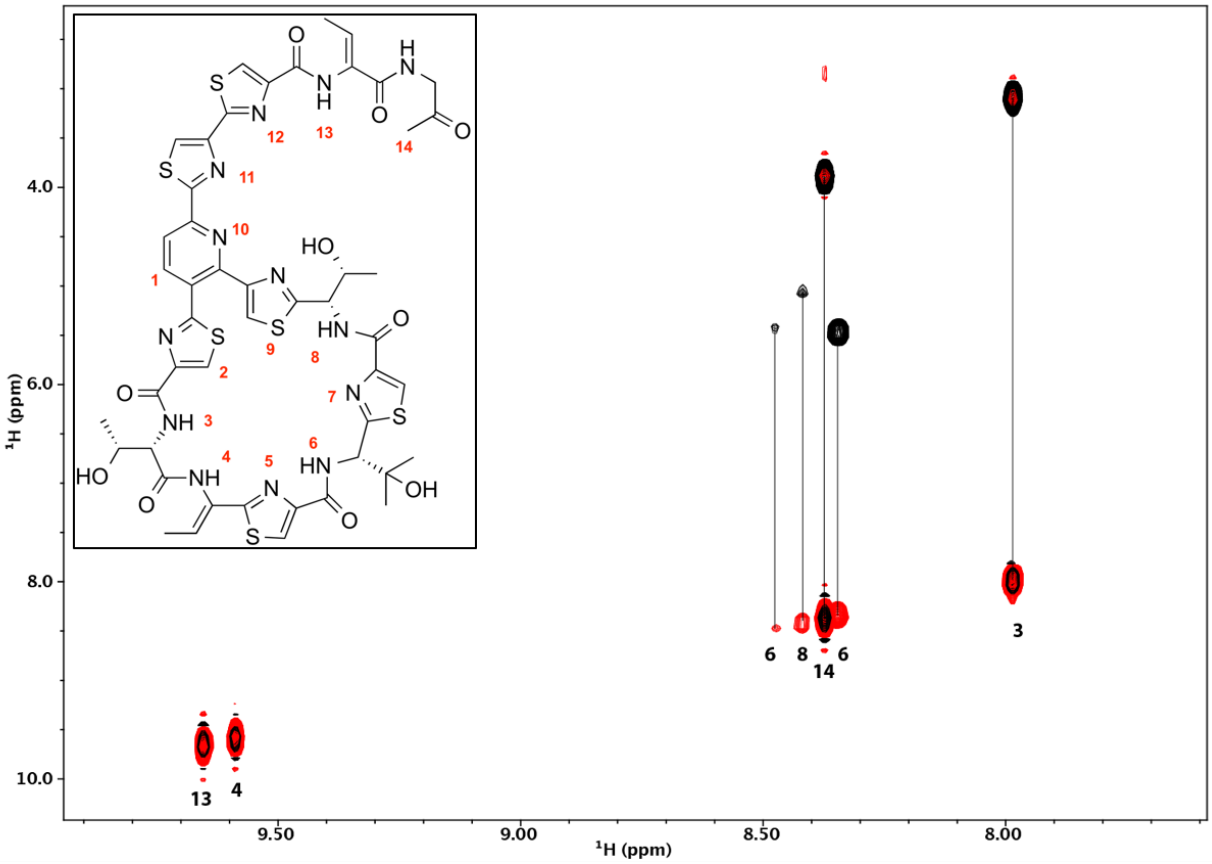

Figure 1-S12: **3D HNHA of [^{15}N] WT Thiocillin YM-266183.** Shown in 2D collapsed along the ^{15}N-axis.

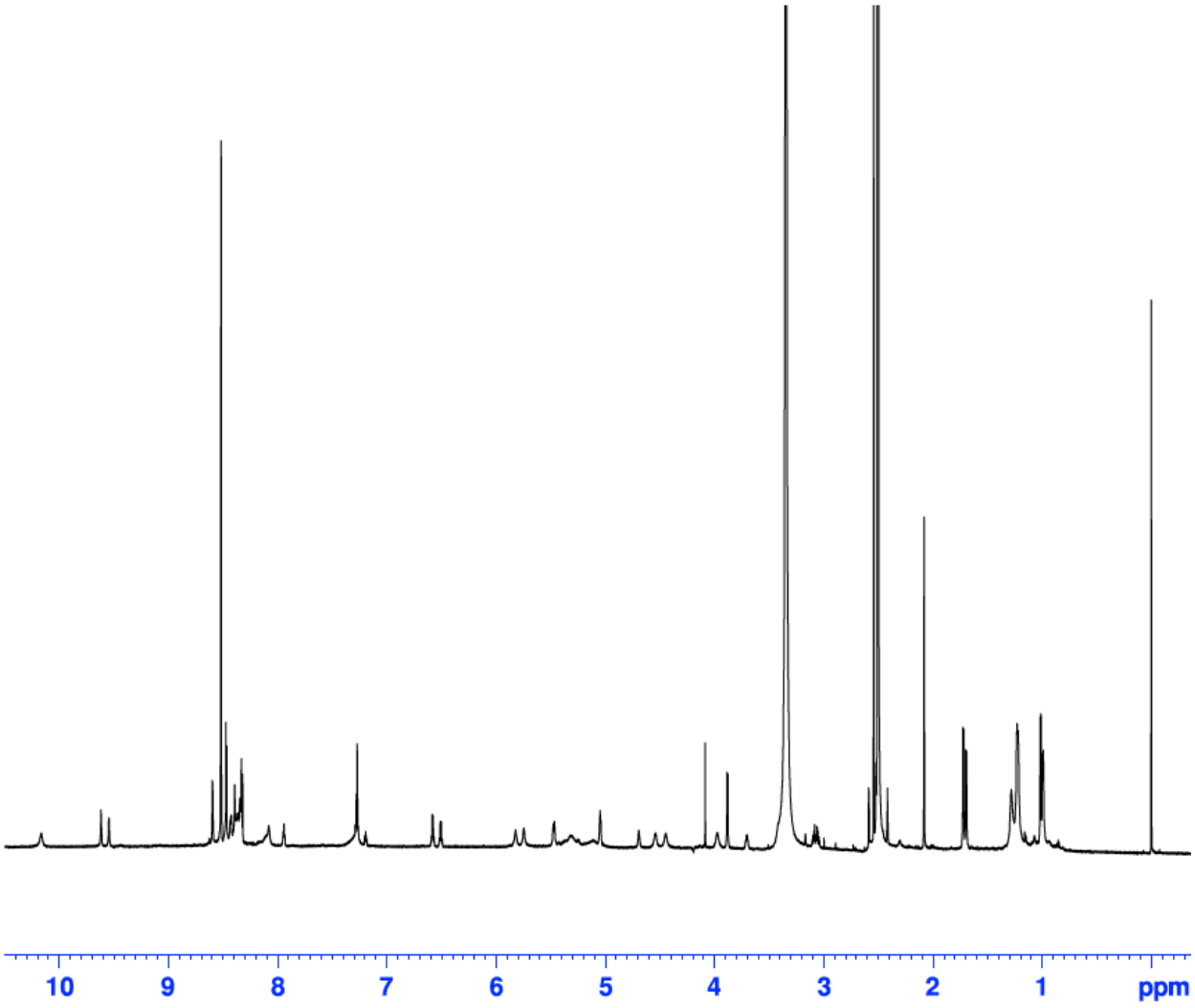

Figure 1-S13: **1D ^{1}H NMR of T4S1**.

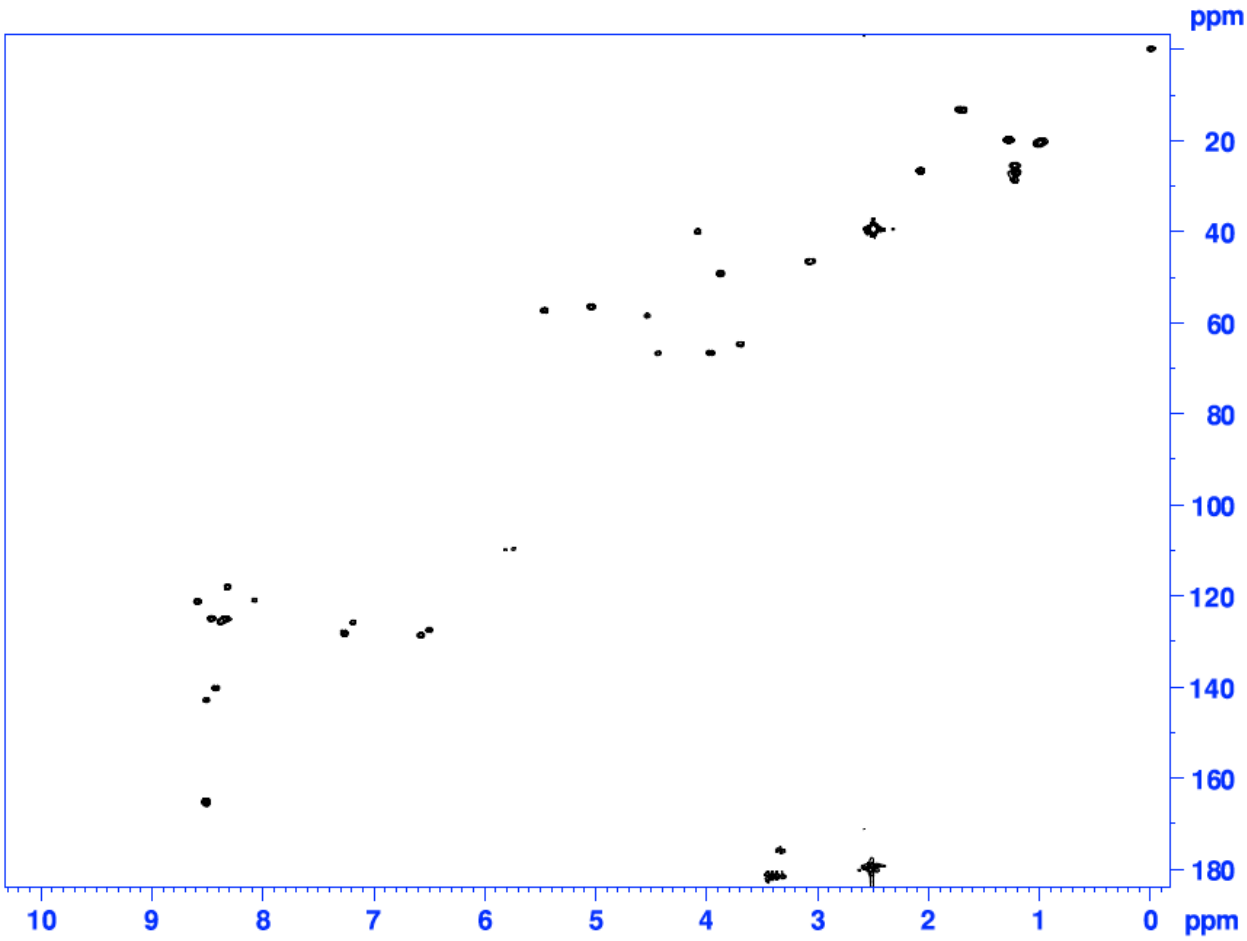

Figure 1-S14: 2D ^{1}H-^{13}C HSQC of T4S1.

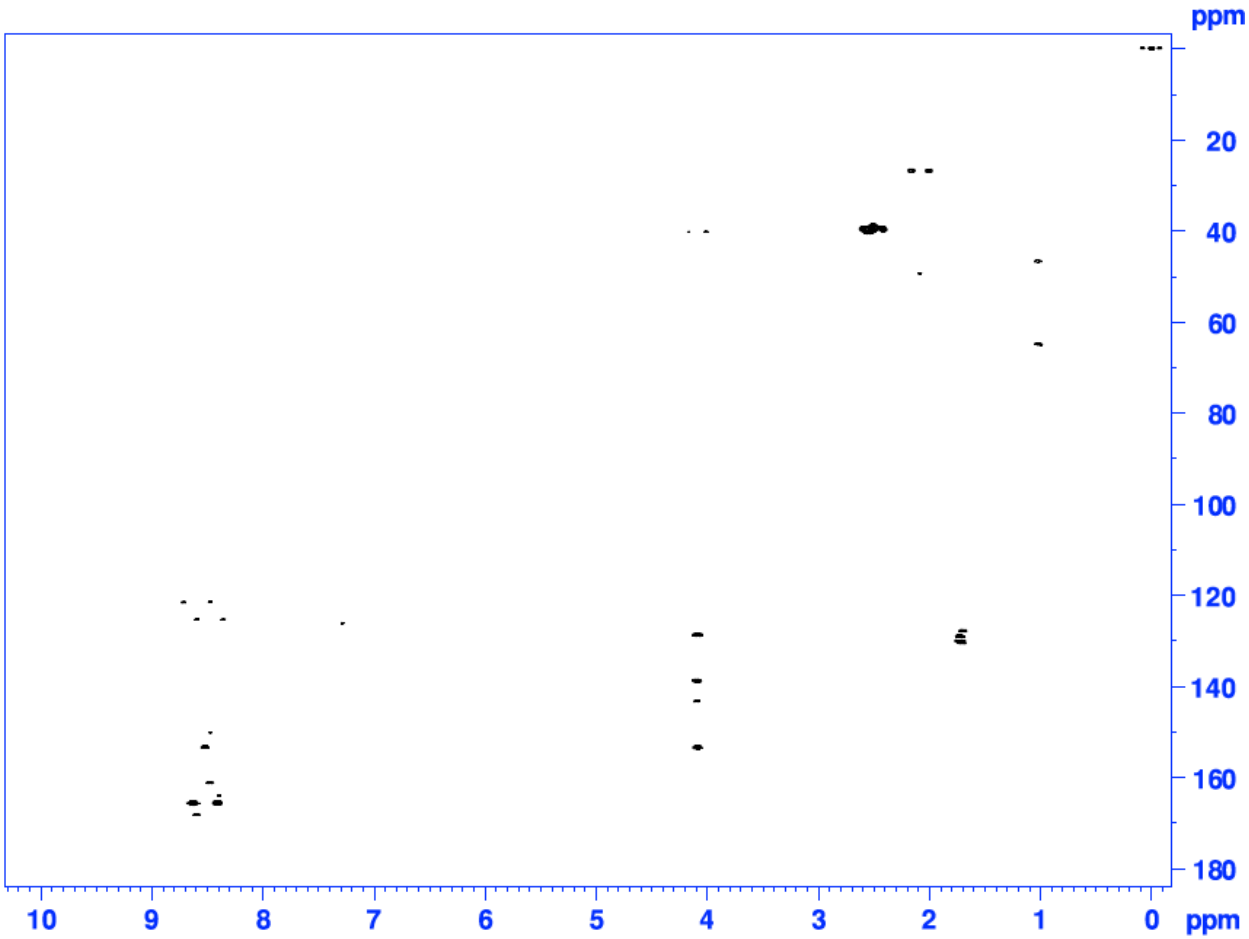

Figure 1-S15: 2D ^{1}H-^{13}C HMBC of T4S1.

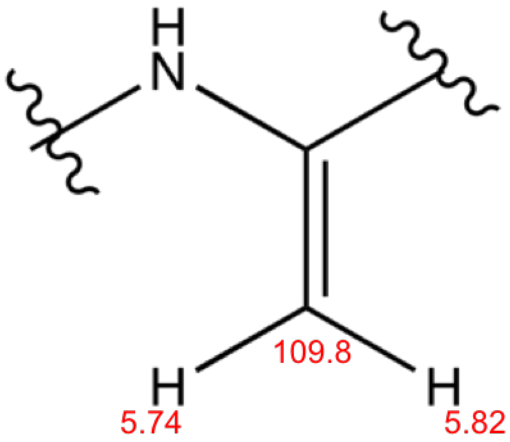

Figure 1-S16: Observed ^{1}H and ^{13}C chemical shifts for the dehydroalanine at residue 4.

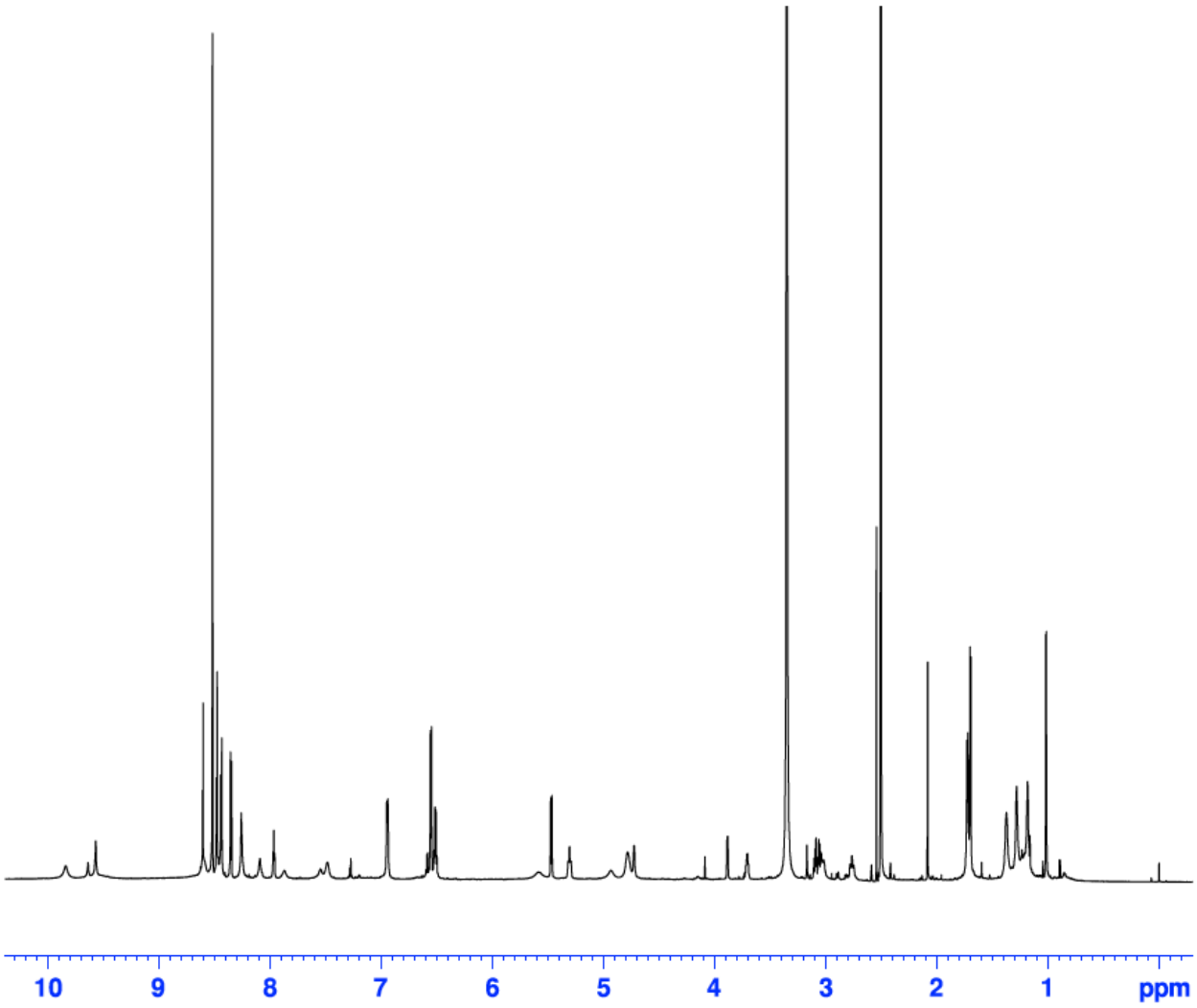

Figure 1-S17: **1D ^{1}H NMR of T8Y1**.

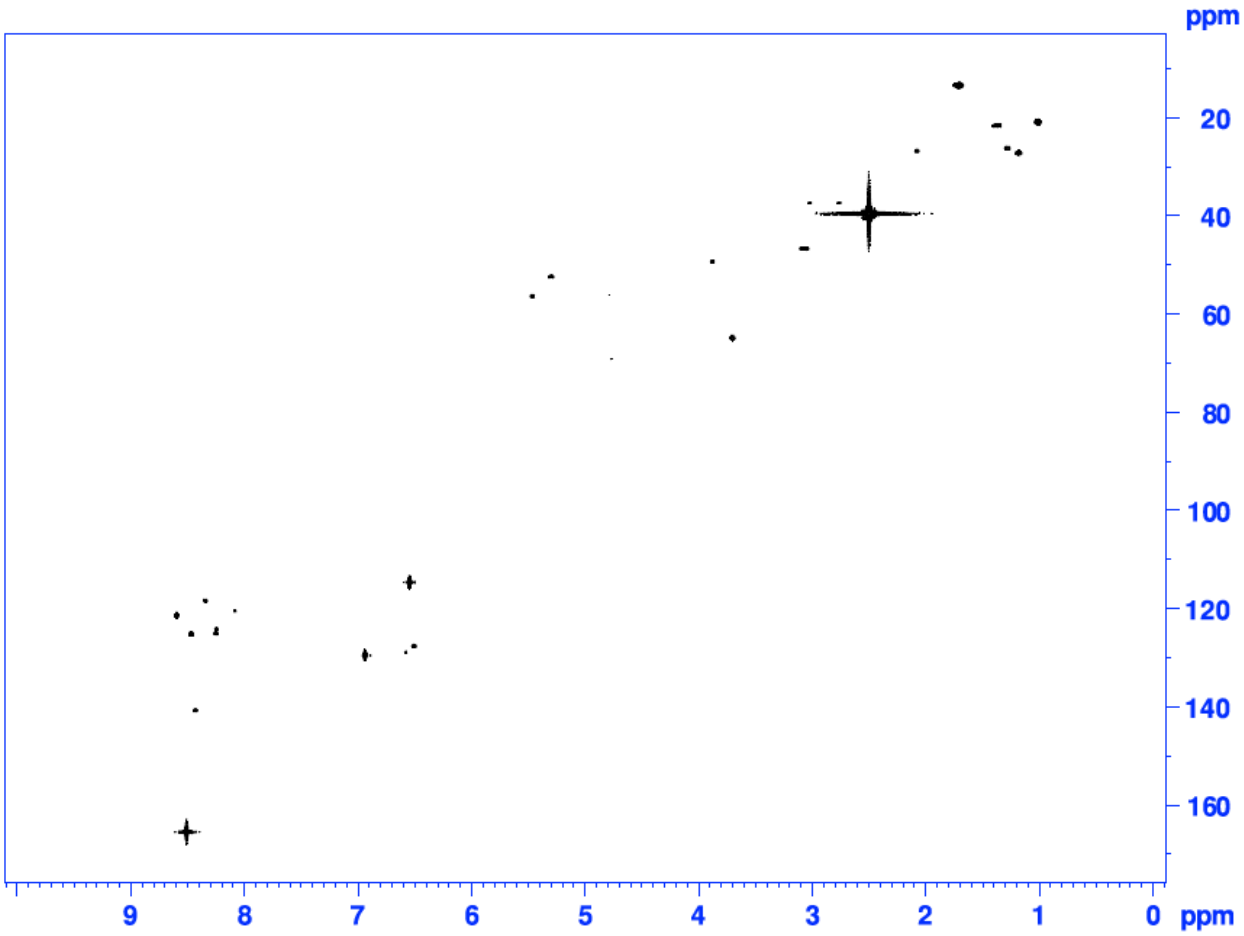

Figure 1-S18: **2D ^{1}H-^{13}C HSQC of T8Y1**.

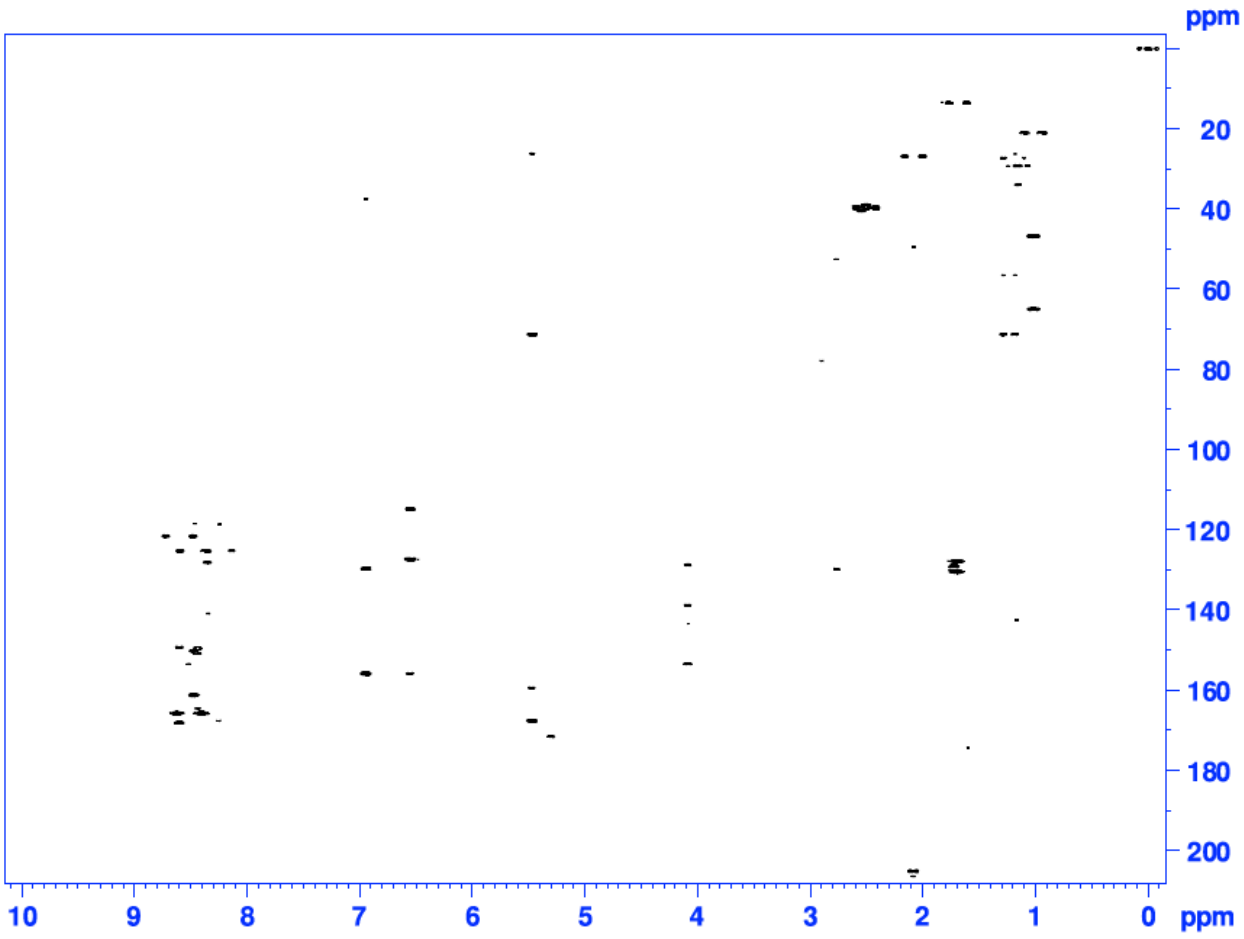

Figure 1-S19: **2D ^{1}H-^{13}C HMBC of T8Y1**.

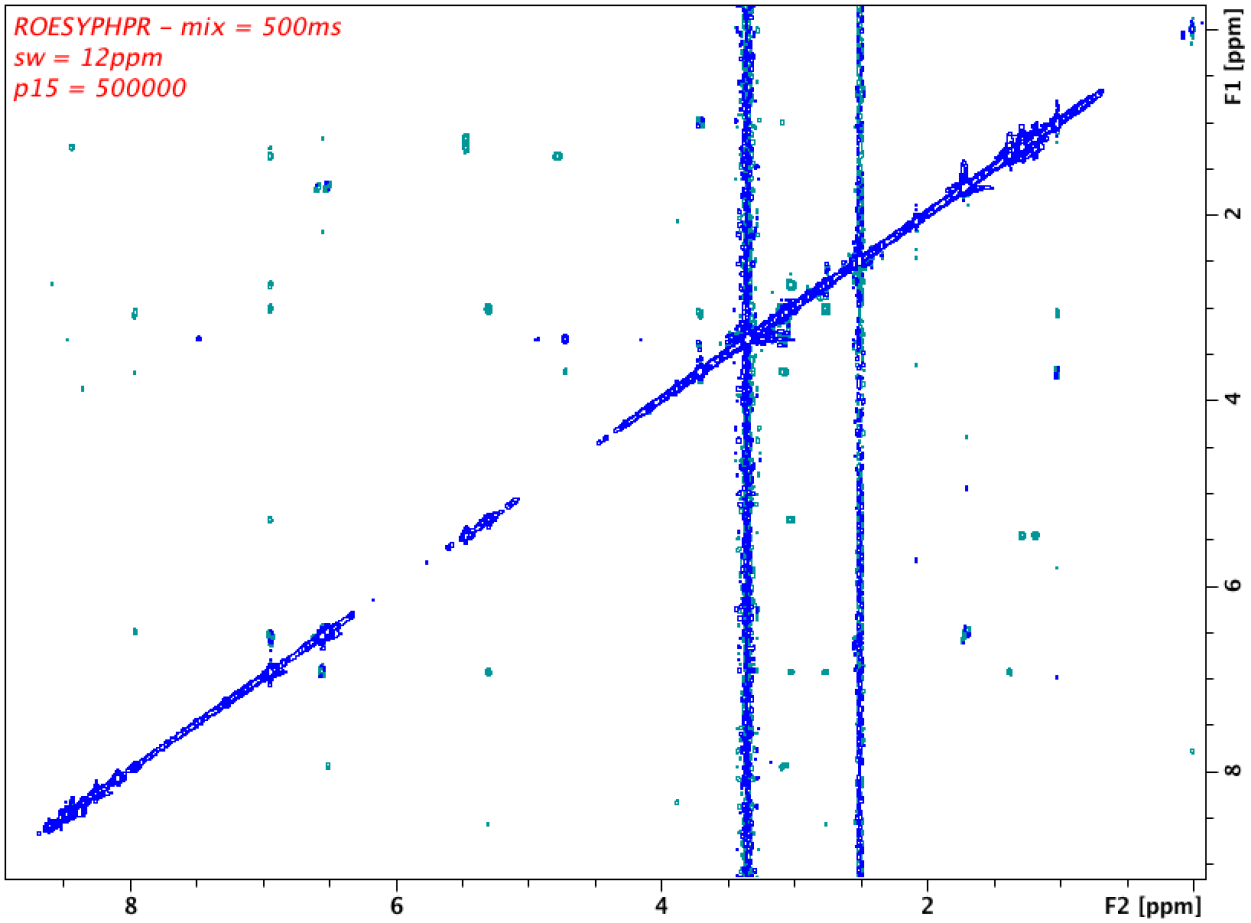

Figure 1-S20: 2D ^{1}H-^{1}H ROESY spectra of T8Y1 with a 500ms mixing time.

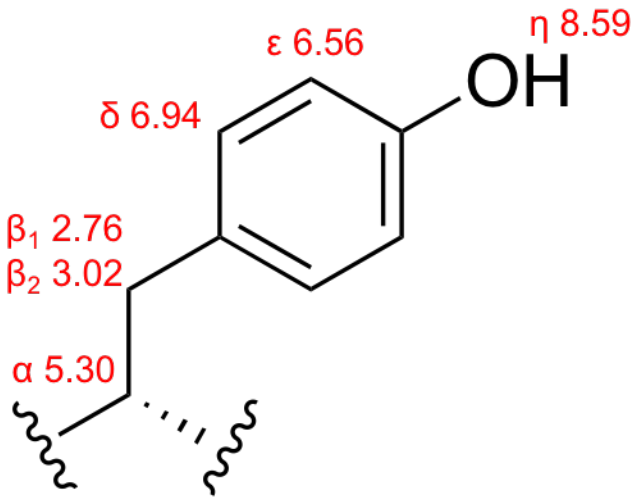

Figure 1-S21: **Proton chemical shift assignments for tyrosine residue in T8Y1**.

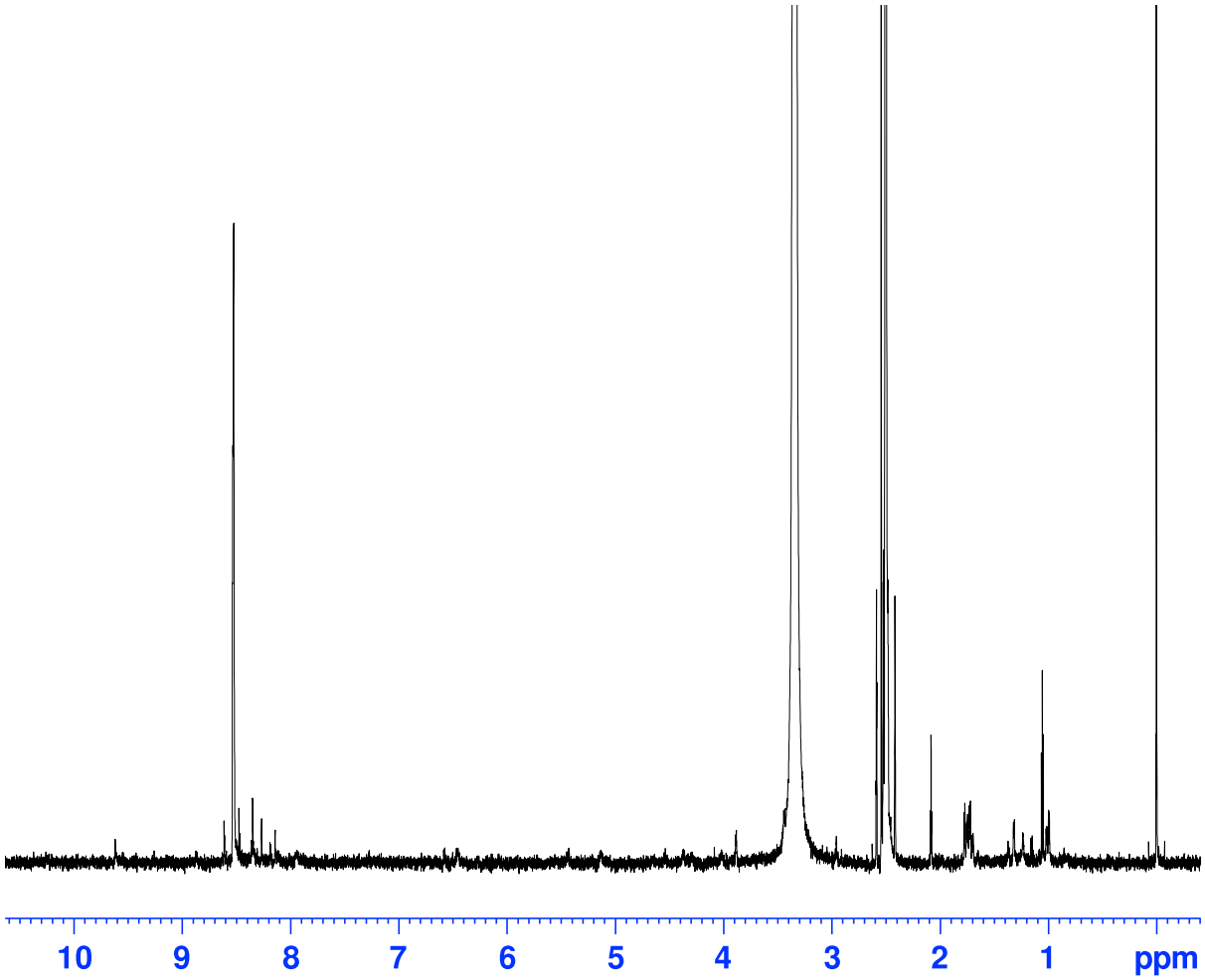

Figure 1-S22: **1D ^{1}H NMR of V6A1**.

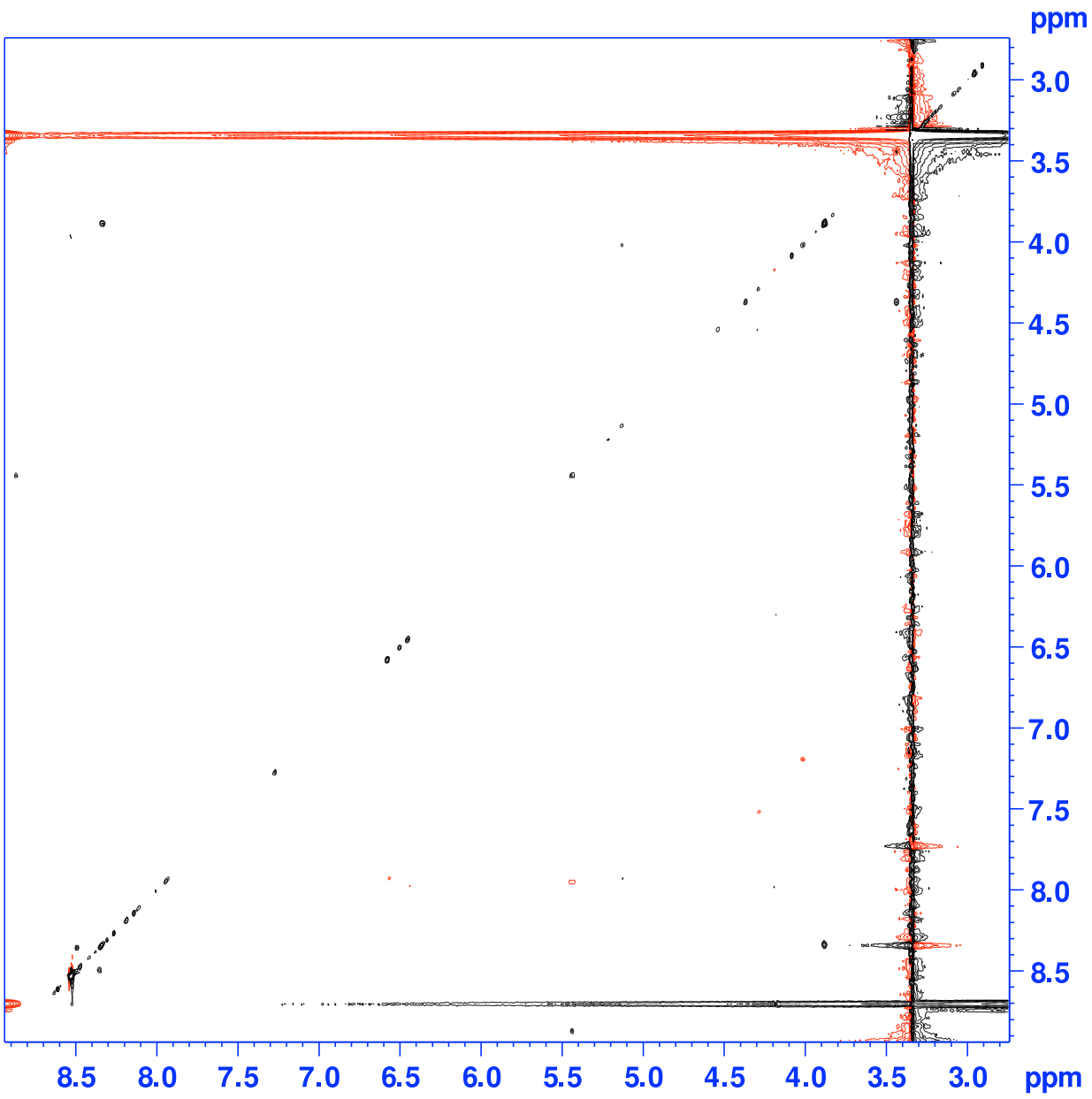

Figure 1-S23: ^{1}**H-**^{1}**H TOCSY spectra of V6A1**. No chemical shift assignments were made due to low sample concentration.

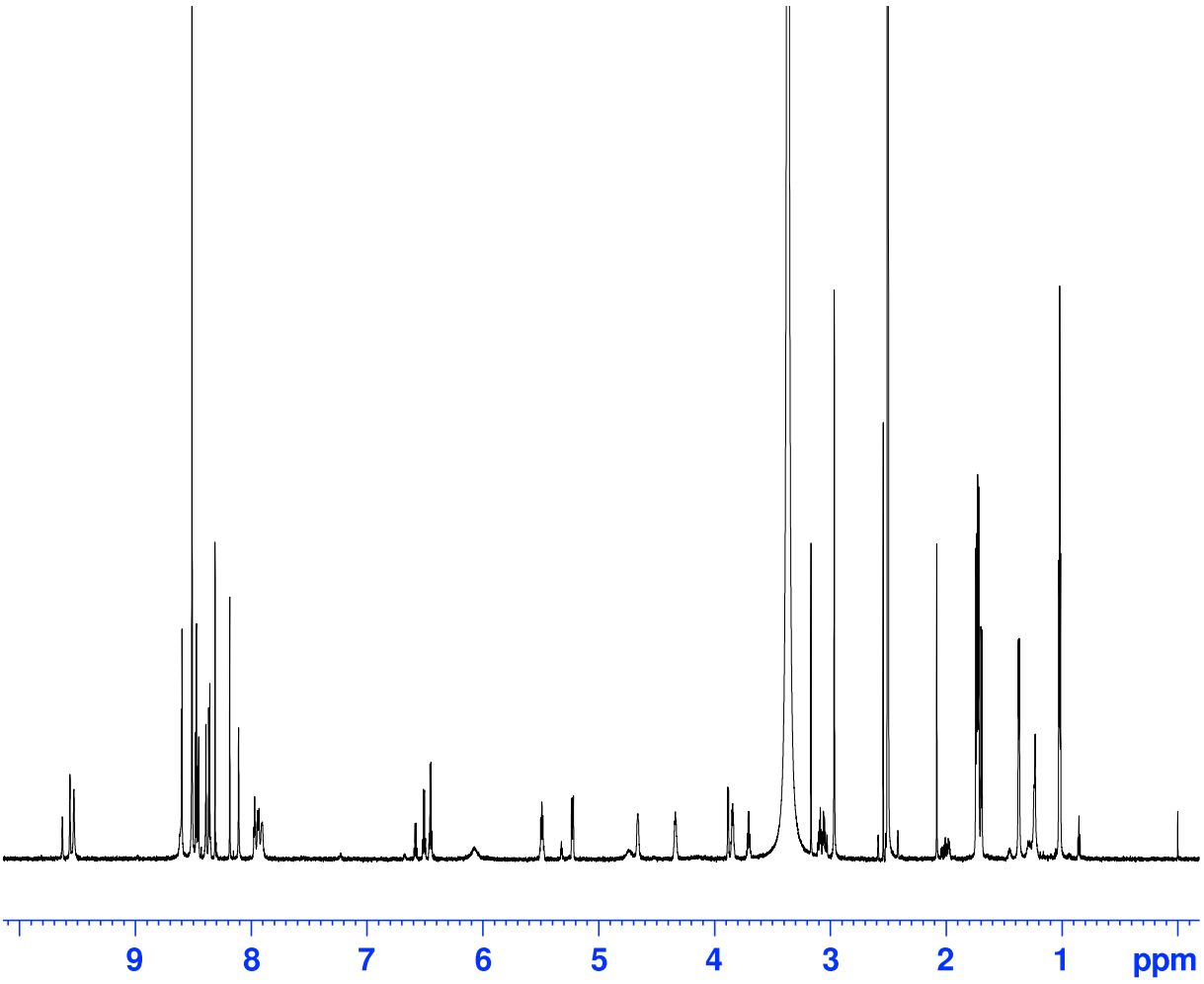

Figure 1-S24: **1D ^{1}H NMR of V6A2**.

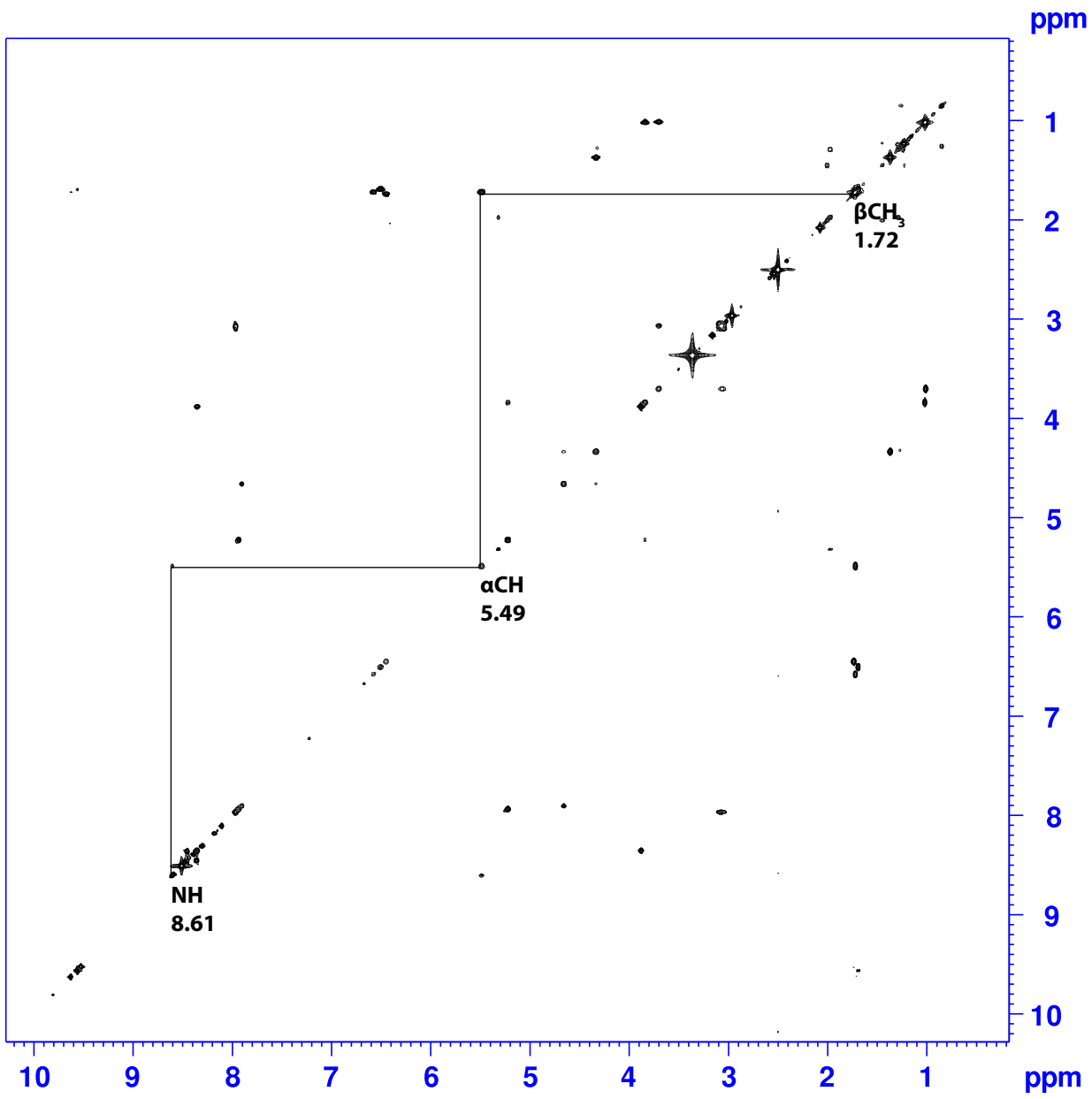

Figure 1-S25: **2D ^{1}H-^{1}H COSY spectra of V6A2**. Proton chemical shift assignments for alanine at residue 6 are shown.

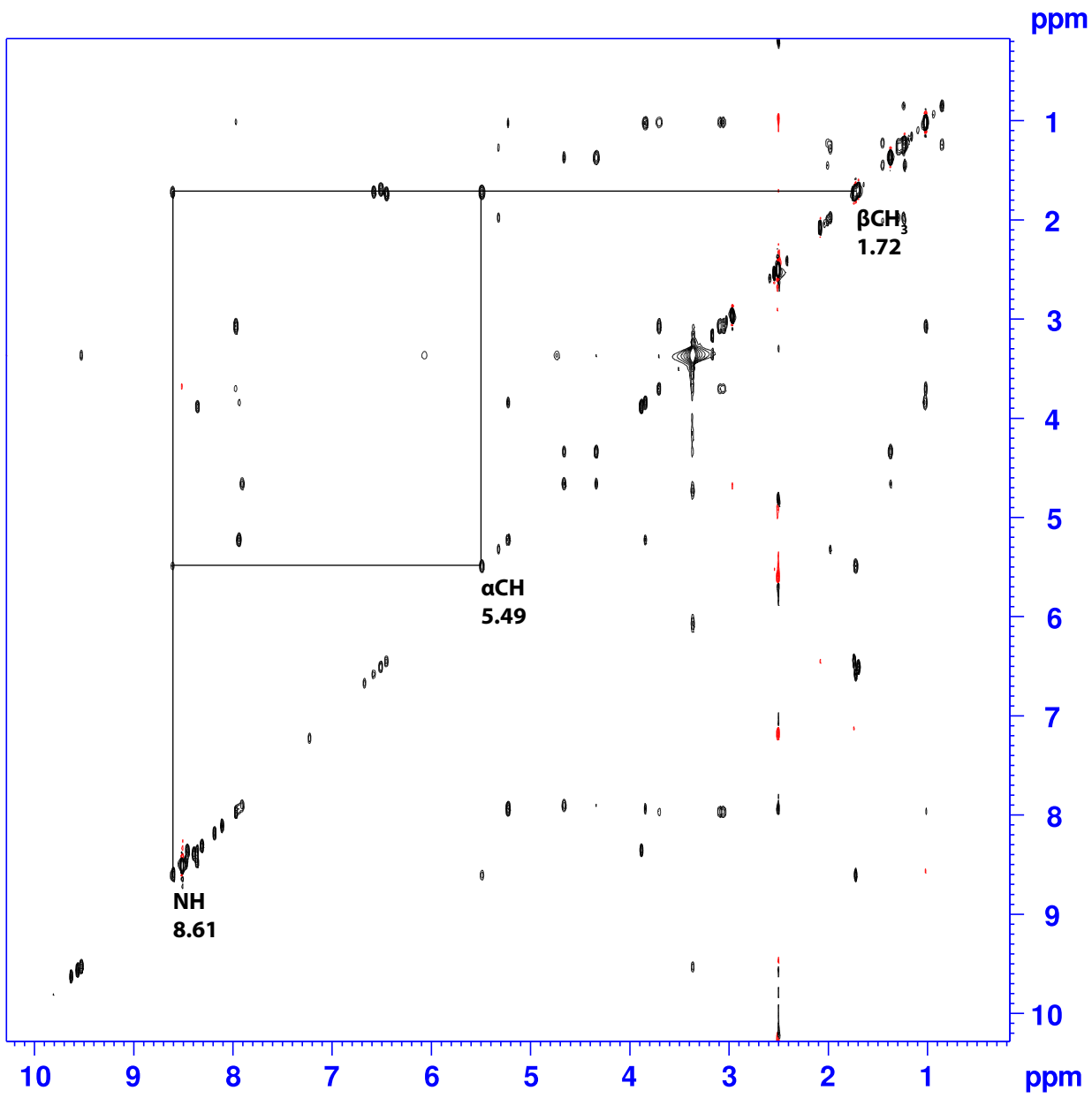

Figure 1-S26: **2D ^{1}H-^{1}H TOCSY spectra of V6A2**. Proton chemical shift assignments for alanine at residue 6 are shown.

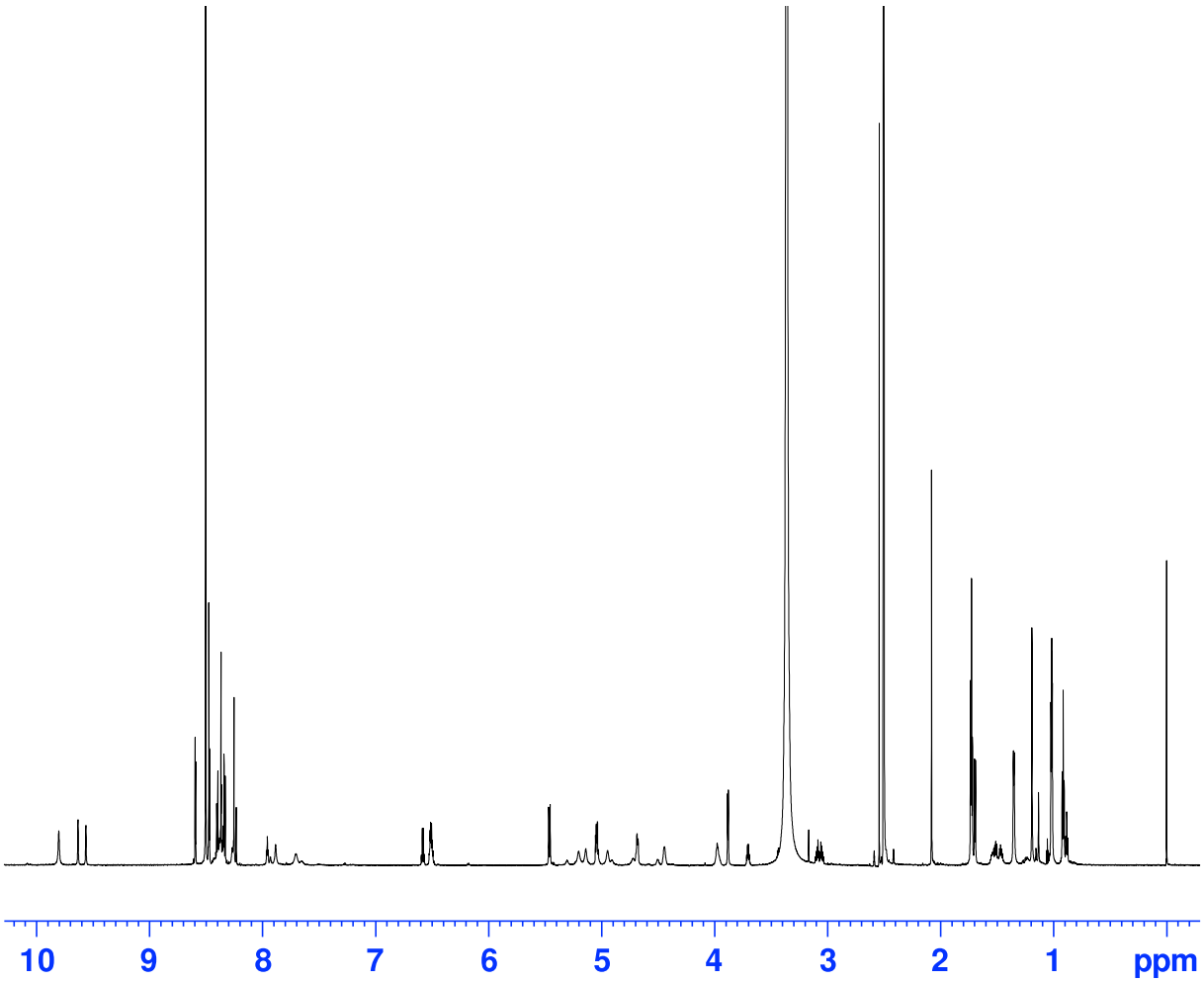

Figure 1-S27: **1D ^{1}H NMR of V6I1**.

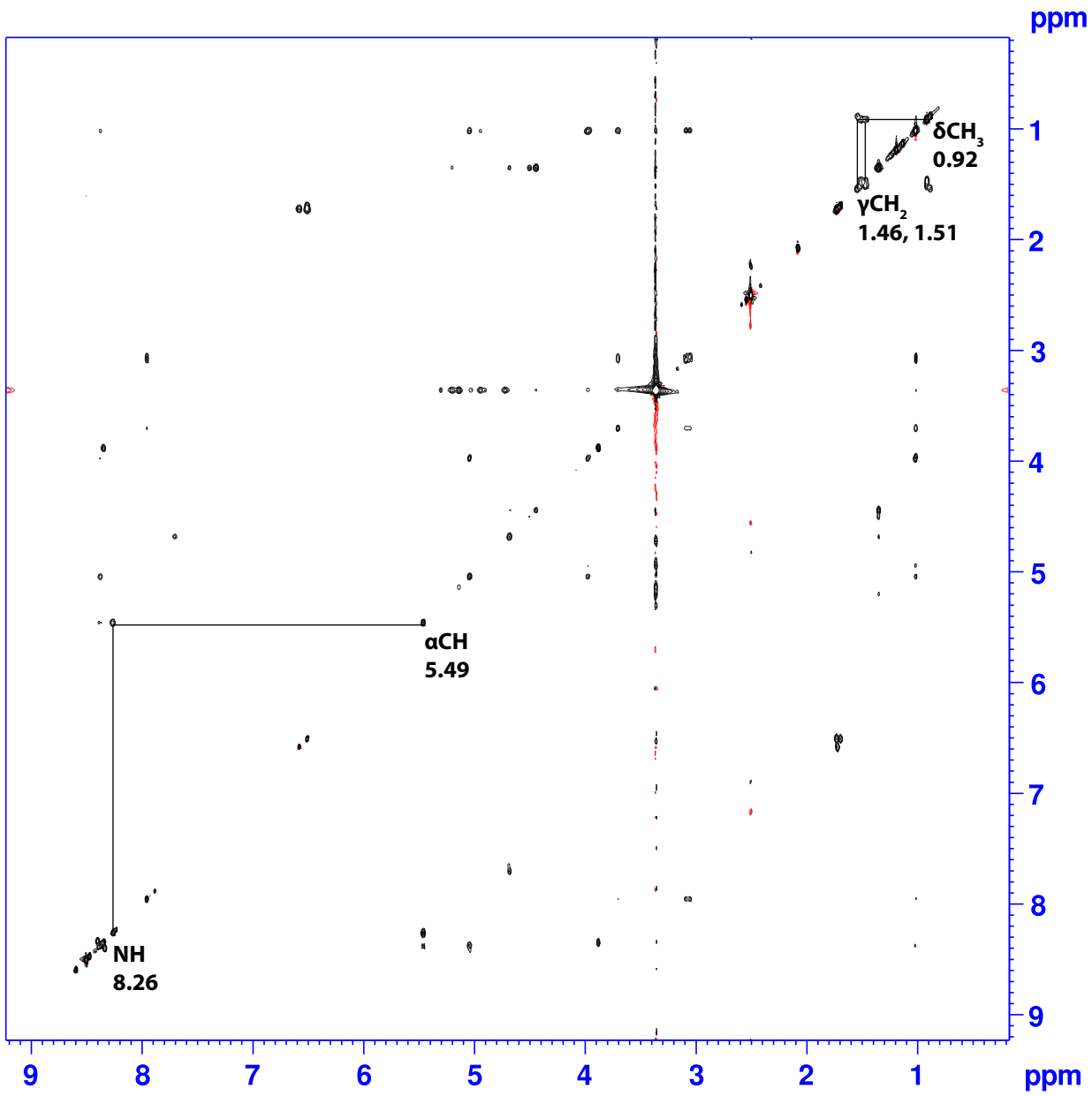

Figure 1-S28: **2D ^{1}H-^{1}H TOCSY spectra of V6I1**. Proton chemical shift assignments for β-hydroxy-isoleucine at residue 6 are shown.

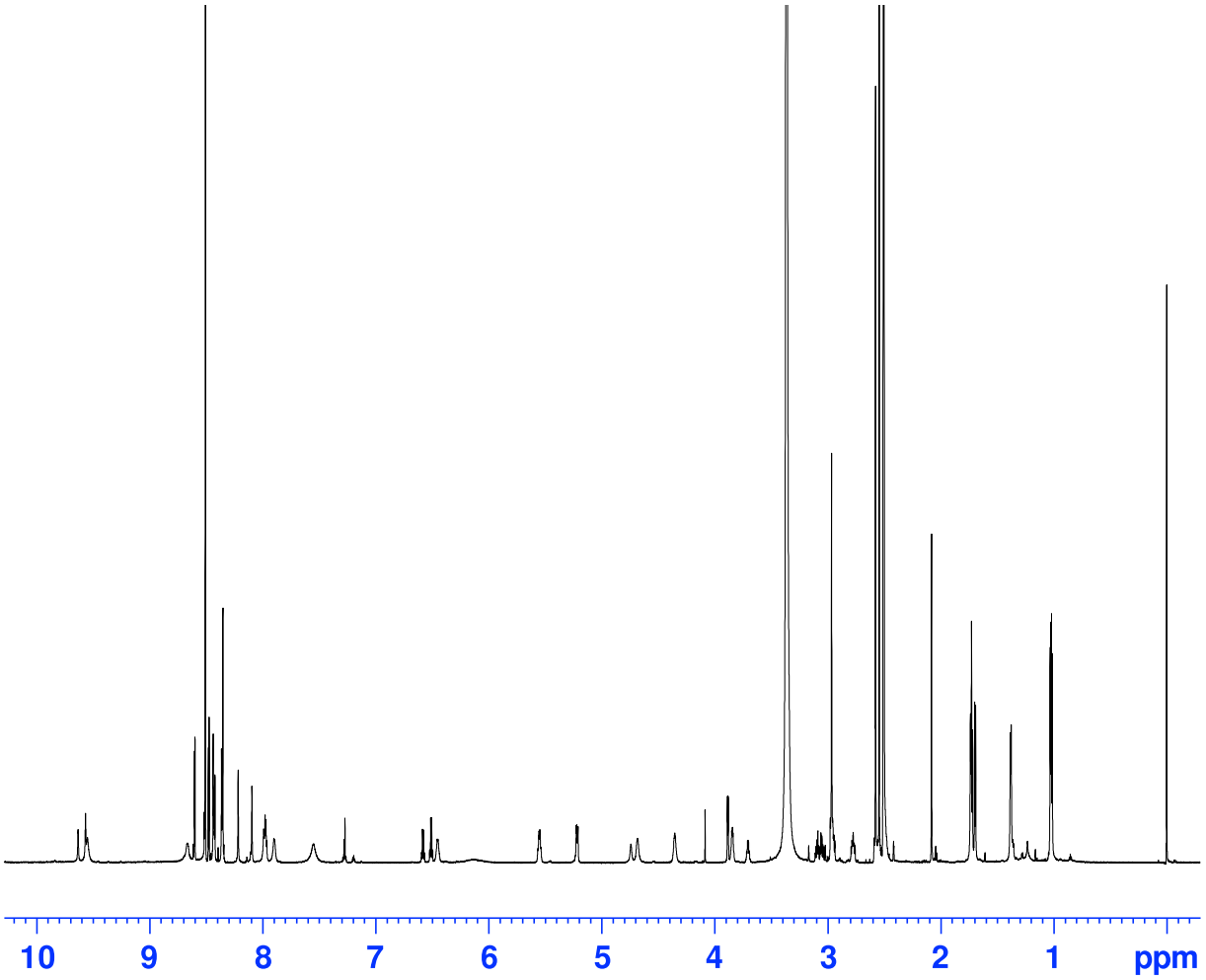

Figure 1-S29: **1D ^{1}H NMR of V6M1**.

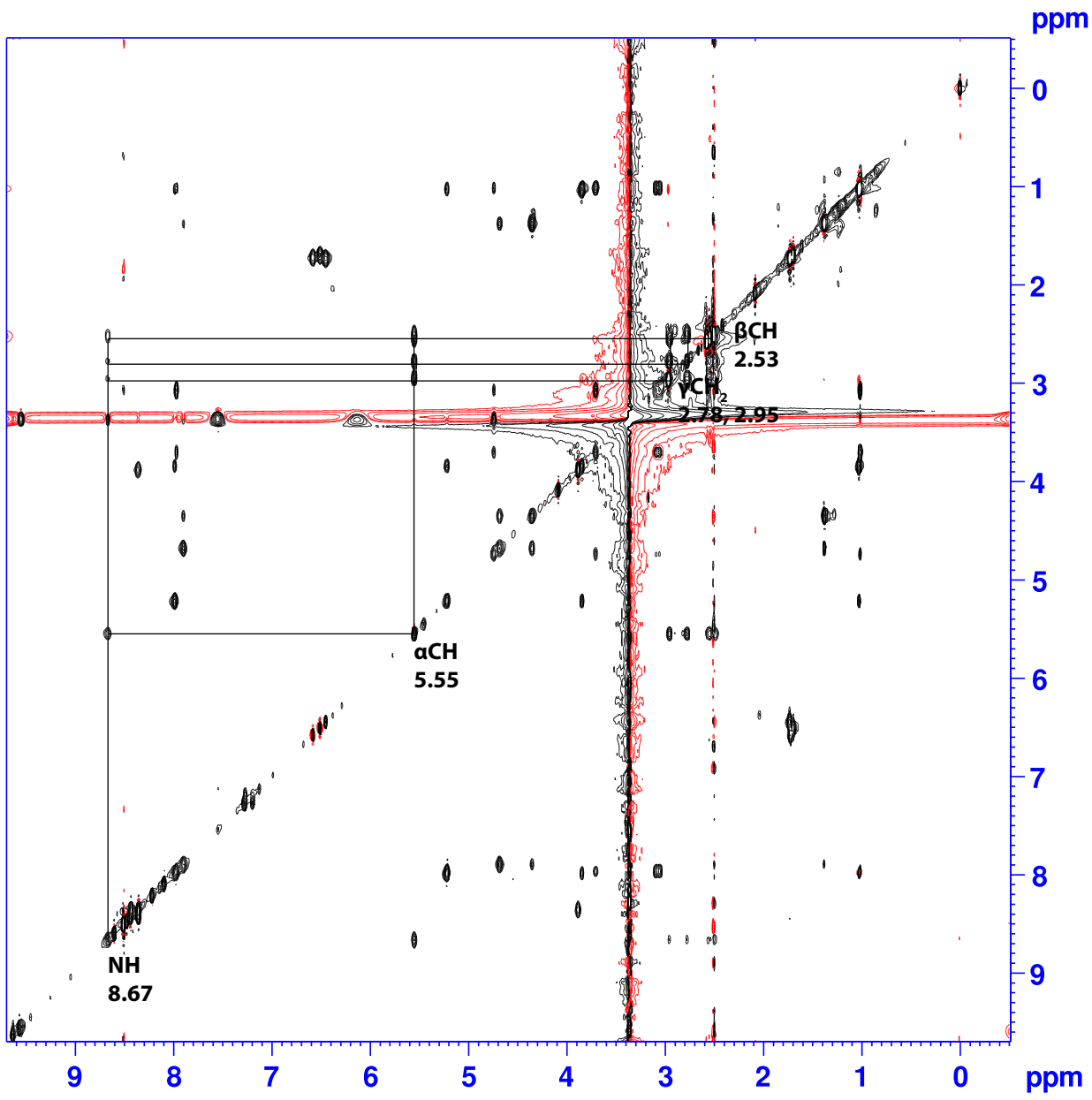

Figure 1-S30: **2D ^{1}H-^{1}H TOCSY spectra of V6M1**. Proton chemical shift assignments for β-hydroxy-methionine at residue 6 are shown.

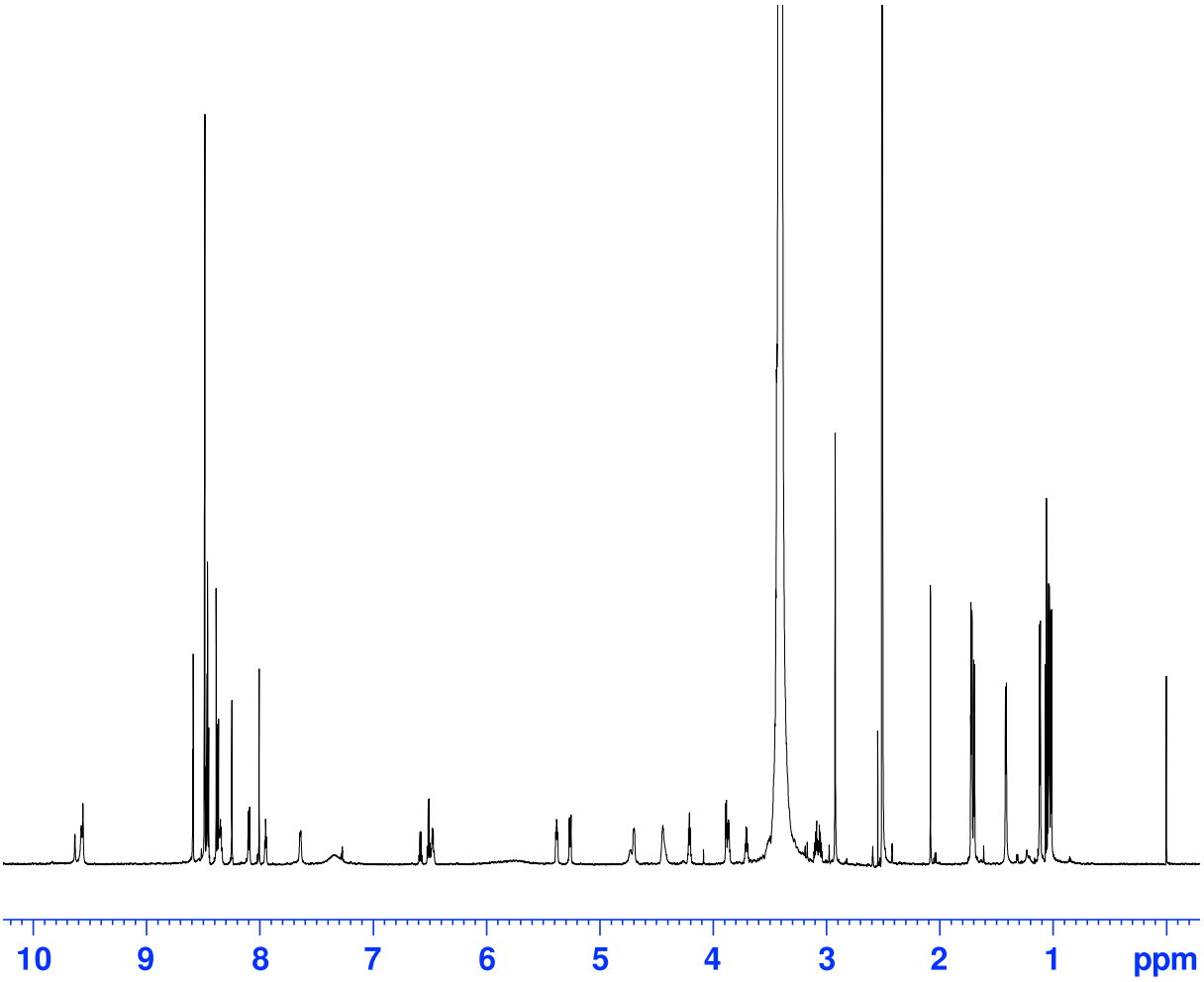

Figure 1-S31: **1D ^{1}H NMR of V6T1**.

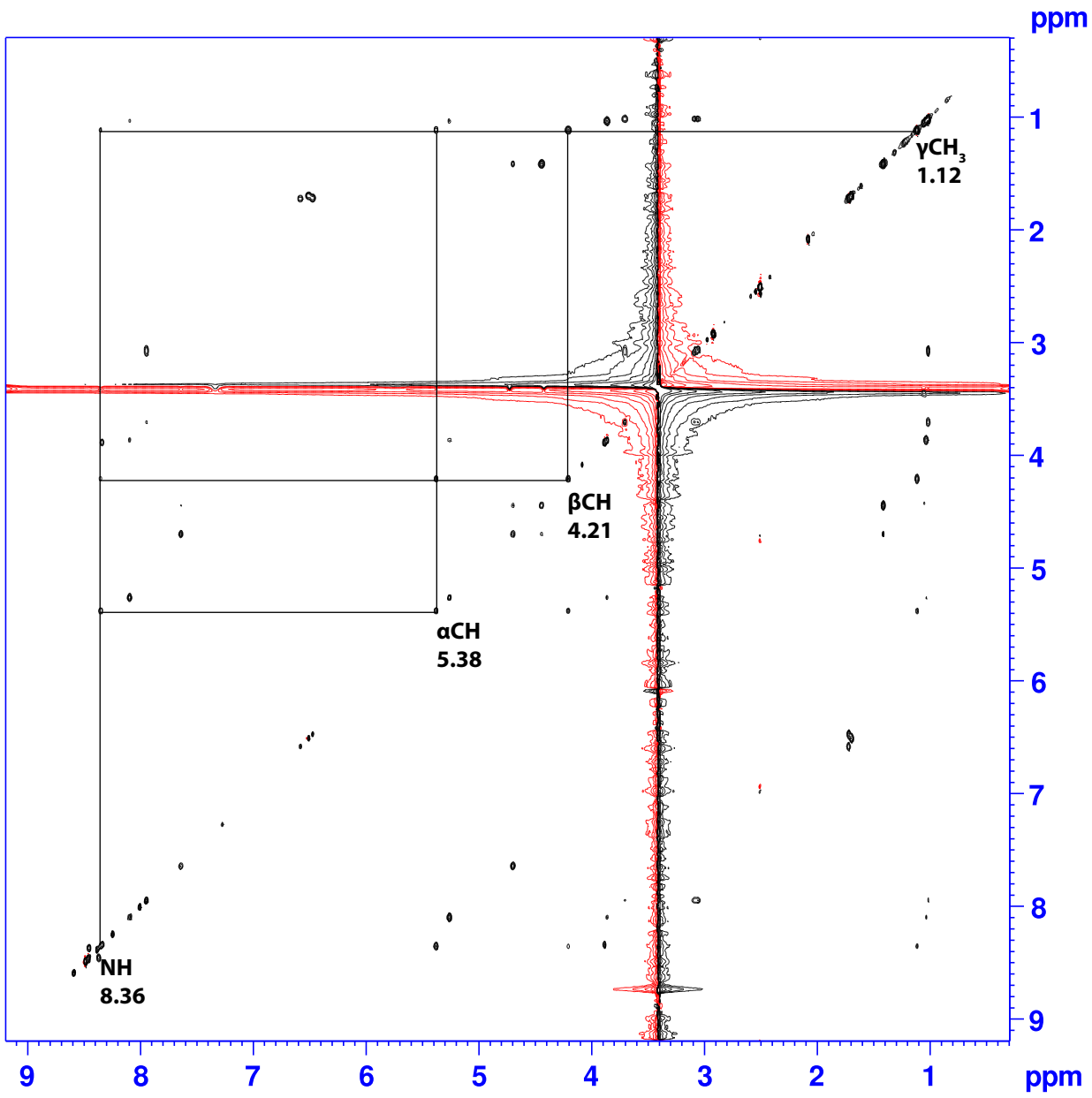

Figure 1-S32: **2D ^{1}H-^{1}H TOCSY spectra of V6T1**. Proton chemical shift assignments for threonine at residue 6 are shown.

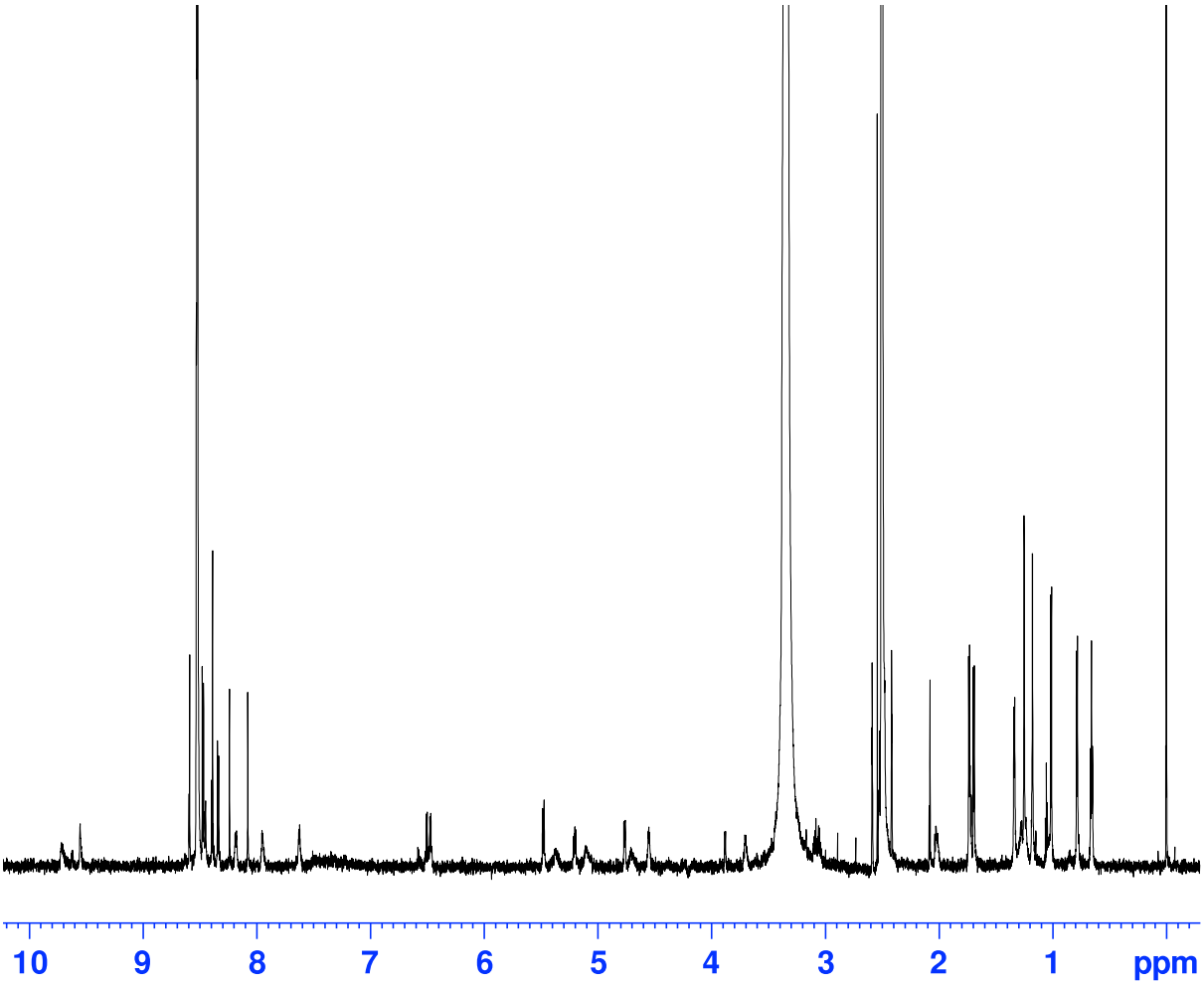

Figure 1-S33: **1D ^{1}H NMR of T8I1**.

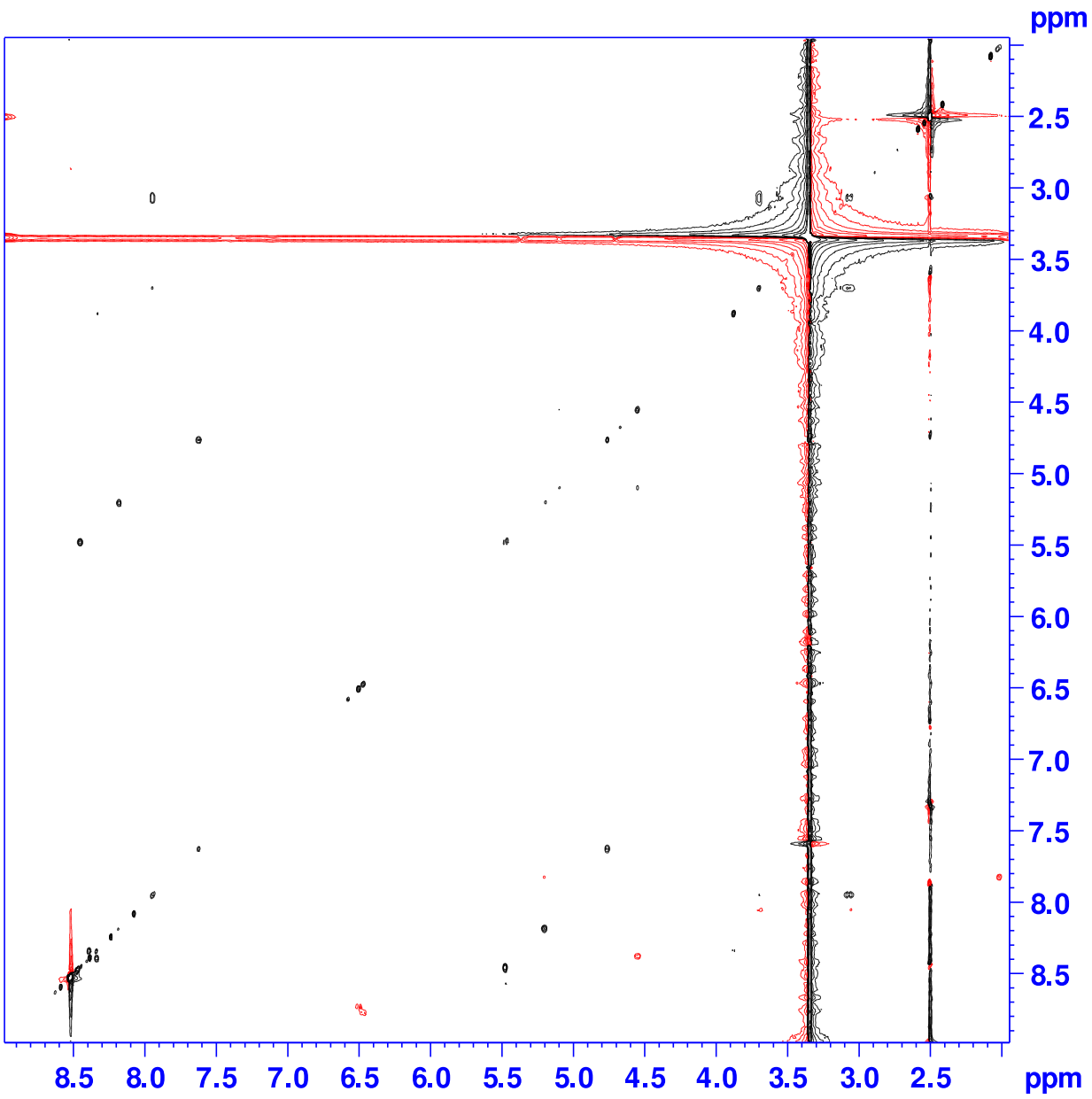

Figure 1-S34: **2D ^{1}H-^{1}H TOCSY spectra of T8I1**. No chemical shift assignments were made due to low sample concentration.

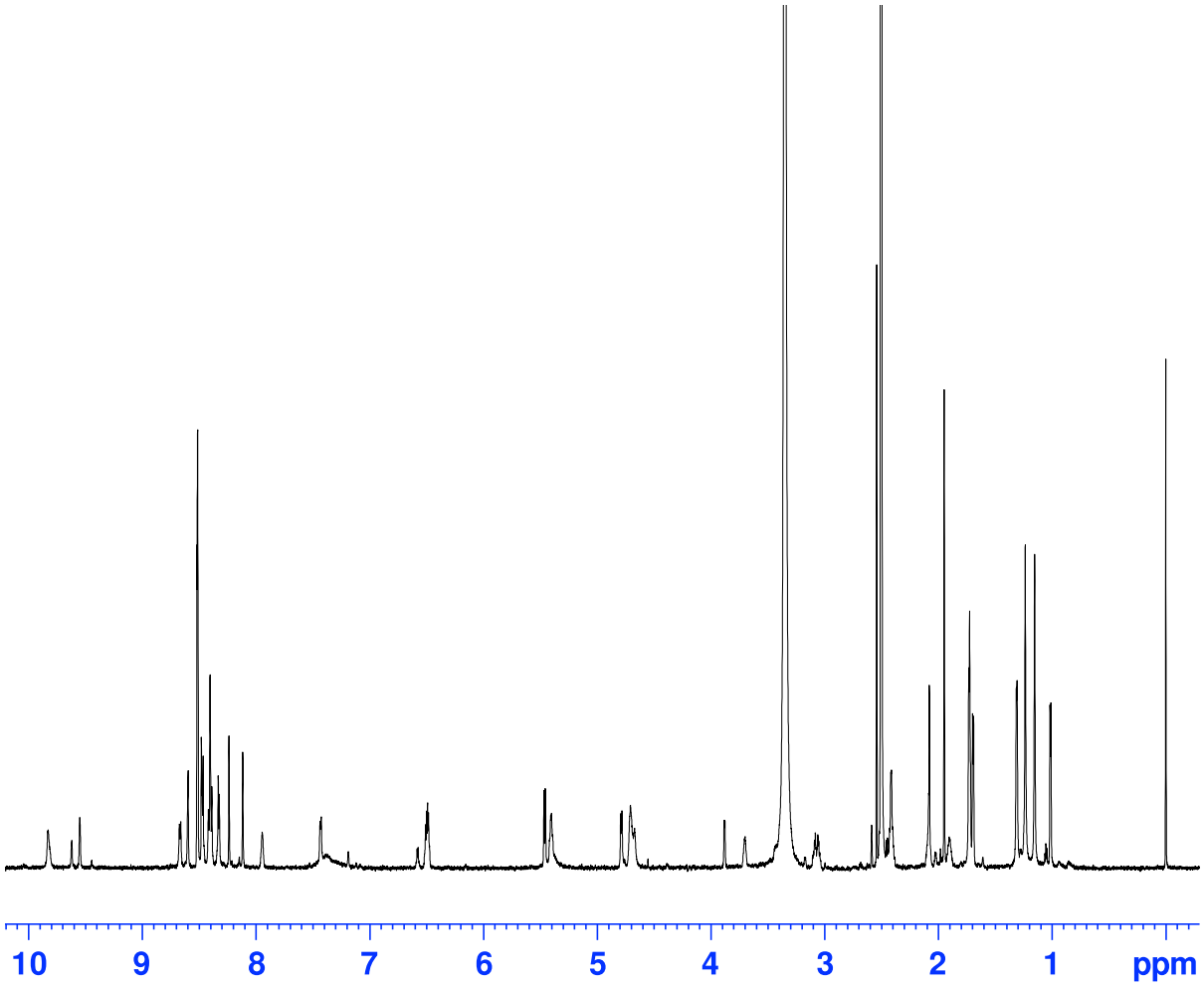

Figure 1-S35: **1D ^{1}H NMR of T8M1**.

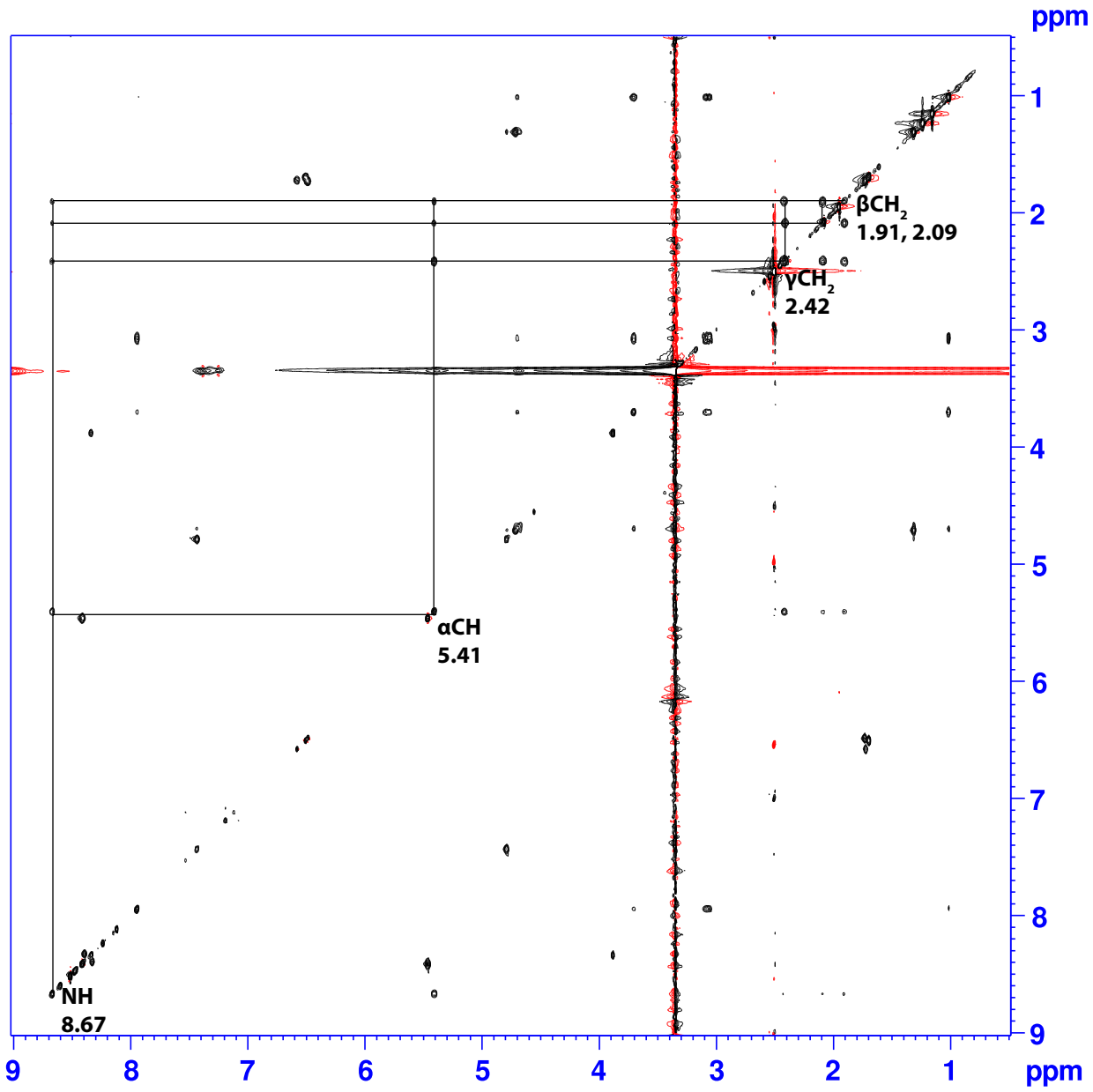

Figure 1-S36: **2D ^{1}H-^{1}H TOCSY spectra of T8M1**. Proton chemical shift assignments for methionine at residue 8 are shown.

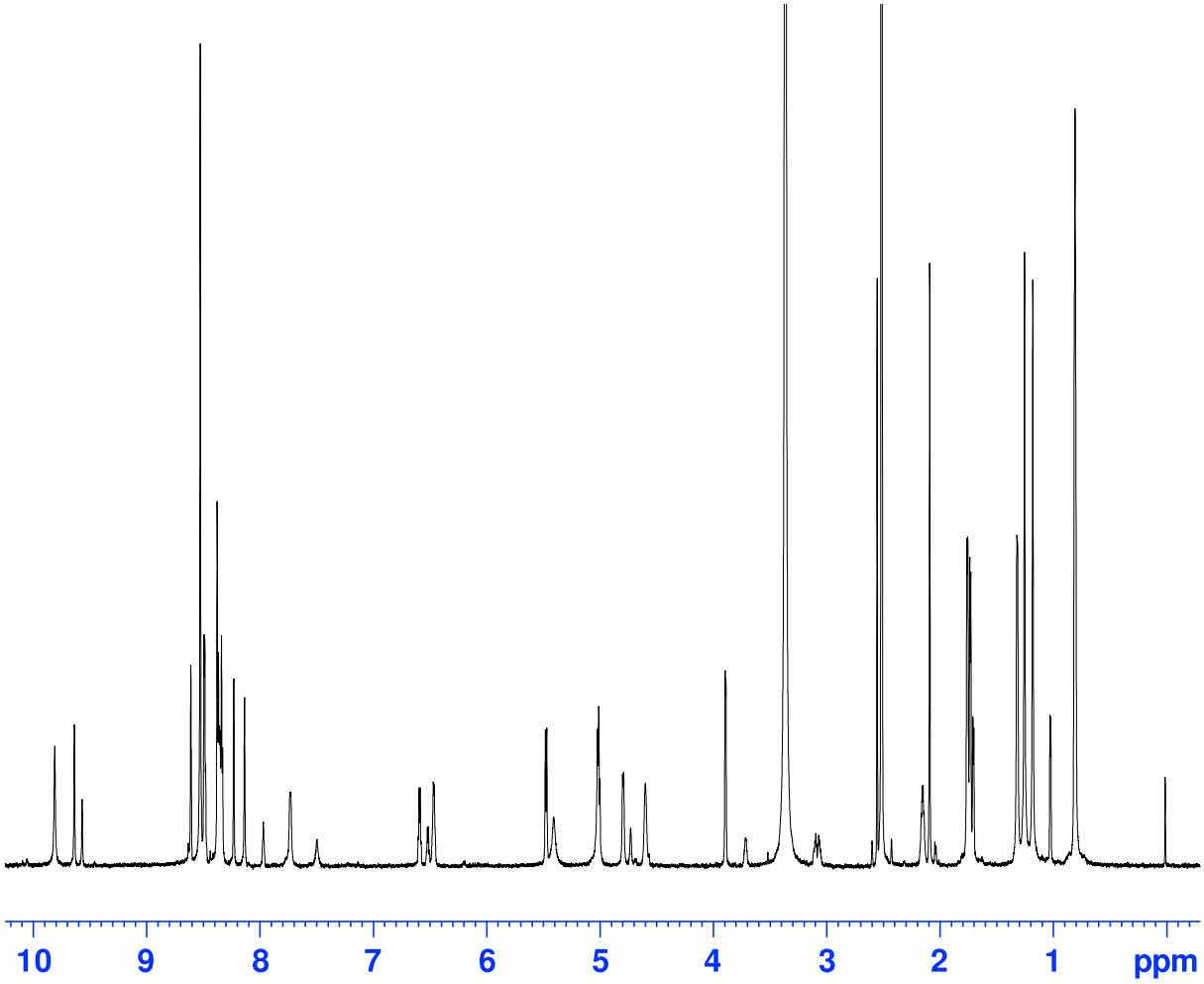

Figure 1-S37: **1D ^{1}H NMR of T8V1**.

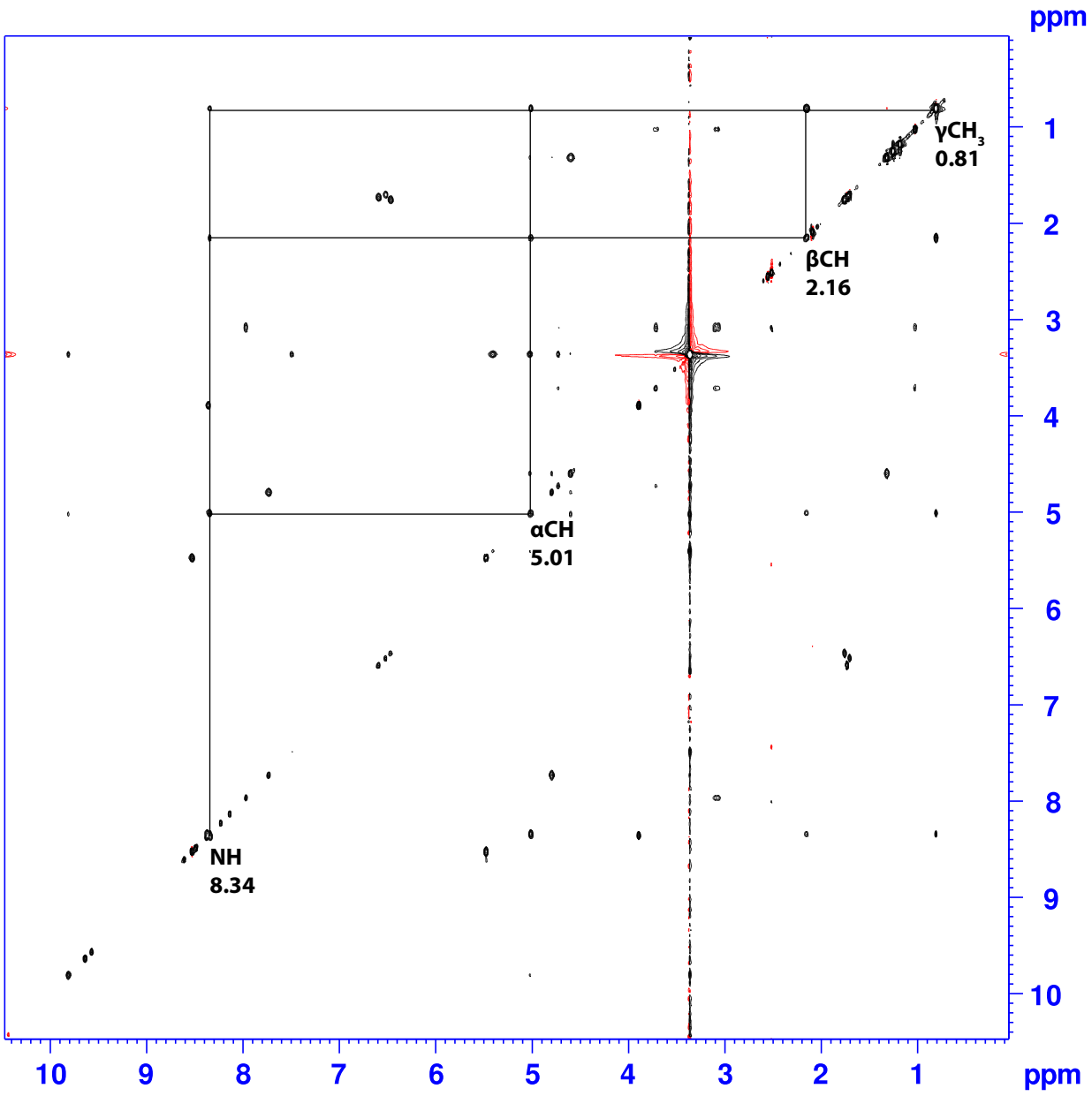

Figure 1-S38: **2D ^{1}H-^{1}H TOCSY spectra of T8V1**. Proton chemical shift assignments for valine at residue 8 are shown.

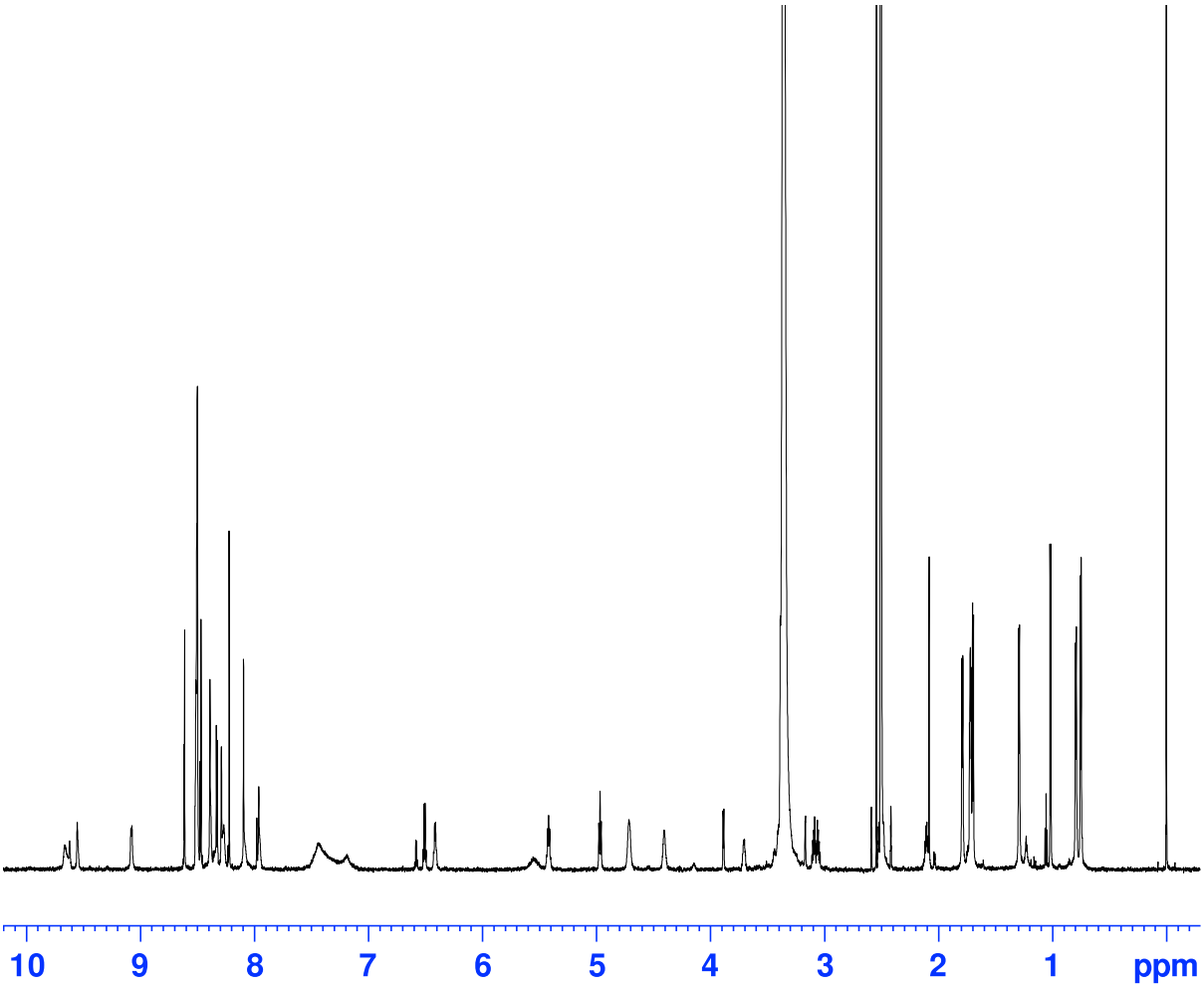

Figure 1-S39: **1D ^{1}H NMR of V6A-T8V1**.

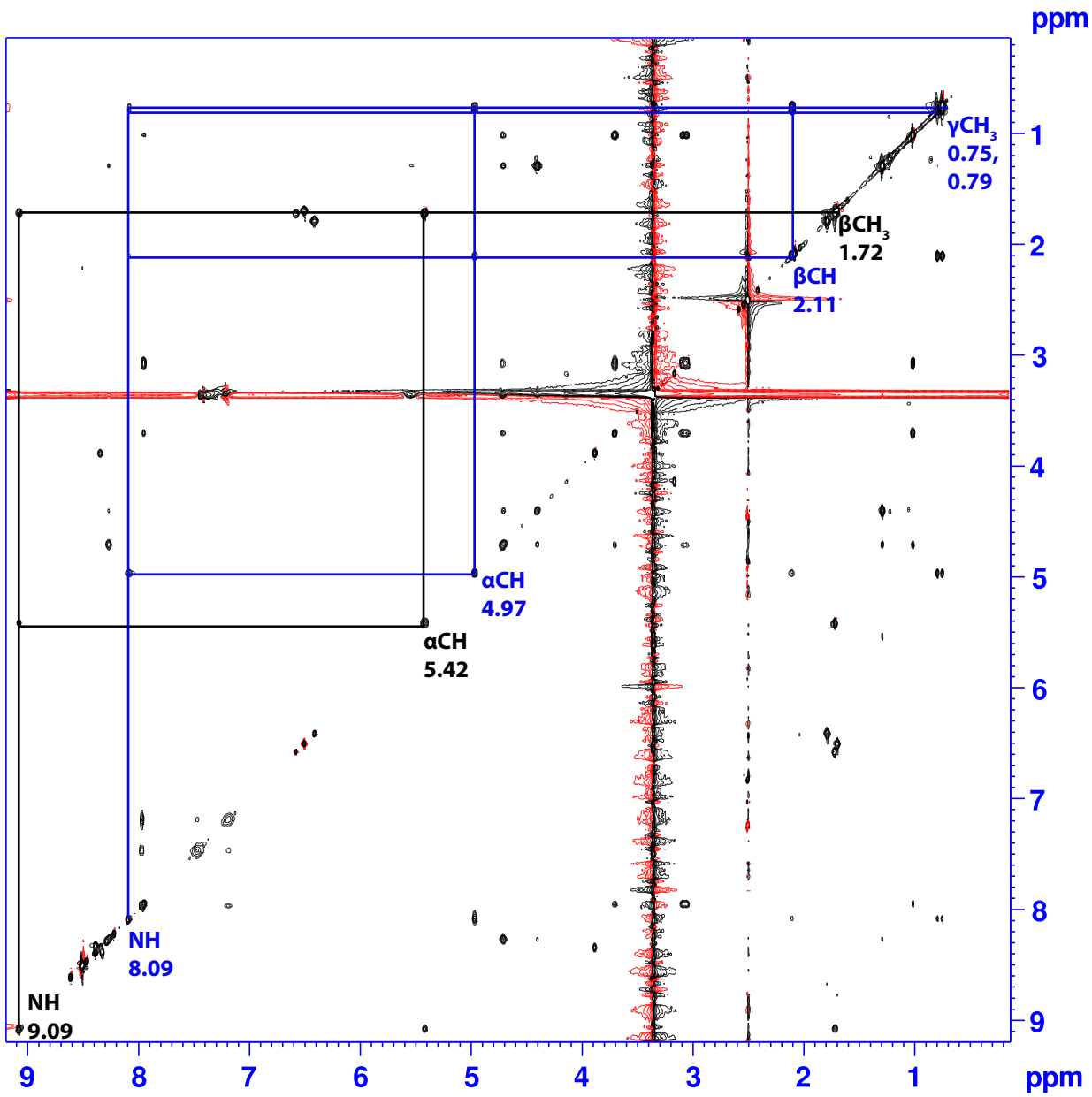

Figure 1-S40: **2D ^{1}H-^{1}H TOCSY spectra of double mutant V6A-T8V1**. Proton chemical shift assignments for alanine at residue 6 are shown in black and valine at residue 8 are shown in blue.

Name	Sequence
tclE-ins-F	ggttgatgttgatgctatgccagaaaacgaagcgcttgaaattatgggagcgtca
tclE-ins-R	gctcattaggcgggctgccccggggacgtctcaagttgtacaacaact
C2A	tgaaattatgggagcgtcaGCTacgacatgcgtatgtacatgcagttgttgtacaacttg
C2D	tgaaattatgggagcgtcaGATacgacatgcgtatgtacatgcagttgttgtacaacttg
C2E	tgaaattatgggagcgtcaGAAacgacatgcgtatgtacatgcagttgttgtacaacttg
C2F	tgaaattatgggagcgtcaTTTacgacatgcgtatgtacatgcagttgttgtacaacttg
C2G	tgaaattatgggagcgtcaGGTacgacatgcgtatgtacatgcagttgttgtacaacttg
C2H	tgaaattatgggagcgtcaCATacgacatgcgtatgtacatgcagttgttgtacaacttg
C2I	tgaaattatgggagcgtcaATTacgacatgcgtatgtacatgcagttgttgtacaacttg
C2K	tgaaattatgggagcgtcaAAAacgacatgcgtatgtacatgcagttgttgtacaacttg
C2L	tgaaattatgggagcgtcaTTAacgacatgcgtatgtacatgcagttgttgtacaacttg
C2M	tgaaattatgggagcgtcaATGacgacatgcgtatgtacatgcagttgttgtacaacttg
C2N	tgaaattatgggagcgtcaAATacgacatgcgtatgtacatgcagttgttgtacaacttg
C2P	tgaaattatgggagcgtcaCCTacgacatgcgtatgtacatgcagttgttgtacaacttg
C2Q	tgaaattatgggagcgtcaCAAacgacatgcgtatgtacatgcagttgttgtacaacttg
C2R	tgaaattatgggagcgtcaCGTacgacatgcgtatgtacatgcagttgttgtacaacttg
C2S	tgaaattatgggagcgtcaTCTacgacatgcgtatgtacatgcagttgttgtacaacttg
C2T	tgaaattatgggagcgtcaACAacgacatgcgtatgtacatgcagttgttgtacaacttg
C2V	tgaaattatgggagcgtcaGTAacgacatgcgtatgtacatgcagttgttgtacaacttg
C2W	tgaaattatgggagcgtcaTGGacgacatgcgtatgtacatgcagttgttgtacaacttg
C2Y	tgaaattatgggagcgtcaTATacgacatgcgtatgtacatgcagttgttgtacaacttg
T3A	gaaattatgggagcgtcatgtGCTacatgcgtatgtacatgcagttgttgtacaacttga
T3C	gaaattatgggagcgtcatgtTGTacatgcgtatgtacatgcagttgttgtacaacttga
T3D	gaaattatgggagcgtcatgtGATacatgcgtatgtacatgcagttgttgtacaacttga
T3E	gaaattatgggagcgtcatgtGAAacatgcgtatgtacatgcagttgttgtacaacttga
T3F	gaaattatgggagcgtcatgtTTTacatgcgtatgtacatgcagttgttgtacaacttga
T3G	gaaattatgggagcgtcatgtGGTacatgcgtatgtacatgcagttgttgtacaacttga
T3H	gaaattatgggagcgtcatgtCATacatgcgtatgtacatgcagttgttgtacaacttga
T3I	gaaattatgggagcgtcatgtATTacatgcgtatgtacatgcagttgttgtacaacttga
T3K	gaaattatgggagcgtcatgtAAAacatgcgtatgtacatgcagttgttgtacaacttga
T3L	gaaattatgggagcgtcatgtTTAacatgcgtatgtacatgcagttgttgtacaacttga
T3M	gaaattatgggagcgtcatgtATGacatgcgtatgtacatgcagttgttgtacaacttga
T3N	gaaattatgggagcgtcatgtAATacatgcgtatgtacatgcagttgttgtacaacttga
T3P	gaaattatgggagcgtcatgtCCTacatgcgtatgtacatgcagttgttgtacaacttga
T3Q	gaaattatgggagcgtcatgtCAAacatgcgtatgtacatgcagttgttgtacaacttga
T3R	gaaattatgggagcgtcatgtCGTacatgcgtatgtacatgcagttgttgtacaacttga
T3S	gaaattatgggagcgtcatgtTCTacatgcgtatgtacatgcagttgttgtacaacttga
T3V	gaaattatgggagcgtcatgtGTAacatgcgtatgtacatgcagttgttgtacaacttga
T3W	gaaattatgggagcgtcatgtTGGacatgcgtatgtacatgcagttgttgtacaacttga
T3Y	gaaattatgggagcgtcatgtTATacatgcgtatgtacatgcagttgttgtacaacttga
T4A	gaaattatgggagcgtcatgtacgGCTtgcgtatgtacatgcagttgttgtacaacttga
T4C	gaaattatgggagcgtcatgtacgTGTtgcgtatgtacatgcagttgttgtacaacttga

Name	Sequence
T4D	gaaattatgggagcgtcatgtacgGATtgcgtatgtacatgcagttgttgtacaacttga
T4E	gaaattatgggagcgtcatgtacgGAAtgcgtatgtacatgcagttgttgtacaacttga
T4F	gaaattatgggagcgtcatgtacgTTTtgcgtatgtacatgcagttgttgtacaacttga
T4G	gaaattatgggagcgtcatgtacgGGTtgcgtatgtacatgcagttgttgtacaacttga
T4H	gaaattatgggagcgtcatgtacgCATtgcgtatgtacatgcagttgttgtacaacttga
T4I	gaaattatgggagcgtcatgtacgATTtgcgtatgtacatgcagttgttgtacaacttga
T4K	gaaattatgggagcgtcatgtacgAAAtgcgtatgtacatgcagttgttgtacaacttga
T4L	gaaattatgggagcgtcatgtacgTTAtgcgtatgtacatgcagttgttgtacaacttga
T4M	gaaattatgggagcgtcatgtacgATGtgcgtatgtacatgcagttgttgtacaacttga
T4N	gaaattatgggagcgtcatgtacgAATtgcgtatgtacatgcagttgttgtacaacttga
T4P	gaaattatgggagcgtcatgtacgCCTtgcgtatgtacatgcagttgttgtacaacttga
T4Q	gaaattatgggagcgtcatgtacgCAAtgcgtatgtacatgcagttgttgtacaacttga
T4R	gaaattatgggagcgtcatgtacgCGTtgcgtatgtacatgcagttgttgtacaacttga
T4S	gaaattatgggagcgtcatgtacgTCTtgcgtatgtacatgcagttgttgtacaacttga
T4V	gaaattatgggagcgtcatgtacgGTAtgcgtatgtacatgcagttgttgtacaacttga
T4W	gaaattatgggagcgtcatgtacgTGGtgcgtatgtacatgcagttgttgtacaacttga
T4Y	gaaattatgggagcgtcatgtacgTATtgcgtatgtacatgcagttgttgtacaacttga
C5A	gaaattatgggagcgtcatgtacgacaGCTgtatgtacatgcagttgttgtacaacttga
C5D	gaaattatgggagcgtcatgtacgacaGATgtatgtacatgcagttgttgtacaacttga
C5E	gaaattatgggagcgtcatgtacgacaGAAgtatgtacatgcagttgttgtacaacttga
C5F	gaaattatgggagcgtcatgtacgacaTTTgtatgtacatgcagttgttgtacaacttga
C5G	gaaattatgggagcgtcatgtacgacaGGTgtatgtacatgcagttgttgtacaacttga
C5H	gaaattatgggagcgtcatgtacgacaCATgtatgtacatgcagttgttgtacaacttga
C5I	gaaattatgggagcgtcatgtacgacaATTgtatgtacatgcagttgttgtacaacttga
C5K	gaaattatgggagcgtcatgtacgacaAAAgtatgtacatgcagttgttgtacaacttga
C5L	gaaattatgggagcgtcatgtacgacaTTAgtatgtacatgcagttgttgtacaacttga
C5M	gaaattatgggagcgtcatgtacgacaATGgtatgtacatgcagttgttgtacaacttga
C5N	gaaattatgggagcgtcatgtacgacaAATgtatgtacatgcagttgttgtacaacttga
C5P	gaaattatgggagcgtcatgtacgacaCCTgtatgtacatgcagttgttgtacaacttga
C5Q	gaaattatgggagcgtcatgtacgacaCAAgtatgtacatgcagttgttgtacaacttga
C5R	gaaattatgggagcgtcatgtacgacaCGTgtatgtacatgcagttgttgtacaacttga
C5S	gaaattatgggagcgtcatgtacgacaTCTgtatgtacatgcagttgttgtacaacttga
C5T	gaaattatgggagcgtcatgtacgacaACAgtatgtacatgcagttgttgtacaacttga
C5V	gaaattatgggagcgtcatgtacgacaGTAgtatgtacatgcagttgttgtacaacttga
C5W	gaaattatgggagcgtcatgtacgacaTGGgtatgtacatgcagttgttgtacaacttga
C5Y	gaaattatgggagcgtcatgtacgacaTATgtatgtacatgcagttgttgtacaacttga
V6A	gaaattatgggagcgtcatgtacgacatgcGCTtgtacatgcagttgttgtacaacttga
V6C	gaaattatgggagcgtcatgtacgacatgcTGTtgtacatgcagttgttgtacaacttga
V6D	gaaattatgggagcgtcatgtacgacatgcGATtgtacatgcagttgttgtacaacttga
V6E	gaaattatgggagcgtcatgtacgacatgcGAAtgtacatgcagttgttgtacaacttga
V6F	gaaattatgggagcgtcatgtacgacatgcTTTtgtacatgcagttgttgtacaacttga
V6G	gaaattatgggagcgtcatgtacgacatgcGGTtgtacatgcagttgttgtacaacttga

Name	Sequence
V6H	gaaattatgggagcgtcatgtacgacatgcCATtgtacatgcagttgttgtacaacttga
V6I	gaaattatgggagcgtcatgtacgacatgcATTtgtacatgcagttgttgtacaacttga
V6K	gaaattatgggagcgtcatgtacgacatgcAAAtgtacatgcagttgttgtacaacttga
V6L	gaaattatgggagcgtcatgtacgacatgcTTAtgtacatgcagttgttgtacaacttga
V6M	gaaattatgggagcgtcatgtacgacatgcATGtgtacatgcagttgttgtacaacttga
V6N	gaaattatgggagcgtcatgtacgacatgcAATtgtacatgcagttgttgtacaacttga
V6P	gaaattatgggagcgtcatgtacgacatgcCCTtgtacatgcagttgttgtacaacttga
V6Q	gaaattatgggagcgtcatgtacgacatgcCAAtgtacatgcagttgttgtacaacttga
V6R	gaaattatgggagcgtcatgtacgacatgcCGTtgtacatgcagttgttgtacaacttga
V6S	gaaattatgggagcgtcatgtacgacatgcTCTtgtacatgcagttgttgtacaacttga
V6T	gaaattatgggagcgtcatgtacgacatgcACAtgtacatgcagttgttgtacaacttga
V6W	gaaattatgggagcgtcatgtacgacatgcTGGtgtacatgcagttgttgtacaacttga
V6Y	gaaattatgggagcgtcatgtacgacatgcTATtgtacatgcagttgttgtacaacttga
C7A	gaaattatgggagcgtcatgtacgacatgcgtaGCTacatgcagttgttgtacaacttga
C7D	gaaattatgggagcgtcatgtacgacatgcgtaGATacatgcagttgttgtacaacttga
C7E	gaaattatgggagcgtcatgtacgacatgcgtaGAAacatgcagttgttgtacaacttga
C7F	gaaattatgggagcgtcatgtacgacatgcgtaTTTacatgcagttgttgtacaacttga
C7G	gaaattatgggagcgtcatgtacgacatgcgtaGGTacatgcagttgttgtacaacttga
C7H	gaaattatgggagcgtcatgtacgacatgcgtaCATacatgcagttgttgtacaacttga
C7I	gaaattatgggagcgtcatgtacgacatgcgtaATTacatgcagttgttgtacaacttga
C7K	gaaattatgggagcgtcatgtacgacatgcgtaAAAacatgcagttgttgtacaacttga
C7L	gaaattatgggagcgtcatgtacgacatgcgtaTTAacatgcagttgttgtacaacttga
C7M	gaaattatgggagcgtcatgtacgacatgcgtaATGacatgcagttgttgtacaacttga
C7N	gaaattatgggagcgtcatgtacgacatgcgtaAATacatgcagttgttgtacaacttga
C7P	gaaattatgggagcgtcatgtacgacatgcgtaCCTacatgcagttgttgtacaacttga
C7Q	gaaattatgggagcgtcatgtacgacatgcgtaCAAacatgcagttgttgtacaacttga
C7R	gaaattatgggagcgtcatgtacgacatgcgtaCGTacatgcagttgttgtacaacttga
C7S	gaaattatgggagcgtcatgtacgacatgcgtaTCTacatgcagttgttgtacaacttga
C7T	gaaattatgggagcgtcatgtacgacatgcgtaACAacatgcagttgttgtacaacttga
C7V	gaaattatgggagcgtcatgtacgacatgcgtaGTAacatgcagttgttgtacaacttga
C7W	gaaattatgggagcgtcatgtacgacatgcgtaTGGacatgcagttgttgtacaacttga
C7Y	gaaattatgggagcgtcatgtacgacatgcgtaTATacatgcagttgttgtacaacttga
T8A	gaaattatgggagcgtcatgtacgacatgcgtatgtGCTtgcagttgttgtacaacttga
T8C	gaaattatgggagcgtcatgtacgacatgcgtatgtTGTtgcagttgttgtacaacttga
T8D	gaaattatgggagcgtcatgtacgacatgcgtatgtGATtgcagttgttgtacaacttga
T8E	gaaattatgggagcgtcatgtacgacatgcgtatgtGAAtgcagttgttgtacaacttga
T8F	gaaattatgggagcgtcatgtacgacatgcgtatgtTTTtgcagttgttgtacaacttga
T8G	gaaattatgggagcgtcatgtacgacatgcgtatgtGGTtgcagttgttgtacaacttga
T8H	gaaattatgggagcgtcatgtacgacatgcgtatgtCATtgcagttgttgtacaacttga
T8I	gaaattatgggagcgtcatgtacgacatgcgtatgtATTtgcagttgttgtacaacttga
T8K	gaaattatgggagcgtcatgtacgacatgcgtatgtAAAtgcagttgttgtacaacttga
T8L	gaaattatgggagcgtcatgtacgacatgcgtatgtTTAtgcagttgttgtacaacttga

Name	Sequence
T8M	gaaattatgggagcgtcatgtacgacatgcgtatgtATGtgcagttgttgtacaacttga
T8N	gaaattatgggagcgtcatgtacgacatgcgtatgtAATtgcagttgttgtacaacttga
T8P	gaaattatgggagcgtcatgtacgacatgcgtatgtCCTtgcagttgttgtacaacttga
T8Q	gaaattatgggagcgtcatgtacgacatgcgtatgtCAAtgcagttgttgtacaacttga
T8R	gaaattatgggagcgtcatgtacgacatgcgtatgtCGTtgcagttgttgtacaacttga
T8S	gaaattatgggagcgtcatgtacgacatgcgtatgtTCTtgcagttgttgtacaacttga
T8V	gaaattatgggagcgtcatgtacgacatgcgtatgtGTAtgcagttgttgtacaacttga
T8W	gaaattatgggagcgtcatgtacgacatgcgtatgtTGGtgcagttgttgtacaacttga
T8Y	gaaattatgggagcgtcatgtacgacatgcgtatgtTATtgcagttgttgtacaacttga
C9A	attatgggagcgtcatgtacgacatgcgtatgtacaGCTagttgttgtacaacttgagac
C9D	attatgggagcgtcatgtacgacatgcgtatgtacaGATagttgttgtacaacttgagac
C9E	attatgggagcgtcatgtacgacatgcgtatgtacaGAAagttgttgtacaacttgagac
C9F	attatgggagcgtcatgtacgacatgcgtatgtacaTTTagttgttgtacaacttgagac
C9G	attatgggagcgtcatgtacgacatgcgtatgtacaGGTagttgttgtacaacttgagac
C9H	attatgggagcgtcatgtacgacatgcgtatgtacaCATagttgttgtacaacttgagac
C9I	attatgggagcgtcatgtacgacatgcgtatgtacaATTagttgttgtacaacttgagac
C9K	attatgggagcgtcatgtacgacatgcgtatgtacaAAAagttgttgtacaacttgagac
C9L	attatgggagcgtcatgtacgacatgcgtatgtacaTTAagttgttgtacaacttgagac
C9M	attatgggagcgtcatgtacgacatgcgtatgtacaATGagttgttgtacaacttgagac
C9N	attatgggagcgtcatgtacgacatgcgtatgtacaAATagttgttgtacaacttgagac
C9P	attatgggagcgtcatgtacgacatgcgtatgtacaCCTagttgttgtacaacttgagac
C9Q	attatgggagcgtcatgtacgacatgcgtatgtacaCAAagttgttgtacaacttgagac
C9R	attatgggagcgtcatgtacgacatgcgtatgtacaCGTagttgttgtacaacttgagac
C9S	attatgggagcgtcatgtacgacatgcgtatgtacaTCTagttgttgtacaacttgagac
C9T	attatgggagcgtcatgtacgacatgcgtatgtacaACAagttgttgtacaacttgagac
C9V	attatgggagcgtcatgtacgacatgcgtatgtacaGTAagttgttgtacaacttgagac
C9W	attatgggagcgtcatgtacgacatgcgtatgtacaTGGagttgttgtacaacttgagac
C9Y	attatgggagcgtcatgtacgacatgcgtatgtacaTATagttgttgtacaacttgagac
68NNK	ggacgtctcaagttgtacaacaactgcaMNNacaMNNgcatgtcgtacatgacgctccc

Table 1-S1: **Primers used to generate all mutants in this study**. Capital letters in sequence indicate mutation.

Mutant	Yield (mg/L)	MIC (µg/mL)	Modifications
WT	3.9	0.5	All variants
V6A-T8I1	1.0	0.5	
V6A-T8V1	1.0	0.25	
V6A-T8Y1	0.7	4	
V6I-T8A	ND	ND	
V6I-T8M	ND	ND	
V6I-T8S	ND	ND	
V6I-T8V	ND	ND	
V6L-T8I	ND	ND	
V6L-T8M	ND	ND	
V6L-T8S	ND	ND	
V6L-T8V	ND	ND	
V6M-T8I1	0.5	0.5	
V6M-T8M	ND	ND	
V6M-T8V1	0.9	1	M6-OH
V6M-T8V2	0.7	1	
V6M-T8Y1	0.4	>8	M6-OH
V6M-T8Y2	0.7	>8	
V6T-T8F	ND	ND	

Table 1-S2: MIC table of active double mutants. ND = not determined.

Mutant	Modifications	Chemical Formula	Expected Mass [M+H]	Observed Mass	Figure
WT	All variants	C48H47N13O10S6	1158.19659	1158.19864	S3A
T3S1	V6-OH	C47H45N13O10S6	1144.18094	1144.18205	S3B
T3S2		C47H45N13O9S6	1128.18602	1128.18843	S3C
T3S3	T8-CH3	C48H47N13O9S6	1142.20167	1142.20401	S3D
T3S4	T3-Dha	C47H43N13O8S6	1110.17546	1110.17857	S3E
T4A1	V6-OH	C47H47N13O10S6	1146.19659	1146.19836	S3F
T4A2		C47H47N13O9S6	1130.20167	1130.20404	S3G
T4S1	T4-Dha; V6-OH	C47H45N13O10S6	1144.18094	1144.18208	S3H
T4S2	T4-Dha; V6-OH; T8-CH3	C48H47N13O10S6	1158.19659	1158.19797	S3I
T4S3	T4-Dha	C47H45N13O9S6	1128.18602	1128.18795	S3J
V6A1		C46H43N13O9S6	1114.17037	1114.17171	S3K
V6A2	T8-CH3	C47H45N13O9S6	1128.18602	1128.18689	S3L
V6I1	I6-OH	C49H49N13O10S6	1172.21224	1172.21319	S3M
V6I2		C49H49N13O9S6	1156.21732	1156.21847	S3N
V6L1	L6-OH; T8-CH3	C50H51N13O10S6	1186.22789	1186.22864	S3O
V6L2	T8-CH3	C50H53N13O9S6	*1172.24862	1172.25000	S3P
V6M1	M6-OH; T8-CH3	C49H49N13O10S7	1204.18431	1204.18549	S3Q
V6M2	T8-CH3	C49H49N13O9S7	1188.18939	1188.19066	S3R
V6S1	T8-CH3	C47H45N13O10S6	1144.18094	1144.18291	S3S
V6T1	T8-CH3	C48H47N13O10S6	1158.19659	1158.19936	S3T
T8A1	V6-OH	C47H45N13O9S6	1128.18602	1128.18840	S3U
T8C1	V6-OH; C8-CH3	C48H47N13O9S7	1174.17374	1174.17637	S3V
T8F1		C53H51N13O8S6	*1190.23806	1190.24049	S3W
T8G1	V6-OH	C46H43N13O9S6	1114.17037	1114.17190	S3X
T8G2		C46H43N13O8S6	1098.17546	1098.17732	S3Y
T8I1	V6-OH	C50H51N13O9S6	1170.23297	1170.23432	S3Z
T8L1	V6-OH	C50H51N13O9S6	1170.23297	1170.23375	S3AA
T8L2		C50H53N13O8S6	*1156.25371	1156.25448	S3BB
T8M1	V6-OH	C49H49N13O9S7	1188.18939	1188.19226	S3CC
T8M2		C49H51N13O8S7	*1174.21013	1174.21150	S3DD
T8S1	V6-OH	C47H45N13O10S6	1144.18094	1144.18211	S3EE
T8S2	V6-OH; S8-Dha	C47H43N13O9S6	1126.17037	1126.17223	S3FF
T8V1	V6-OH	C49H49N13O9S6	1156.21732	1156.21959	S3GG
T8V2		C49H51N13O8S6	*1142.23806	1142.23920	S3HH
T8Y1	V6-OH	C53H49N13O10S6	1220.21224	1220.21448	S3II
T8Y2		C53H51N13O9S6	*1206.23297	1206.23292	S3JJ
V6A-T8I1		C48H47N13O8S6	1126.20676	1126.20849	S3KK
V6A-T8V1		C47H45N13O8S6	1112.19111	1112.19422	S3LL
V6A-T8Y1		C51H45N13O9S6	1176.18602	1176.18810	S3MM
V6M-T8I1		C50H53N13O8S7	*1188.22578	1188.22679	S3NN
V6M-T8V1	M6-OH	C49H49N13O9S7	1188.18939	1188.19102	S3OO
V6M-T8V2		C49H49N13O8S7	1172.19448	1172.19607	S3PP
V6M-T8Y1	M6-OH	C53H49N13O10S7	1252.18431	1252.18618	S3QQ

Mutant	Modifications	Chemical Formula	Expected Mass [M+H]	Observed Mass	Figure
V6M-T8Y2		C53H49N13O9S7	1236.18939	1236.19122	S3RR

Table 1-S3: **HRMS data for all compounds in this study**. Expected [M+H] are shown for compounds containing an aminoacetone residue at position 14. * indicates an expected [M+H] for an aminoisopropanol residue at position 14.

Residue	Group	δ ^{1}H (ppm)	δ ^{13}C (ppm)	δ ^{15}N (ppm)
Thr 3	NH	7.98		107.65
	CH (α)	3.09	47.40	
	CH (β)	3.71	65.49	
	CH_3 (γ)	1.03	21.68	
Dhb 4	NH	9.59		117.34
	C (α)		131.07	
	CH (β)	6.51	128.41	
	CH_3 (γ)	1.70	14.04	
Val 6 (β-OH)	NH	8.35		115.84
	CH (α)	5.48	57.87	
	C (β)		71.77	
	CH_3 (γ1)	1.23	27.94	
	CH_3 (γ2)	1.25	26.43	
Thr 8	NH	8.42		116.73
	CH (α)	5.06	57.22	
	CH (β)	3.96	67.55	
	CH_3 (γ)	1.02	21.45	
Dhb 13	NH	9.65		116.67
	C (α)		130.69	
	CH (β)	6.59	129.63	
	CH_3 (γ)	1.73	14.04	
Thr 14	NH	8.37		103.73
(aminoacetone)	CH_2 (α)	3.88	50.05	
	CO (β)		205.59	
	CH_3 (γ)	2.09	27.55	

Table 1-S4: Chemical shift assignments for WT thiocillin YM-266183.

Model	Thr 3	Val 6	Thr 8	Occupancy
$^3J_{HNHA}$	7.0	9.2	8.6	
$^3J_{HNHA}$ Torsion	±142	±165	±157	
WT_1	158.4	-129.1	176.8	37%
WT_2	148.4	-134.1	138.6	16%
WT_3	63.6	-141.6	53.2	16%
WT_4	163.2	-72.3	65.3	9%
WT_5	161.1	-29.0	163.9	7%

Table 1-S5: Phi angles of thiocillin NMR models. Experimentally determined NMR $^3J_{HNHA}$ coupling constants (Hz) and the corresponding torsion angles (°) calculated from the Karplus equation. Three macrocycle phi angles (°) and percent occupancy are listed for the top five computationally constrained models of thiocillin.

References

(1) Wieland Brown, L. C.; Acker, M. G.; Clardy, J.; Walsh, C. T.; Fischbach, M. A. *Proc Natl Acad Sci U S A* **2009**, *106*, 2549.

(2) Li, C.; Zhang, F.; Kelly, W. L. *Mol Biosyst* **2011**, *7*, 82.

(3) Harms, J. M.; Wilson, D. N.; Schluenzen, F.; Connell, S. R.; Stachelhaus, T.; Zaborowska, Z.; Spahn, C. M.; Fucini, P. *Mol Cell* **2008**, *30*, 26.

(4) Oman, T. J.; van der Donk, W. A. *Nat Chem Biol* **2010**, *6*, 9.

(5) Walsh, C. T.; Malcolmson, S. J.; Young, T. S. *ACS Chem Biol* **2012**, *7*, 429.

(6) Bowers, A. A.; Walsh, C. T.; Acker, M. G. *J Am Chem Soc* **2010**, *132*, 12182.

(7) Wever, W. J.; Bogart, J. W.; Baccile, J. A.; Chan, A. N.; Schroeder, F. C.; Bowers, A. A. *J Am Chem Soc* **2015**, *137*, 3494.

(8) Bowers, A. A.; Acker, M. G.; Koglin, A.; Walsh, C. T. *J Am Chem Soc* **2010**, *132*, 7519.

(9) Bowers, A. A.; Acker, M. G.; Young, T. S.; Walsh, C. T. *J Am Chem Soc* **2012**, *134*, 10313.

(10) Luo, X.; Zambaldo, C.; Liu, T.; Zhang, Y.; Xuan, W.; Wang, C.; Reed, S. A.; Yang, P. Y.; Wang, R. E.; Javahishvili, T.; Schultz, P. G.; Young, T. S. *Proc Natl Acad Sci U S A* **2016**, *113*, 3615.

(11) Just-Baringo, X.; Albericio, F.; Alvarez, M. *Angew Chem Int Ed Engl* **2014**, *53*, 6602.

(12) Coutsias, E. A.; Lexa, K. W.; Wester, M. J.; Pollock, S. N.; Jacobson, M. P. *J Chem Theory Comput* **2016**, *12*, 4674.

(13) Gavrish, E.; Sit, C. S.; Cao, S.; Kandror, O.; Spoering, A.; Peoples, A.; Ling, L.; Fetterman, A.; Hughes, D.; Bissell, A.; Torrey, H.; Akopian, T.; Mueller, A.; Epstein, S.; Goldberg, A.; Clardy, J.; Lewis, K. *Chem Biol* **2014**, *21*, 509.

(14) Vuister, G. W.; Bax, A. *J Am Chem Soc* **1993**, *115*, 7772.

(15) Turgeon, N.; Laflamme, C.; Ho, J.; Duchaine, C. J Microbiol Methods 2006, 67, 543.

(16) Acker, M. G.; Bowers, A. A.; Walsh, C. T. J Am Chem Soc 2009, 131, 17563.

Chapter 2

Site-Specific Labelling of Engineered Methionine Residues on Thiocillin

Hai L. Tran, and James A. Wells

Abstract

The ability to modify chemical compounds found in nature has been a powerful tool to study their biological role and develop many natural products into therapeutics. We chose to study the ribosomal natural product, thiocillin, based on our previous work studying its structure-activity relationship by saturation mutagenesis and molecular modelling. This study demonstrates the first use of the ReACT oxaziridine reagent to site-specifically label methionine residues on engineered thiocillin natural products. Alkyne or azide click handles can be installed on the natural product robustly. This enables the semi-synthesis of thiocillin analogs by click-chemistry. We demonstrate the simplicity of generating semi-synthetic analogs using the ReACT reagent followed by click-chemistry. However, our attempts to generate a soluble prodrug of thiocillin has led to a loss of antibiotic activity. Further studies are needed to fully understand the implications of labelling with the ReACT reagent on membrane permeability, solubility, and activity.

Introduction

Thiocillin is a ribosomally synthesized and post-translationally modified peptide (RiPPs) natural product.[1,2] Thiocillin exhibits potent antimicrobial activity against gram-positive bacteria including dangerous pathogens such as methicillin-resistant *Staphylococcus aureus* (MRSA) and vancomycin-resistant *Enterococci* (VRE). Its target is the interface between ribosomal protein L11 and the 23S rRNA.[3] Due to thiocillin's genetically encoded peptide scaffold, it has been the subject of many mutational studies ranging from alanine-scanning, saturation mutagenesis, ring-size variations, to incorporation of unnatural amino acids.[4-9] Our previous work with thiocillin has elucidated much of the structure-activity relationship critical for activity.[9]

Solubility has been one of the major issues plaguing the use of thiopeptides as clinical drugs. Despite this challenge, Novartis improved the solubility of the thiopeptide GE2270A in the development in their clinical candidate, LFF571, which is currently in Phase II clinical trials.[10-12] This exemplifies the potential for thiopeptides to be developed as drugs. However, using traditional medicinal chemistry methods to modify natural products can be quite challenging. This study seeks to use site-specific methods to enable semi-synthesis of thiocillin.

The ability to site-specifically label natural products has many potential uses from tagging to changing its chemical properties. Site-specific chemistry relies on taking advantage of a unique functional group. Since thiocillin is genetically encoded, one method would be to introduce a unique residue amenable to modification. A favorite amongst chemical biologists is to introduce reactive cysteines. However, free cysteines are not well tolerated in thiocillin and are often converted into thiazole residues. An

alternative successful method would be to incorporate an unnatural amino acid. This has been previously demonstrated, but this method suffers from low yields.[6]

In this study, we target a natural amino acid, methionine, for site-specific labelling. From our previous study, methionine mutations are well tolerated and generally result in good yields. We will use a redox-activated chemical tagging (ReACT) system which was recently developed for the bioconjugation of methionine residues.[13] This system has been demonstrated to work on native proteins and our study is the first use of this reagent on a natural product. The ReACT system uses an oxaziridine warhead which targets the sulfur atom on methionine to form a stable sulfimide bond. The oxaziridine reagent can be modified to carry a chemical handle. In our case, we install an alkyne or azide handle which will enable downstream copper catalyzed click chemistry. The reaction scheme for the ReACT-enabled semi-synthesis is shown in **Figure 2-1**.

Materials and Methods

Production of thiocillin mutants.

Cloning, expression, and purification of thiocillin mutants are described in the Chapter 1 Supplemental Information section.

Chemical synthesis

10-fold excess ReACT reagent was added to T8M1 analog in 9:1 DMSO:H_2O. Reaction was stirred for 24 hours at room temperature and HPLC purified. For click chemistry, all reagents were dissolved in DMSO unless otherwise stated. 5 eq azide reagent was added to T8M1-alkyne. 0.2 eq CuSO4-TBTA mixture (in 55% DMSO and 45% H_2O) is added followed by 0.4 eq ascorbic acid. Reaction was stirred overnight at room temperature and purified by HPLC.

Purification of compounds

After each step, all compounds are purified by HPLC over a Waters XBridge Prep C18 5 μm OBD 19 x 50 mm column.

LC/MS analysis

Details on the LC/MS analysis are described in the Chapter 1 Supplemental Information section.

MIC assay

The MIC assay is described in detail in the Chapter 1 Supplemental Information section. Detergent MIC assay was performed the same way with the addition of 0.025% Tween-80.

Results and Discussion

Sites on thiocillin were profiled for acceptance of a methionine mutation. Our previous mutagenesis study showed that residues Thr-3, Thr-4, Val-6, and Thr-8 in the macrocycle tolerate methionine mutations well with yields greater than 1 mg/L.[9] In addition, we profiled the remaining two non-thiazole residues, Thr-13 and Thr-14. Both of these residues tolerated a methionine substitution, however, their yields were significantly decreased by over 10-fold. In total, all six non-thiazole and non-pyridine-forming residues were able to accept a methionine substitution. T3M and T4M showed no activity, while T13M and T14M showed reduced activity and low yield. We decided to move forward with the T8M mutation due to its high yield and its known tolerance to accept large amino acids at this site.

The large-scale purification of the T8M mutant led to the formation of two major products: T8M1 containing a β-hydroxy valine PTM at residue 6; and T8M1 with a standard valine at residue 6. We continued with T8M1 due to its higher activity of 1 μg/mL MIC and slightly higher solubility. **Figure 2-1** describes the reactioin scheme used in this study to generate semi-synthetic analogs. We demonstrate the use of the oxaziridine-alkyne ReACT reagent to specifically label the methionine on T8M1 to generate T8M1-alkyne. In addition, T8M1-azide can be generated with an oxaziridine-azide reagent.

Installing a chemical handle, such as biotin, on a natural product can advance the study of its biological role. An example of this is with the thiopeptide, thiostrepton, where a biotin handle was installed on the natural product in order to find its target in

human breast cancer cells, MCF-7.[14] We demonstrate the use of click-chemistry for the attachment of biotin onto thiocillin. We reacted T8M1-alkyne with an azide-PEG3-biotin reagent in the presence of catalytic amounts of $CuSO_4$-TBTA and ascorbic acid to generate T8M1-biotin (**Figure 2-2**).[15] This compound can now be used as a chemical handle for future affinity pull-down studies. In theory, we can also use this method to attach other chemical handles such as fluorophores or photoreactive crosslinkers.

To investigate the extent to which improving solubility can improve activity, we repeated the MIC assay performed in our previous study on a library of thiocillin analogs in the presence of 0.025% Tween-80 detergent (**Table 2-1**). Detergents help to break up insoluble aggregates into its monodispersed form.[16] Our results show an across the board increase in potency. To exemplify the role compound solubility plays, analog T8F1 was active when screened on solid agarose media and lost activity in liquid culture, but regained activity in the presence of detergents. Increasing the solubility may have a dual role of improving drug delivery and improving activity.

To improve solubility, we decided to explore a prodrug approach to derivatize thiocillin. **Figure 2-3** shows this approach with several proposed analogs. This approach will install solubilizing groups such as phosphates and esters onto thiocillin to improve solubility for IV dosing. Once the drug is delivered, serum phosphatases and esterases can cleave the prodrug to release an active antibiotic. In order for this strategy to work, the cleaved form must be active. We synthesized the T8M1-hydroxyethyl cleaved prodrug product by using click chemistry to install an azidoethanol onto T8M1-alkyne.

An MIC assay was performed on T8M1-alkyne and T8M1-hydroxyethyl to see if activity was preserved (**Table 2-2**). These two analogs did not retain activity which

shows that in this particular case, labelling at this site or labelling methionines in general is not a viable solubilizing strategy. The addition of the sulfimide and alkyne group ablated activity. This could be due to changing membrane transport properties or influencing target engagement. Although mutant T13M has a lower yield, attempting to use the ReACT system on the tail region of thiocillin may rule out any adverse effects of directly labelling the macrocycle. Future work is necessary to determine if the ReACT reagent has inherent properties that prevent membrane permeability.

In conclusion, we demonstrate the use of the ReACT oxiziridine reagent to site-specifically label engineered methionines on thiocillin. The ReACT chemistry followed by click chemistry is a very robust system to generate semi-synthetic analogs. Chemical handles such as alkynes, azides, and biotin have been successfully installed onto thiocillin. Chemical handles can also be installed onto many of the thiocillin mutants previously discovered. These biotin-conjugated thiocillins may be useful for future affinity pull-down studies to identify targets in mammalian cells or other model organisms. Although the use of the ReACT reagent did not lead to active antibiotics, the strategy described here may be applicable to other natural product systems. This study illustrates how difficult medicinal chemistry can be to improve specific properties of a natural product compound.

Acknowledgments

We thank Dr. Shixian Lin and Professor Christopher Chang for graciously providing the oxaziridine reagents. We also thank Professors Adam Renslo, Michael Fischbach, and Susan Miller for helpful discussion.

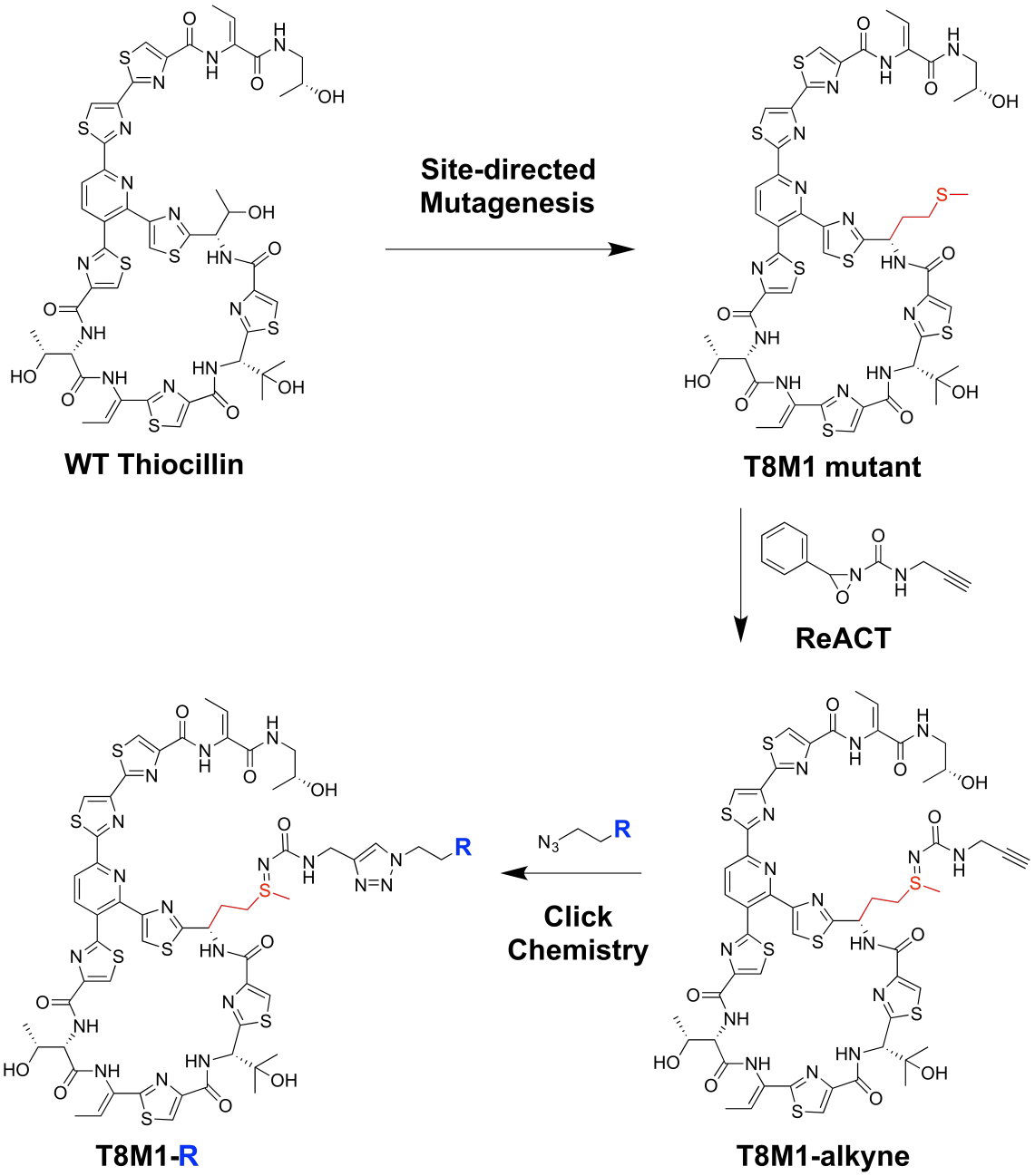

Figure 2-1) Reaction scheme for ReACT-enabled semi-synthesis. Site-directed mutagenesis is used to generate a methionine mutant. Spontaneous reaction of T8M1 analog with oxaziridine-alkyne reagent (in 9:1 DMSO:H_2O) generates the alkyne labelled thiocillin. Copper catalyzed click chemistry is then used to generate semi-synthetic analogs.

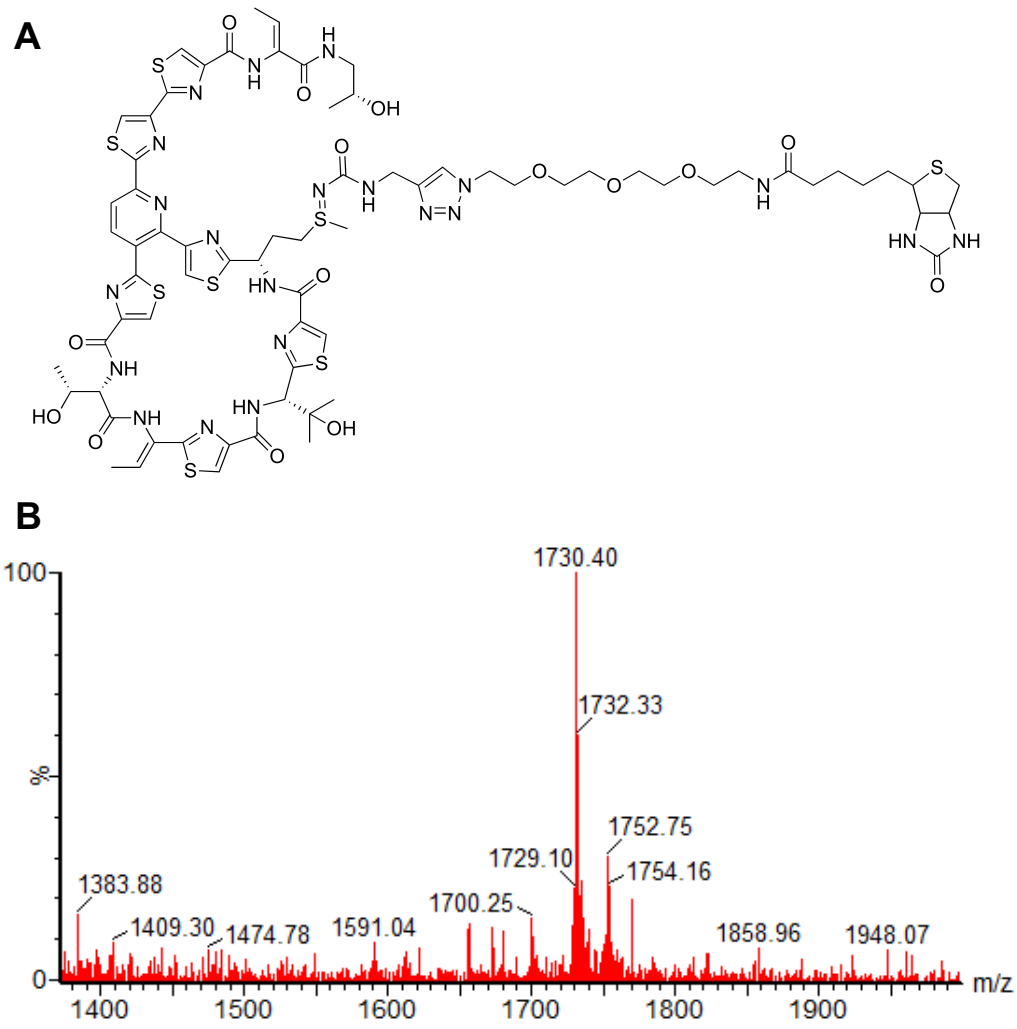

Figure 2-2: Thiocillin analog T8M1-biotin. A) T8M1-biotin was synthesized from T8M1-alkyne via click chemistry. **B)** Expected [M+H] = 1730.45.

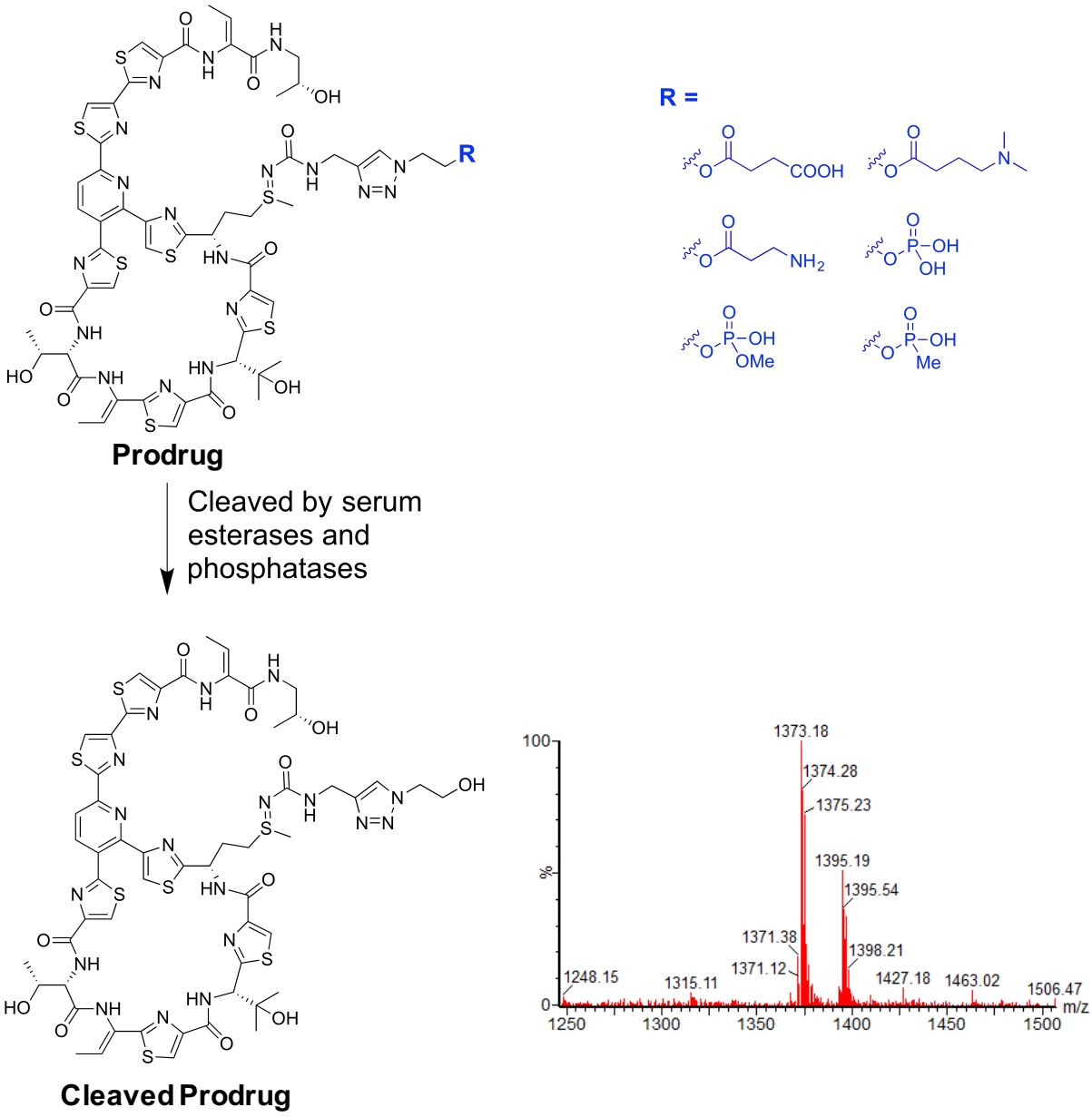

Figure 2-3: Prodrug analogs of thiocillin. Proposed solubilizing R-groups shown in blue. The prodrug will be cleaved phosphatases or esterases in serum. Expected [M+H] of the cleavage product is 1372.27.

Mutant[a]	Yield[b]	MIC[c]	MIC[c] + 0.025% Tween-80	Modifications[d]
WT	3.9	0.5	0.03	All variants
T3S1	1.3	>8	0.25	V6-OH
T3S2	1.9	>8	0.25	
T3S3	0.3	>8	2	T8-CH_3
T3S4	0.3	>8	>8	T3-Dha
T4A1 (-)	0.7	>8	>8	V6-OH
T4A2 (-)	1.1	>8	>8	
T4S1	0.6	2	0.5	T4-Dha; V6-OH
T4S2	0.3	1	0.25	T4-Dha; V6-OH; T8-CH_3
T4S3	0.1	>8	>8	T4-Dha
V6A1	0.5	1	0.13	
V6A2	1.9	0.06	0.03	T8-CH_3
V6I1	2.1	0.5	0.03	I6-OH
V6I2	0.3	0.5	0.06	
V6L1	0.3	0.5	0.06	L6-OH; T8-CH_3
V6L2	0.5	2	0.25	T8-CH_3
V6M1	1.1	0.25	0.06	M6-OH; T8-CH_3
V6M2	2.4	0.13	0.03	T8-CH_3
V6S1	0.6	0.5	0.13	T8-CH_3
V6T1	1.6	0.13	0.03	T8-CH_3
T8A1	1.2	0.5	0.06	V6-OH
T8C1	0.4	8	0.5	V6-OH; C8-CH_3
T8F1	1.0	>8	1	
T8G1	0.9	2	0.13	V6-OH
T8G2	0.4	0.5	0.13	
T8I1	0.7	0.13	0.13	V6-OH
T8L1	1.3	1	0.25	V6-OH
T8L2	0.7	>8	>8	
T8M1	1.4	1	0.25	V6-OH
T8M2	1.3	2	0.13	
T8S1	0.9	>8	0.13	V6-OH
T8S2	0.1	1	0.13	V6-OH; S8-Dha
T8V1	2.0	0.13	0.03	V6-OH
T8V2	0.3	1	0.25	
T8Y1	1.6	0.25	0.06	V6-OH
T8Y2	2.1	1	0.25	

Table 2-1: MIC table of thiocillin analogs with detergent. [a]Compound numbering is in order of chromatographic retention time. (-) indicates an inactive negative control. [b]mg/L. [c]μg/mL. [d]Modifications are predicted based on high-resolution MS, retention time, and NMR (structural characterizations are included in the SI). Compounds were screened against *Bacillus subtilis* 168.

Analog	MIC
WT	0.5
T8M	1
T8M-Alkyne	>8
T8M-Cleaved Prodrug	>8

Table 2-2: MIC table of semi-synthesis products. Compounds were screened against *Bacillus subtilis* 168.

References

(1) Arnison, P. G.; Bibb, M. J.; Bierbaum, G.; Bowers, A. A.; Bugni, T. S.; Bulaj, G.; Camarero, J. A.; Campopiano, D. J.; Challis, G. L.; Clardy, J.; Cotter, P. D.; Craik, D. J.; Dawson, M.; Dittmann, E.; Donadio, S.; Dorrestein, P. C.; Entian, K. D.; Fischbach, M. A.; Garavelli, J. S.; Goransson, U.; Gruber, C. W.; Haft, D. H.; Hemscheidt, T. K.; Hertweck, C.; Hill, C.; Horswill, A. R.; Jaspars, M.; Kelly, W. L.; Klinman, J. P.; Kuipers, O. P.; Link, A. J.; Liu, W.; Marahiel, M. A.; Mitchell, D. A.; Moll, G. N.; Moore, B. S.; Muller, R.; Nair, S. K.; Nes, I. F.; Norris, G. E.; Olivera, B. M.; Onaka, H.; Patchett, M. L.; Piel, J.; Reaney, M. J.; Rebuffat, S.; Ross, R. P.; Sahl, H. G.; Schmidt, E. W.; Selsted, M. E.; Severinov, K.; Shen, B.; Sivonen, K.; Smith, L.; Stein, T.; Sussmuth, R. D.; Tagg, J. R.; Tang, G. L.; Truman, A. W.; Vederas, J. C.; Walsh, C. T.; Walton, J. D.; Wenzel, S. C.; Willey, J. M.; van der Donk, W. A. *Nat Prod Rep* **2013**, *30*, 108.

(2) Wieland Brown, L. C.; Acker, M. G.; Clardy, J.; Walsh, C. T.; Fischbach, M. A. *Proc Natl Acad Sci U S A* **2009**, *106*, 2549.

(3) Harms, J. M.; Wilson, D. N.; Schluenzen, F.; Connell, S. R.; Stachelhaus, T.; Zaborowska, Z.; Spahn, C. M.; Fucini, P. *Mol Cell* **2008**, *30*, 26.

(4) Bowers, A. A.; Acker, M. G.; Koglin, A.; Walsh, C. T. *J Am Chem Soc* **2010**, *132*, 7519.

(5) Bowers, A. A.; Acker, M. G.; Young, T. S.; Walsh, C. T. *J Am Chem Soc* **2012**, *134*, 10313.

(6) Luo, X.; Zambaldo, C.; Liu, T.; Zhang, Y.; Xuan, W.; Wang, C.; Reed, S. A.; Yang, P. Y.; Wang, R. E.; Javahishvili, T.; Schultz, P. G.; Young, T. S. *Proc Natl Acad Sci U S A* **2016**, *113*, 3615.

(7) Just-Baringo, X.; Albericio, F.; Alvarez, M. *Angew Chem Int Ed Engl* **2014**, *53*, 6602.

(8) Acker, M. G.; Bowers, A. A.; Walsh, C. T. *J Am Chem Soc* **2009**, *131*, 17563.

(9) Tran, H. L.; Lexa, K. W.; Julien, O.; Young, T. S.; Walsh, C. T.; Jacobson, M. P.; Wells, J. A. *J Am Chem Soc* **2017**, *139*, 2541.

(10) Leeds, J. A.; LaMarche, M. J.; Brewer, J. T.; Bushell, S. M.; Deng, G.; Dewhurst, J. M.; Dzink-Fox, J.; Gangl, E.; Jain, A.; Lee, L.; Lilly, M.; Manni, K.; Mullin, S.; Neckermann, G.; Osborne, C.; Palestrant, D.; Patane, M. A.; Raimondi, A.; Ranjitkar, S.; Rann, E. M.; Sachdeva, M.; Shao, J.; Tiamfook, S.; Whitehead, L.; Yu, D. *Antimicrob Agents Chemother* **2011**, *55*, 5277.

(11) LaMarche, M. J.; Leeds, J. A.; Amaral, A.; Brewer, J. T.; Bushell, S. M.; Deng, G.; Dewhurst, J. M.; Ding, J.; Dzink-Fox, J.; Gamber, G.; Jain, A.; Lee, K.; Lee, L.; Lister, T.; McKenney, D.; Mullin, S.; Osborne, C.; Palestrant, D.; Patane, M. A.; Rann, E. M.; Sachdeva, M.; Shao, J.; Tiamfook, S.; Trzasko, A.; Whitehead, L.; Yifru, A.; Yu, D.; Yan, W.; Zhu, Q. *J Med Chem* **2012**, *55*, 2376.

(12) Trzasko, A.; Leeds, J. A.; Praestgaard, J.; Lamarche, M. J.; McKenney, D. *Antimicrob Agents Chemother* **2012**, *56*, 4459.

(13) Lin, S.; Yang, X.; Jia, S.; Weeks, A. M.; Hornsby, M.; Lee, P. S.; Nichiporuk, R. V.; Iavarone, A. T.; Wells, J. A.; Toste, F. D.; Chang, C. J. *Science* **2017**, *355*, 597.

(14) Hegde, N. S.; Sanders, D. A.; Rodriguez, R.; Balasubramanian, S. *Nat Chem* **2011**, *3*, 725.

(15) Chan, T. R.; Hilgraf, R.; Sharpless, K. B.; Fokin, V. V. *Org Lett* **2004**, *6*, 2853.

(16) Coan, K. E.; Shoichet, B. K. *J Am Chem Soc* **2008**, *130*, 9606.

Publishing Agreement

It is the policy of the University to encourage the distribution of all theses, dissertations, and manuscripts. Copies of all UCSF theses, dissertations, and manuscripts will be routed to the library via the Graduate Division. The library will make all theses, dissertations, and manuscripts accessible to the public and will preserve these to the best of their abilities, in perpetuity.

Please sign the following statement:

I hereby grant permission to the Graduate Division of the University of California, San Francisco to release copies of my thesis, dissertation, or manuscript to the Campus Library to provide access and preservation, in whole or in part, in perpetuity.

Author Signature

3/21/2017

Date